Integrated Research/Education University Aircraft Design Program
Development

Eli Livne
UNIVERSITY OF WASHINGTON
4333 BROOKLYN AVE NE
SEATTLE, WA 981950001

04/06/2017
Final Report

Air Force Research Laboratory
AF Office Of Scientific Research (AFOSR)/RTA1

REPORT DOCUMENTATION PAGE

Form Approved
OMB No. 0704-0188

The public reporting burden for this collection of information is estimated to average 1 hour per response, including the time for reviewing instructions, searching existing data sources, gathering and maintaining the data needed, and completing and reviewing the collection of information. Send comments regarding this burden estimate or any other aspect of this collection of information, including suggestions for reducing the burden, to Department of Defense, Executive Services, Directorate (0704-0188). Respondents should be aware that notwithstanding any other provision of law, no person shall be subject to any penalty for failing to comply with a collection of information if it does not display a currently valid OMB control number.
PLEASE DO NOT RETURN YOUR FORM TO THE ABOVE ORGANIZATION.

1. REPORT DATE *(DD-MM-YYYY)* 06-04-2017	2. REPORT TYPE Final Performance	3. DATES COVERED *(From - To)* 01 Jan 2014 to 31 Dec 2016

4. TITLE AND SUBTITLE Integrated Research/Education University Aircraft Design Program Development	5a. CONTRACT NUMBER
	5b. GRANT NUMBER FA9550-14-1-0027
	5c. PROGRAM ELEMENT NUMBER 61102F
6. AUTHOR(S) Eli Livne, John Valasek, Ryan Starkey, Thomas Strganac	5d. PROJECT NUMBER
	5e. TASK NUMBER
	5f. WORK UNIT NUMBER

7. PERFORMING ORGANIZATION NAME(S) AND ADDRESS(ES) UNIVERSITY OF WASHINGTON 4333 BROOKLYN AVE NE SEATTLE, WA 981950001 US	8. PERFORMING ORGANIZATION REPORT NUMBER

9. SPONSORING/MONITORING AGENCY NAME(S) AND ADDRESS(ES) AF Office of Scientific Research 875 N. Randolph St. Room 3112 Arlington, VA 22203	10. SPONSOR/MONITOR'S ACRONYM(S) AFRL/AFOSR RTA1
	11. SPONSOR/MONITOR'S REPORT NUMBER(S) AFRL-AFOSR-VA-TR-2017-0077

12. DISTRIBUTION/AVAILABILITY STATEMENT
DISTRIBUTION A: Distribution approved for public release.

13. SUPPLEMENTARY NOTES

14. ABSTRACT
Progress in both areas of capstone airplane design education development and supersonic tailless configurations research in the project years is reported. Seniors at the University of Washington designed, analyzed, ground-tested, and built advanced research UAVs for the flight testing of low-speed flight characteristics of tailless supersonic aircraft. Integrated with the undergraduates was a graduate student who then proceeded to carry out more advanced research, at the graduate level, focusing on the controllability at high angles of attack of tailless supersonic configurations. In parallel to University of Washington work in the advanced airplane design education / airplane design areas, the University of Colorado, Boulder, and Texas A&M developed integrated education / research programs in the airplane design area, each adding its particular perspective. The University of Colorado focused on the development of a supersonic UAV while Texas A&M focused on airplane design in general and on the control of tailless supersonic configurations.

15. SUBJECT TERMS

16. SECURITY CLASSIFICATION OF:			17. LIMITATION OF ABSTRACT	18. NUMBER OF PAGES	19a. NAME OF RESPONSIBLE PERSON TILEY, JAIMIE
a. REPORT	b. ABSTRACT	c. THIS PAGE			
Unclassified	Unclassified	Unclassified	UU		19b. TELEPHONE NUMBER *(Include area code)* 703-588-8316

Standard Form 298 (Rev. 8/98)
Prescribed by ANSI Std. Z39.18

Final Report

AFOSR Grant FA9550-14-1-0027

"Integrated Research/Education University Aircraft Design Program Development"

March 28, 2017

By

Eli Livne

Boeing Endowed Professor of Aeronautics & Astronautics

University of Washington

Seattle, WA 98195-2400

eli@aa.washington.edu

Abstract

Progress in both areas of capstone airplane design education development and supersonic tailless configurations research in the project years is reported. Seniors at the University of Washington designed, analyzed, ground-tested, and built advanced research UAVs for the flight testing of low-speed flight characteristics of tailless supersonic aircraft. Integrated with the undergraduates was a graduate student who then proceeded to carry out more advanced research, at the graduate level, focusing on the controllability at high angles of attack of tailless supersonic configurations. In parallel to University of Washington work in the advanced airplane design education / airplane design areas, the University of Colorado, Boulder, and Texas A&M developed integrated education / research programs in the airplane design area, each adding its particular perspective. The University of Colorado focused on the development of a supersonic UAV while Texas A&M focused on airplane design in general and on the control of tailless supersonic configurations.

Annual Progress Report

AFOSR Grant FA9550-14-1-0027

"Integrated Research/Education University Aircraft Design Program Development"

Introduction

The two major goals of AFOSR Grant FA9550-14-1-0027, "Integrated Research/Education University Aircraft Design Program Development", were (a) to contribute to the development cutting edge capstone airplane design courses in U.S. universities. Such courses would take advantage of the most recent developments in software and hardware systems and tools as well as systems design technology to bring into aerospace engineering undergraduate and graduate programs a systems integration perspective and the experience of designing, building, and flying, supported by rigorous analysis and tests, of advanced research unmanned aerial vehicles (UAVs); (b) to contribute to the understanding of design options and tradeoffs that would lead to efficient long-range supersonic aircraft without tail surfaces. No tail surfaces or reduced size tail surfaces may lead to less drag, less weight, lower construction cost, and smaller stealth signatures. The elimination or size-reduction of tail surfaces must be well understood regarding the impact on flight stability and control, especially at low-speed takeoff, approach and landing conditions, and in the context of thorough multidisciplinary optimization that would account for all design criteria, constraints, and objectives. New contributions to tailless or minimal-tail supersonic long-range flight are of importance to the future of both military and civil aircraft.

The grant supported efforts by three universities: The University of Washington in Seattle, Texas A&M University, and the University of Colorado, Boulder. Leading the work at Texas A&M were Professors John Valasek and Tom Strganac. At the University of Colorado – Prof. Ryan Starkey. At the University of Washington – Prof. Eli Livne.

In the following, work done at the University of Washington during 2015 will be presented first. Because funds for Year II of the project were delayed significantly and arrived very late in 2015, work at Texas A&M and the University of Colorado, after the conclusion of successful Year I efforts, could not proceed as planned. With a grant extension in place later, Project Year II work could be completed at all three universities and is reported here.

The University of Washington 2016 Capstone Airplane Design Project was a third effort, after the 2013 and 2014 projects, to examine features of supersonic tailless configuration design that were not studied earlier. In particular, the 2016 design challenge focused on yaw control by directional thrust vectoring and wing tip winglet / rudders. To focus on these aspects of the configuration with as little risk as possible in other areas, a three-surface configuration was selected by the students. Such a configuration takes advantage of the control flexibility and possible redundancy offered longitudinally and laterally by integrated operation of wing control surfaces, canards, and tail surfaces.

Thirty-five seniors in the William E. Boeing Department of Aeronautics and Astronautics, over twenty academic weeks of the 2016 winter and spring quarters, designed, analyzed, ground tested, and worked on building the 2016 Research UAV (R-UAV), as described in the presentation below.

All key elements of the UW's approach to aircraft design education were pursued:

A complex cutting-edge design challenge with the opportunity to contribute to the state of the art;

Substantial engineering analysis using industry-standard simulation techniques and tools;

Substantial testing and analysis / test correlation experience;

System analysis and integration;

Airplane design team work, including team multi-discipline information exchange and interaction;

Multidisciplinary tradeoffs;

Engineering communication and presentation;

Project execution to meet budget and schedule constraints;

Consideration of environmental / societal impacts of airplane design decisions.

Wind tunnel tests showed that with the particular planform selected for the 2016 R-UAV, wing-tip devices were not effective for yaw control.

Details of the project progress and accomplishments are presented next.

In addition to the work carried out by the seniors, a graduate student who was a TA for the airplane design course, proceeded with graduate level research work that focused on the controllability at high angles of attack of tailless supersonic configurations. The success of the resulting MSAA work would, hopefully, lead to stronger integration of undergraduate and graduate student work in the design, development, construction, and testing of advanced flight vehicle configurations that would be a contribution to the state of the art in airplane design.

Each year, design of different supersonic configurations was pursued, including detailed CAD definitions of the geometry, low-speed wind tunnel tests, analysis, using commercial simulation tools, of the aerodynamic, structural, performance, and stability and control characteristics of the configurations. The resulting information produced by analysis and tests provides an important data base that can support future development of supersonic configurations.

The UW configurations developed with AF support

The following figures show the University of Washington research UAV designs from 2013 to 2016. Each configuration was developed to study different design features that would contribute to the low-speed handling qualities of long-range supersonic configurations. Details are provided in each year's final design reports and presentations.
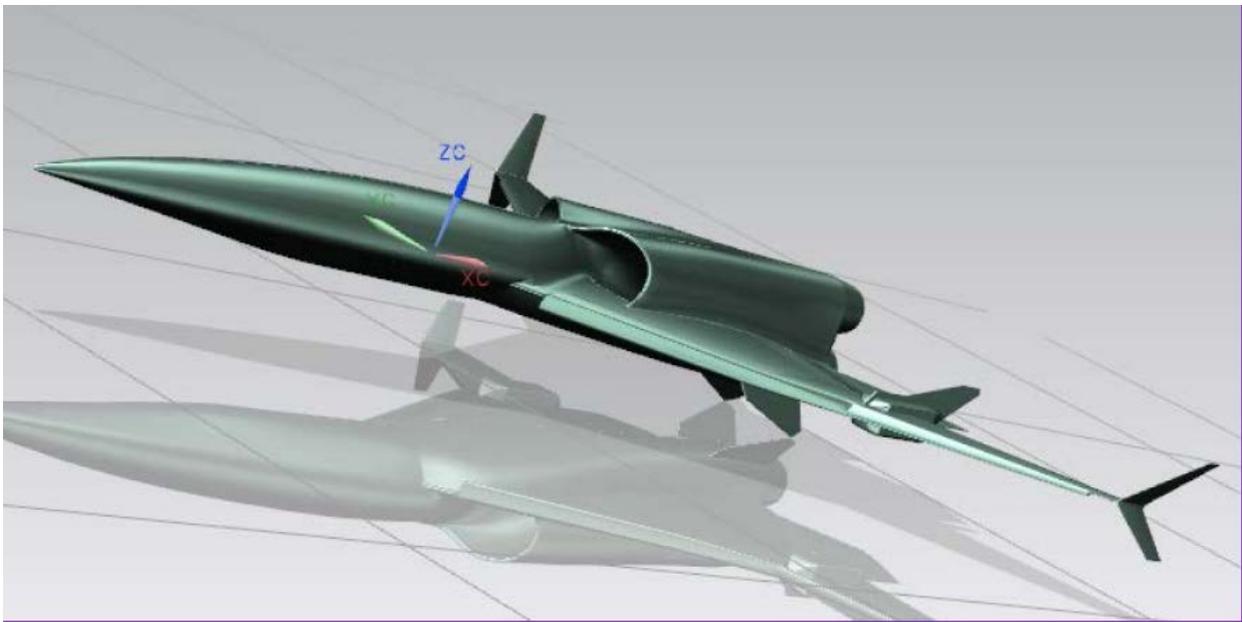
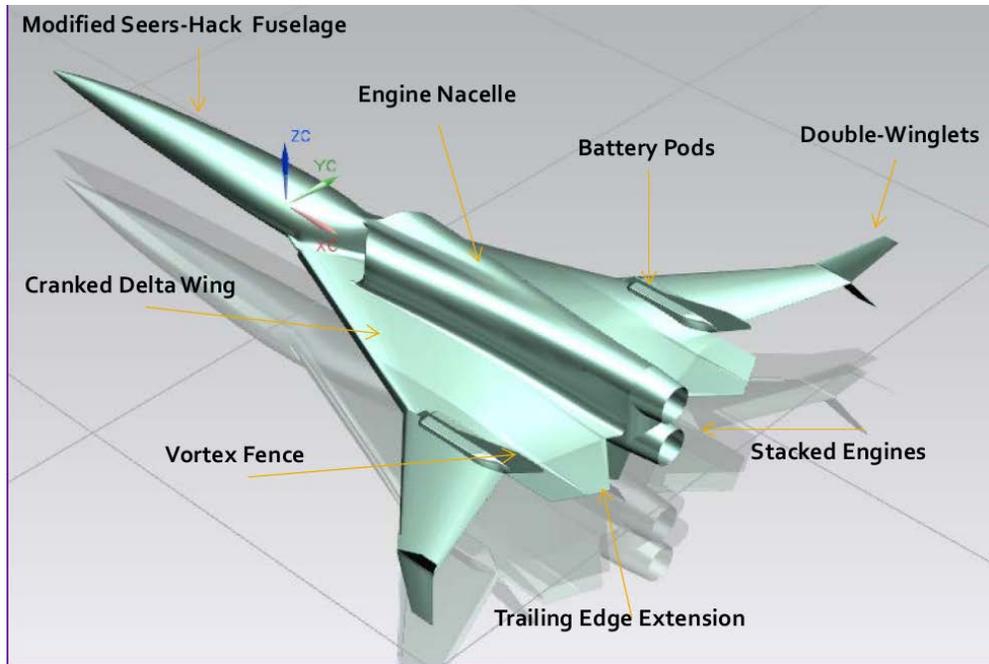Figure 1: The 2013 configuration

Figure 2: The 2013 Configuration
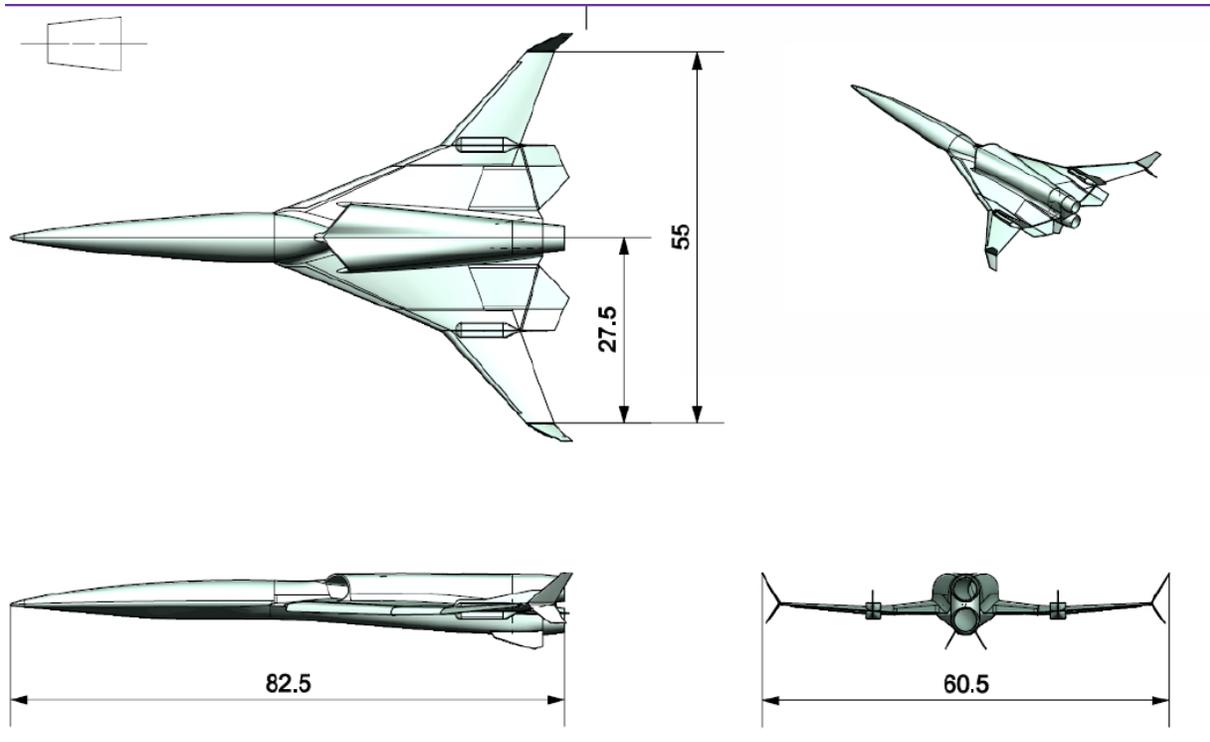

Figure 3: The 2013 Wind Tunnel Model
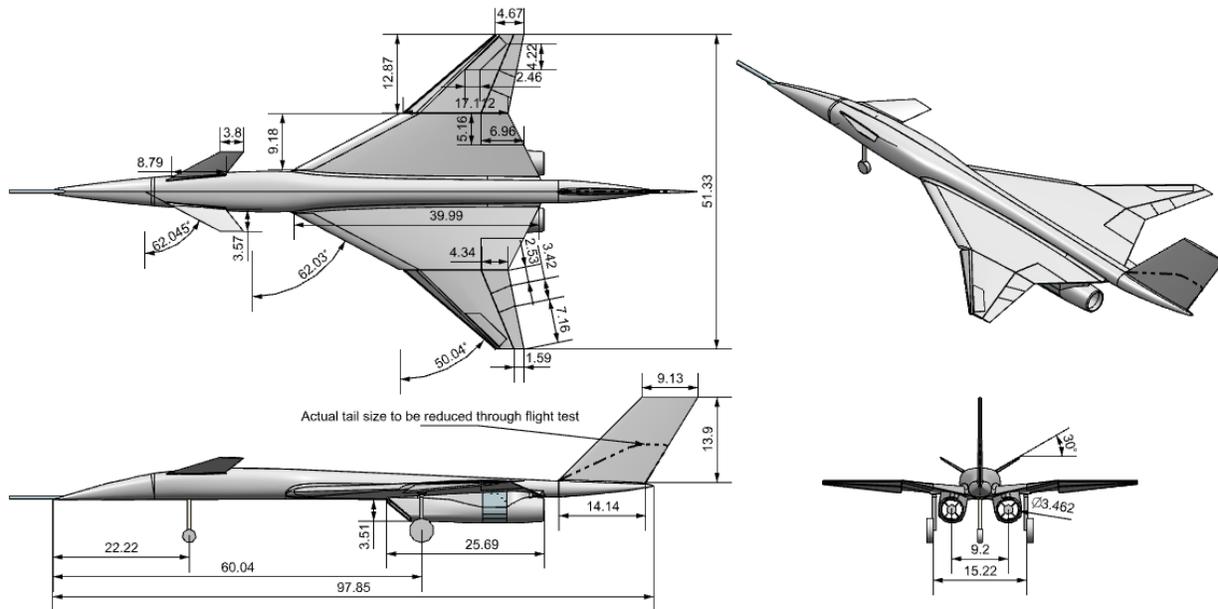
Figure 4: The 2013 configuration

Figure 5: The 2014 UAV

Figure 6: The 2014 Wind Tunnel Mode

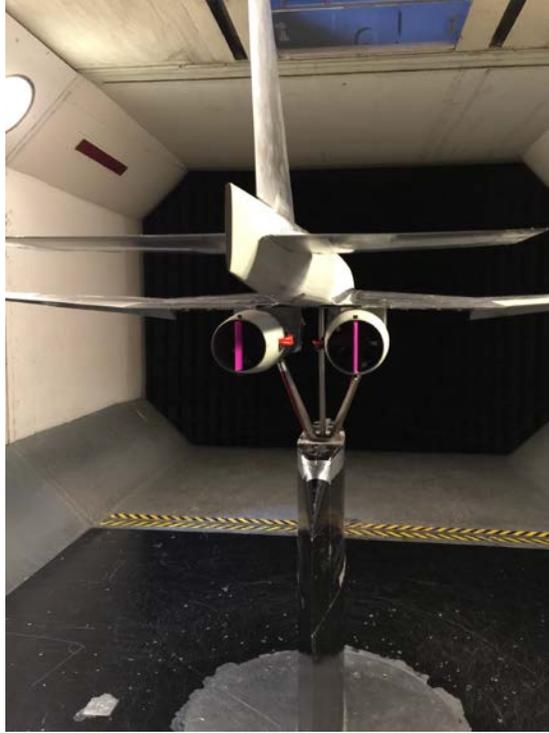Figure 7: The 2014 UAV with full-size vertical tail

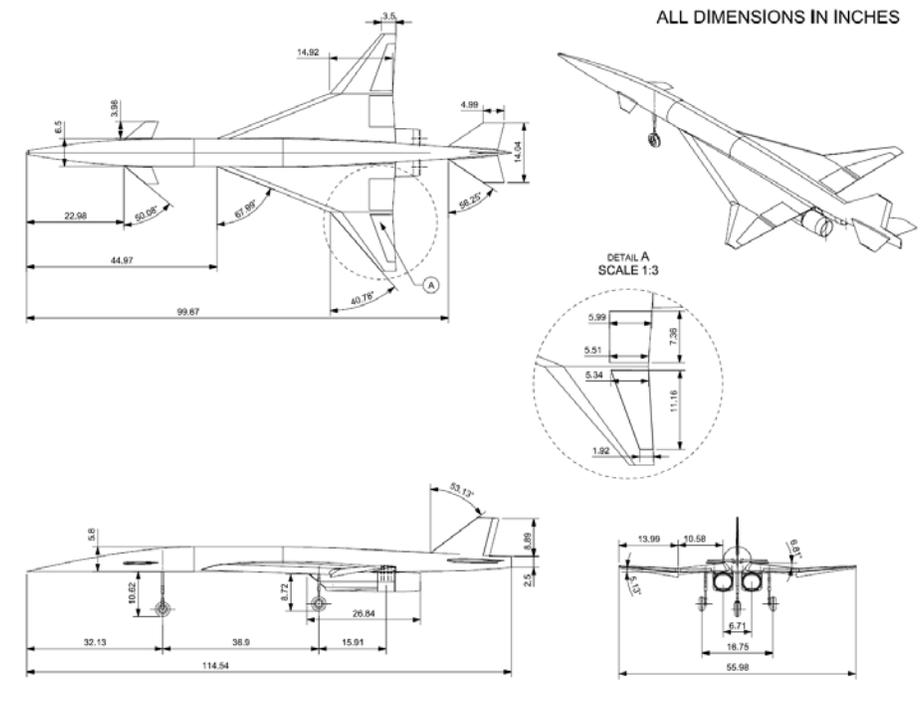Figure 8: Thrust vectoring on the 2015 wind tunnel model

Figure 9: The 2015 UW UAV

Figure 10: The 2015 UW UAV without vertical tail and boom

Figure 11: The 2015 UW wind tunnel model

Figure 12: The 2016 Wind Tunnel Model
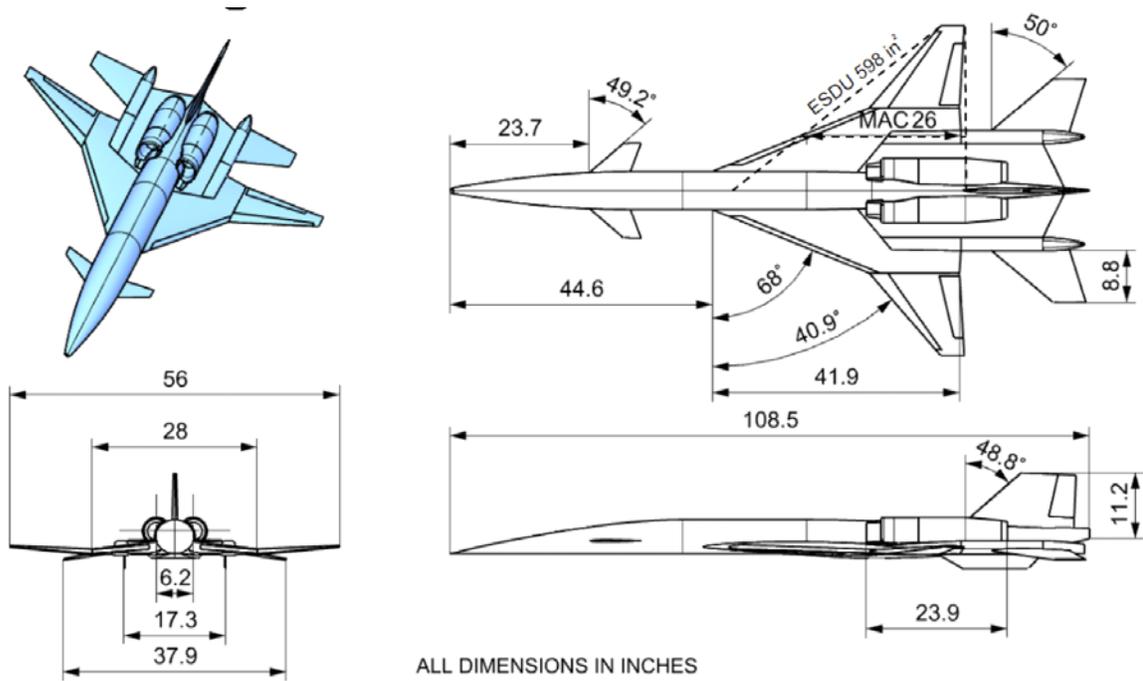

ALL DIMENSIONS IN INCHES
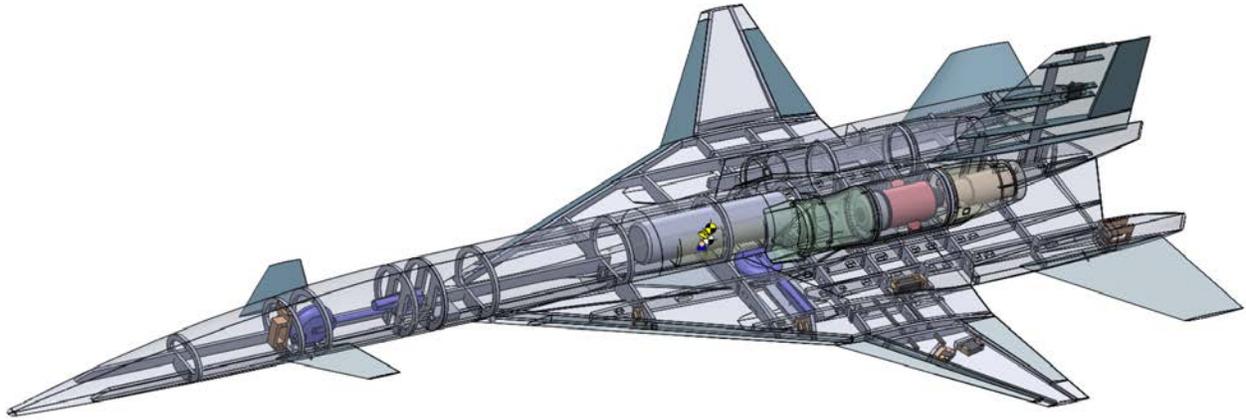
Figure 13: The 2016 configuration

Figure 14: Structural layout of the 2016 UAV

Figure 15: The 2016 UAV under construction

The different configurations developed and tested all had slender low-boom high supersonic cruise efficiency features. The 2013 configuration studied a British Lightning like placement of engines to reduce yawing moments and the need for a vertical tail in the case of engine loss. Top-mounted nacelles for low sonic boom and reduced ground noise signature as well as wing tip rudder/winglet devices were studied. The focus in 2014 was on lateral-directional control using a rich array of control surfaces: canards, an array of wing trailing edge control surfaces and spoilers. The vehicle was built with a modular vertical tail that could be reduced to a no vertical tail configuration. In 2015 the focus was again on wing tip devices for directional control and on directional thrust vectoring. Improvements were sought in 2016, moving from electric ducted fans to jet engines, studying different options for a three-surface configuration and nacelle placement, plus moving leading edge flaps and a retractable landing gear.

The two-quarter limit on the capstone airplane design course at the UW presents a major challenge regarding the completion of development of UAVs as complex and innovative as the one the UW program strives to develop. Over many years of capstone airplane design at the UW research UAVs were completed and flight tested. The tailless long-range supersonic challenge tackled in 2013-2016 added complexity and difficulty.

While from the educational perspective all educational goals were achieved and the students involved completed the design of cutting-edge new configurations, construction in a number of cases was not fully completed. The 2013 UAV was not completed. The 2014 and 2015 UAVs were completed, with the 2014 UAV taxi-tested and the 2015 UAV (now used to train capstone design students in systems and testing of UAVs) currently being prepared for flight. The 2016 UAV was about 80% completed. Lessons from the 2013-2016 years were used to improve the program to meet the 20-week schedule constraint while developing cutting-edge innovative complex UAVs.

Education

The number of seniors at the University of Washington's William E. Boeing Department of Aeronautics and Astronautics pursuing capstone airplane design and benefiting from our program, is by year, as follows:

2013 - 40

2014 - 34

2015 - 35

2016 - 25

That is, 134 students at the undergraduate level designed, analyzed, built, and ground tested airplanes that are among the most advanced and difficult pursued today. In addition, one student completed an impressive masters thesis on the subject of tailless supersonic long-range configurations. The work has been published in:

Langston, S, Nelson, C.P., and Livne, E., "Low-Speed Stability and Control of a Reduced Scale Long-Range Supersonic Configuration with Reduced-Size or No Vertical Tail", AIAA Paper 2016-1036, AIAA SciTech2016 Conference, San Diego, CA January 2016.

Integrated Research/Education
University Aircraft Design Program Development
Phase II Final Report

31 December 2016

Prepared For

Dr. Eli Livne
Boeing Endowed Professor of Aeronautics & Astronautics
Adjunct Professor, Department of Mechanical Engineering
University of Washington
Seattle, WA

Submitted By

Dr. John Valasek
Vehicle Systems & Control Laboratory
Aerospace Engineering Department
Texas A&M University, College Station, TX

1. EXECUTIVE SUMMARY

Phase II of the Air Force Research Laboratory's Integrated Research/Education University Aircraft Design Program Development project sought to demonstrate the results from Phase I, which were to investigate public domain information and practices with regards to a senior capstone design project of a tailless supersonic flight vehicle and to introduce systems engineering topics and methods into the aerospace engineering curriculum.

2. RESEARCH PROCESS

In pursuit of the stated objective—that is, demonstrating controllable flight of a supersonic-type airframe without use of vertical stabilizers, an appropriate research plan is described and discussed. As a high level summary, this process can be divided into interlinked tasks. First, an alternative actuator capable of providing yaw control authority must be identified. Based on this selection, development of a flight model for a supersonic-type airframe is necessary to enable simulation. This simulation capability allows for synthesis and testing of control laws that allow controllable tailless flight. Once evaluated in simulation, these control laws can then be demonstrated in flight.

2.1   Actuator Selection

Our starting point in working towards the stated objective is to identify, in the absence of traditional vertical stabilizer control surfaces, alternative actuator options capable of providing the yaw control authority required for controllable flight. Due to fixed-wing aerospace stability and control fundamentals, a vehicle without sufficient or properly placed vertical stabilizer surface area will intrinsically be unstable about its yaw axis. Instability in and of itself is not necessarily problematic in system design and control. Depending on the degree and nature of the instability, an unstable system can still be operated, either manually or with assistance. Stability augmentation systems (SAS), to illustrate, are now commonplace in the aerospace industry, allowing, amongst other things, for the safe control and operation of vehicles that would otherwise be deemed uncontrollable with an unassisted manual pilot. The implicit requirement in this situation, however, is that the vehicle must provide adequate control authority to overcome the instability. This is relevant when considering a tailless vehicle because removal of the vertical tails not only destabilizes the vehicle, but it also removes the vertical tail control surfaces. In this condition and without further modification, the vehicle simply does not have yaw control authority to overcome the resulting instability. For this reason, an alternative actuator must be identified in the absence of a vertical stabilizer.

Alternative actuator options for achieving yaw control authority include thrust vectoring, twin-engine asymmetric thrust control, "rudderons", or an otherwise asymmetric spoiler configuration, to name a few. Thrust vectoring is the process in which the direction of engine

thrust is controllable to some degree. If we define 2D thrust vectoring as an instance in which the direction of thrust from a single engine is controllable with two degrees of freedom, a single 2DOF thrust vectoring engine is capable of providing both pitch and yaw control authority. A twin-engine configuration, with each engine capable of 2DOF thrust vectoring, provides pitch, yaw, and roll control authority--3D thrust vectoring. Some degree of yaw control authority can also be achieved with asymmetric thrust control in the case of a twin-engine configuration. This alone, however, is unlikely to be preferable to thrust vectoring, especially in the case of a supersonic-type airframe, simply because it only provides 1DOF of limited additional control authority. The required additional control authority can also be achieved using "rudderons", aerodynamic control surfaces capable of providing both roll and yaw control authority. These typically take the form of outboard split ailerons that can act as both traditional ailerons, providing roll control, and asymmetric air brakes, providing yaw control. "Rudderons" have been successfully demonstrated on various fixed-wing vehicles and are an actuator of choice for any flying wing vehicle configuration. Yaw authority could similarly be achieved with asymmetric spoiler actuation in general, though this is typically not seen.

Given the supersonic airframe requirement and the goal of demonstrating tailless control on an RC model vehicle, 3D thrust vectoring was selected for further evaluation and testing in this work. Asymmetric aerodynamic spoiler configurations, though likely capable of providing adequate yaw control authority, particularly in the case of rudderons, were deemed too mechanically complex for the desired scale of RC vehicle intended for implementation. These solutions would have necessitated a vehicle that would have exceeded budgetary constraints in the form of either requiring a large COTS RC airframe or a smaller custom-built airframe. The decision to focus on 3D thrust vectoring over asymmetric thrust control was additionally driven by RC vehicle scale and cost. Thrust vectoring is a feature now frequently provided on even relatively low-cost electric COTS RC airframes. For the scale implicitly bounded by budgetary constraints, however, these vehicles typically use a single ducted fan, which rules out asymmetric thrust control.

2.2 Modeling (Flight testing of thrust vectoring, Wind tunnel testing, CFD,

Recalling the described high level process, a flight model must be developed for an airframe with the selected yaw control actuation method to enable simulation and later control synthesis. The methods used in generating this model, however, notably have to exclude online or offline system identification from flight testing due to the fact that the vehicle will be uncontrollable for a manual RC pilot without its vertical stabilizers. Alternate methods must therefore be used. The process outlined here involves first evaluating the performance of the implemented thrust vectoring system and then using both wind tunnel testing and computational fluid dynamics (CFD) simulation to generate appropriate flight models.

The first step in this process is to evaluate the performance of 3D thrust vectoring as implemented on a selected airframe with its standard vertical stabilizers and control surfaces. Thrust vectoring control authority can first be done qualitatively by manually flying the RC vehicle in three configurations: first, with both thrust vectoring and rudder control enabled; second, with rudder control enabled and thrust vectoring disabled; and third, with thrust vectoring enabled and rudder control disabled. The first configuration is used to set a benchmark performance for the stock vehicle. The second configuration is used to allow for qualitative comparison with the benchmark, evaluating the impact of the additional control authority provided by the thrust vectoring. Finally, the third configuration is used to assess 3D thrust vectoring control authority coupled with aileron roll authority in the presence of passive yaw axis stabilization. Essentially, this configuration is a simple way to determine if the vehicle is controllable when the only yaw axis control authority is provided by thrust vectoring but assisted by the passive stabilization of the vertical tails. If controllable flight is not achievable with thrust vectoring when assisted by passive vertical stabilizers, additional yaw control authority will be required before the vertical tails can feasibly be removed. Follow-up quantitative analysis can be performed by repeating these three configurations for a fixed set of maneuvers and logging relevant vehicle states.

Assuming the above testing deems the implemented thrust vectoring to be plausibly capable of providing the required control authority in the absence of vertical tail control surfaces, further development of a flight model for the vehicle without its vertical stabilizers can proceed. Because, as mentioned, the vehicle cannot be manually piloted in this condition, online and offline system identification methods are not available as options here. The preferred alternative options are based on CFD simulation and/or wind tunnel testing. By performing a series of tests involving different combinations of angle of attack and sideslip, fundamental fixed-wing vehicle stability coefficients can be derived and in turn converted into the state matrix for a linear model of the vehicle at a specific flight condition. Repeating these $\alpha - \beta$ sweeps for several different thrust vectoring actuator positions can furthermore determine the thrust vectoring contribution to the input matrix of the linear model.

For verification and validation purposes, the safest approach here is to first perform this wind tunnel / CFD testing for the stock airframe with its vertical tails. By doing so, flight models can be generated, simulated, and then compared with data collected on manually piloted flights. Once it has been demonstrated that an accurate flight model can be generated for the vehicle *with* its vertical stabilizers, the process can be repeated to generate models for the vehicle *without* its vertical tails. The motivation here is driven by the fact that the vehicle cannot be manually flown without its vertical tails. That is, the model cannot be validated until after a controller is implemented. First generating and validating a model for the stock airframe would provide additional confidence in the subsequent modeling of the modified tailless airframe.

3. CONTROL DESIGN

3.1 Flight Control Problem

The flight control problem seeks to develop and implement algorithms to close the loop between sensor measurements and control inputs to obtain a good-flying aircraft that is able to accomplish its mission. A "good-flying" aircraft is judged by relevant performance metrics and systems such as the Cooper-Harper flying qualities rating scale. This is equivalent to stating that the closed-loop dynamics have the desired properties (e.g. damping and natural frequencies). The generic flight control problem can be described with the following high-level block diagram, which shows a tracking controller structure with actuator dynamics, disturbances, and noisy sensor measurements.
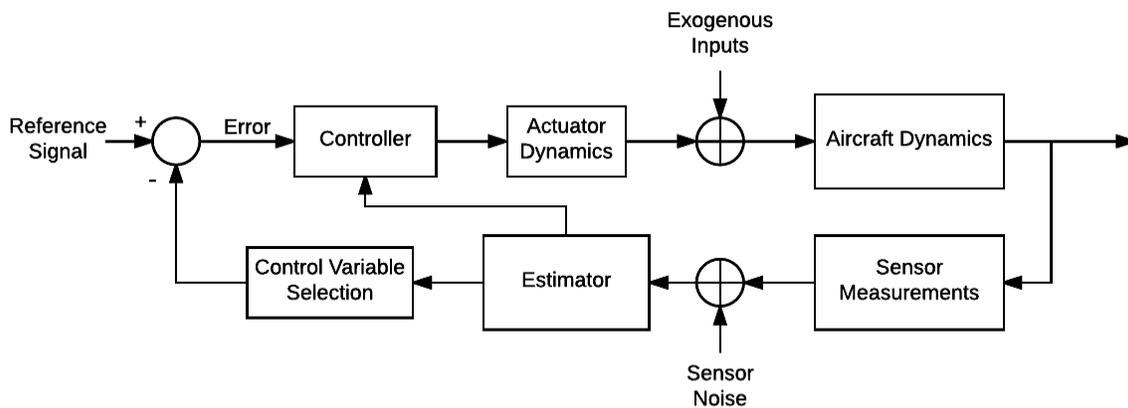
The objective is the design of the controller (and, if applicable, the state estimator) to obtain the desired tracking/regulation performance in the presence of noisy and incomplete measurements and exogenous disturbances.

3.2 Nonlinear Aircraft Dynamics

Aircraft dynamics can be represented as the first-order state-space system shown below,

$$\dot{x} = f(x, u),$$
$$y = h(x, u),$$

where $x \in R^n$ is the state vector, $u \in R^m$ is the control vector, and $y \in R^p$ is the measurement vector. The functions f and h are nonlinear functions of the state and controls. A rigid aircraft has twelve degrees-of-freedom: six translational and six rotational. The translational equations of motion are of the form

$$m(\dot{V} + \omega \times V) = F_A + F_p,$$

where m is the aircraft mass, V is the body-axis translational velocity vector, ω is the angular velocity vector, F_A are the aerodynamic forces, and F_P are the propulsive forces. The translational position is then obtained by transforming the body-axis velocity vector into the inertial coordinate system and integrating. Similarly, the rotational equations of motion are of the form

$$\dot{I} + \omega \times I\omega = L_A + L_P,$$

where I is the inertia tensor, L_A are the aerodynamic moments, and L_P are the propulsive moments. The attitude dynamics are another set of first-order equations dependent upon the choice of attitude parameterization used, e.g. Euler angles or quaternions.

Traditionally, the aerodynamics forces and moments are modeled using a coefficient build up method, where the forces and moments are represented as nondimensional coefficients multiplied against the dynamic pressure ($\bar{q} = \frac{1}{2}\rho V^2$) and appropriate reference geometry. For example, the lift force can be modeled as

$$L = C_L \bar{q} S = (C_{L_1} + C_{L_\alpha}\alpha + C_{L_{\dot{\alpha}}}\dot{\alpha} + C_{L_q}\frac{q\bar{c}}{2V_T} + C_{L_{\delta_E}}\delta_E)\bar{q}S.$$

The terms in the above example such as C_{L_α} are nondimensional stability derivatives. This method of parametrizing the aerodynamic effects is valid for both linear and nonlinear models; nonlinear models can add nonlinear terms or make the stability derivatives functions of relevant variables. Determination of these coefficients is an important part of the modeling process, discussed above.

For conventional aircraft with an xz plane of symmetry flying at near zero bank angle, the equations of motion can be separated into two sets, the longitudinal axis and the lateral/directional (lat/d) axes. The longitudinal states are, in the stability axis system, the forward velocity u, angle-of-attack α, body-axis pitch rate q, and pitch attitude angle θ. Standard longitudinal control effectors are throttle δ_T and elevator δ_E. For the lat/d axes, the stability axis state variables are the sideslip angle β, body-axis roll rate p, body-axis yaw rate r, bank angle ϕ, and heading angle ψ. The standard lat/d control effectors are the ailerons δ_A and rudder δ_R.

3.3   Linearized Aircraft Dynamics

Certain state and control combinations result in equilibrium points of the equations of motion: $f(x_1, u_1) = 0$. These are called trim conditions. Jacobian linearization results in a linear state-space model

$$\dot{x} = Ax + Bu,$$

$$y = Cx + Du,$$

that describes the locally linear dynamics of the aircraft and is suitable for linear control design methods. Here, the matrix A is referred to as the state matrix, the matrix B is the control distribution matrix, the matrix C is the output matrix, and the matrix D is the carry-through or feedforward matrix. The elements of the A and B matrices derive from the dimensional stability derivatives. The pair (A, B) determines the controllability of the linear system, while the pair (C, A) determines the observability of the system states from the outputs.

This linearized form of the dynamics is amenable for both Multi-Input, Multi-Ouput (MIMO) and Single-Input, Single-Output (SISO) design techniques; for the latter, the transfer function matrix can be obtained as

$$H(s) = C(sI - A)^{-1}B + D.$$

A common approach to the flight control problem is to linearize the nonlinear equations of motion about several trim conditions, design linear controllers at each condition (usually parameterized by dynamic pressure, or a Mach/altitude combination), and then switch the resulting gains as the aircraft flies between different flight conditions. This approach is termed gain scheduling.

3.4 Performance Metrics

The performance requirements for flight control laws derive from military flying qualities requirements. These requirements are specified in MIL-STD-1797 and the older MIL-F-8785. MIL-STD-1797 in particular features updated requirements for highly-augmented airplanes such as the Control Anticipation Parameter for the longitudinal axis, but is limited distribution and accordingly difficult to use in an academic environment. As a result, MIL-F-8785C is used as a source of requirements. For a supersonic tailless aircraft, the requirements for a Class IV aircraft in a Category A flight phase are used.

3.5 Challenges of Tailless Aircraft

The lack of vertical tails results in a directionally unstable configuration (i.e., the static directional stability derivative C_{n_β} is negative; this effect is also referred to as weathercock stability). As a result, any perturbation in sideslip angle results in near immediate departure from controlled flight. For supersonic configurations, this is extremely difficult to recover from. For this reason, most current fighter aircraft are directionally stable, although some, like the F-16, become directionally unstable at high angle-of-attack. The control laws on these aircraft almost uniformly feature alpha-limiters to prevent such departures from occurring. This improves the aircraft stability, but reduces the performance envelope and the ability to point the aircraft nose.

Since conventional configurations feature side area aft of the aerodynamic center via tails and, on some aircraft, fillets and ventral fins, maintaining the directional stability of the aircraft is a combination of inherent stability provided by these devices and directional control surfaces such as rudders. For less stable aircraft, actuators with high bandwidth are required for stabilization; the F-16 rudder integrated servoactuator for example has position limits of ±30 deg and rate limits of 120 deg/s. A tailless aircraft, in contrast, effectively uses only control effectors to maintain stability, further increasing these requirements, and necessitating active control.

3.6　Flight Control Systems

Flight control systems can be broadly separated into Stability Augmentation Systems (SAS), Command Augmentation Systems (CAS), and autopilots. The first two systems assist the pilot in flying the aircraft, whereas autopilots are autonomous systems that manage the aircraft guidance, navigation, and control to relieve the pilot's workload. This section focuses on SAS and CAS systems.

3.7　Stability Augmentation Systems

The simplest form of stabilization is a SAS. Here, feedback is used to modify the aircraft damping to obtain the desired flying qualities. For the lateral/directional axes, a yaw damper is a commonly used SAS. Traditionally, a yaw damper consists of yaw rate feedback to generate rudder commands to oppose yaw rate perturbations, and a washout filter to prevent the system from fighting pilot commands for coordinated turns by only passing through transient signals. A SAS is typically a limited authority system, i.e. the SAS only can use a certain percentage of the control authority available, the rest being allocated to the pilot's direct control.
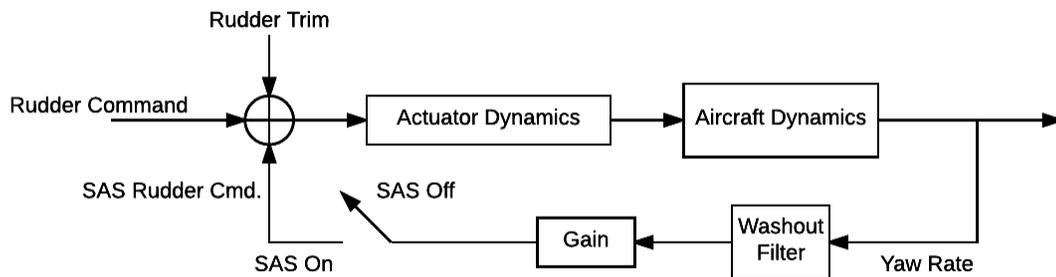
3.8　Command Augmentation Systems

While yaw dampers have been used successfully for many years, the advent of more powerful avionics and increased performance envelopes for modern fighter aircraft has resulted in most aircraft now using a CAS, where the pilot uses stick input to command a controlled variable, and the flight control laws use this as the reference command. Unlike a SAS, a CAS is a full-authority system where the flight control system has complete control over the actuators. A CAS

has the benefit of reducing pilot workload, allowing the pilot to focus less on flying the aircraft and more on accomplishing mission objectives. A block diagram for a generic CAS is shown below.
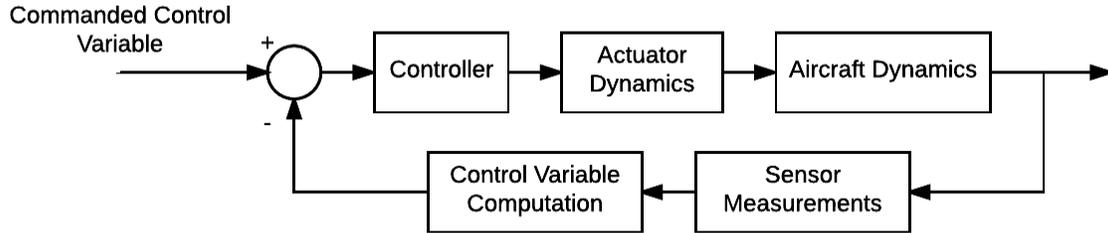
A simple CAS for the directional axis could regulate sideslip angle or stability axis yaw rate. A more complex multivariable flight control approach is proposed in WL-TR-96-3099, which defines a yaw control variable of

$$NCV = (1 - F_{LAT})NCV_{lo\bar{q}} + F_{LAT}NCV_{hi\bar{q}}$$

where

$$NCV_{lo\bar{q}} = r$$

and

$$NCV_{hi\bar{q}} = (r_s + K_\beta \beta + trim) - \frac{g}{V}cos\theta sin\phi$$

with

$$trim = \frac{\omega_{ny}}{s} \times (K_{ny}\,ny - NCV_{hi\bar{q}})\text{for zero pedal input.}$$

Here, the variable F_{LAT} is the control transition function which controls the transition between low and high dynamic pressure controlled variables. Various control methodologies can be used to achieve this; WL-TR-96-3099 considers eigenstructure assignment, dynamic inversion, and μ-synthesis.

3.9   Implementation

Currently, implementation of flight control systems occurs almost uniformly on digital computers. Digital computers operate in discrete time, and use measurements converted to digital values from analog signals via a sample and hold mechanism. Other issues are present, such as computation time, aliasing, etc. Most control systems, however, are designed in the continuous domain and are then discretized during implementation, with the approach of sampling as fast as possible to approximate continuous-time. Direct digital design, by contrast, begins with accounting for the effects of sampling and computation in the synthesis procedure.

Implementation issues such as actuator saturation, integrator windup, and system nonlinearities such as pilot-induced oscillations are well-known and additionally require addressing during the flight control system design.

4.   CONTROL TECHNIQUES

Several control methodologies are well-suited for the flight control problem. This section discusses a subset of commonly used synthesis techniques.

4.1   Classical Successive Loop Closure

Classical SISO techniques for flight control generally revolve around the practice of successive loop closure, wherein a series of SISO control loops are closed. As an example, consider a bank angle command and hold system as shown in the block diagram below. First, a controller is designed based on the transfer function from the aileron to the roll rate in order to obtain the desired roll damping, closing the first loop. Next, the output of the closed loop aileron to roll rate transfer function is integrated to obtain the bank angle, and a controller is designed to minimize the error between the desired and actual bank angle. (Note that the block diagram shows the implementation form, where the needed states are obtained from the aircraft measurement outputs.) These controllers range from simple gains to dynamic compensating elements such as lead-lag compensators depending on the vehicle dynamics.
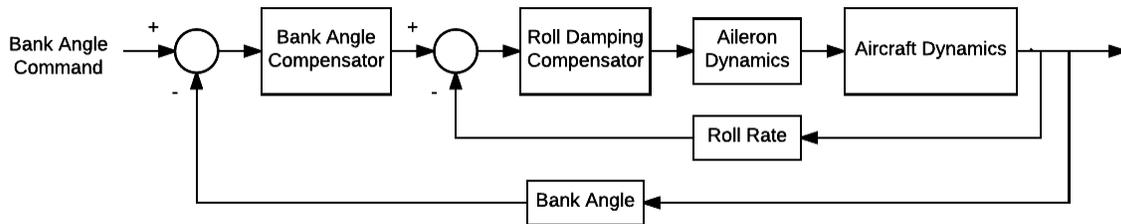
Successive loop closure is a tedious design method that requires multiple design iterations and loop shaping compared to MIMO control methods. Despite the drawbacks, loop closure and classical methods are the design methods most commonly taught at the undergraduate level, where control theory courses almost entirely consist of classical methods. Direct digital design using these methods is possible via the z-transform and z-plane root locus.

4.2   Linear Quadratic Regulator

Perhaps the simplest multi-input, multi-output (MIMO) control algorithm is the Linear Quadratic Regulator (LQR), which uses a quadratic cost function to penalize state and control deviations. The cost function for the infinite horizon LQR problem is shown below.

$$J = \frac{1}{2}\int_0^\infty (x^T Q x + u^T R u)dt$$

Here, the matrices $Q \geq 0$ and $R > 0$ are chosen by the designer to obtain the desired performance. This performance index can be minimized in several ways to obtain the optimal control

$$u = -Kx = -R^{-1}B^T Px,$$

where P is the solution to the continuous algebraic Riccati equation,

$$A^T P + PA - PBR^{-1}B^T P + Q = 0.$$

LQR assumes full-state feedback, that is, all vehicle states can be measured. LQR can be used as the basis for several different structures, with modifications including the addition of a proportional-integral filter for better steady-state performance, non-zero setpoint tracking, control rate weighting for minimization of pilot-induced oscillations, and Command Generator Tracking/Servo LQR for tracking arbitrary reference inputs.

4.3   Sampled Data Regulator

For direct digital design, a modified form of the LQR controller called the *sampled data regulator* (SDR) is available. This modifies the LQR performance index to include a zero-order hold on the control value at each sampling time. This performance index is

$$J = \frac{1}{2}x^T(N)Sx(N) + \frac{1}{2}\sum_{k=0}^{N-1}(x^T(k)\hat{Q}x(k) + 2x^T(k)Mu(k) + u^T(k)\hat{R}u(k))$$

where the control input is then $u(t) = u(kT)$ for $t \in [kT, (k+1)T)$. The optimal control is then

$$u(k) = -(\hat{R} + \Gamma^T P(k+1)\Gamma)^{-1}(M^T + \Gamma^T P(k+1)\Phi)x(k),$$

subject to the discrete Riccati equation

$$P(k) = \hat{Q} + \Phi^T P(k+1)\Phi - (M + \Phi^T P(k+1)\Gamma)(\hat{R} + \Gamma^T P(k+1)\Gamma)^{-1}(M^T + \Gamma^T P(k+1)\Phi)$$

with $P(N) = S$. The system (Φ, Γ) is the discrete-time version of (A, B) using a zero-order hold.

4.4   Linear Quadratic Gaussian

The Linear Quadratic Gaussian (LQG) controller extends the LQR framework to systems with output feedback and stochastic disturbances and measurement noise modeled as Gaussian random variables. The linear dynamics can be represented as

$$\dot{x} = Ax + Bu + v$$
$$y = Cx + w,$$

where v and w are Gaussian with covariances V and W. The infinite horizon performance index is then

$$J = E\left[\int_0^\infty (x^T Q x + u^T R u) dt\right],$$

where E is the expected value. The optimal control is a combination of an LQR controller using the estimated state as feedback and a Kalman filter estimator:

$$\dot{\hat{x}} = A\hat{x} + Bu + L(y - C\hat{x}), \hat{x}(0) = E[x(0)]$$
$$u = -K\hat{x}$$

where the Kalman gain $L = PC^T W^{-1}$ results from the solution of the Linear Quadratic Estimator (LQE) problem and the feedback gain K results from the solution of the LQR problem. The LQE problem is a dual of the LQR problem. As a result of the separation principle, the optimal estimator and optimal controller may be designed separately.

A sampled-data approach to LQG can also be used by using a continuous-discrete Kalman filter and the SDR technique.

5.   PRELIMINARY RESULTS

Having fully described the planned course of action regarding demonstration of controllable flight of a tailless supersonic-type air vehicle, results obtained to-date are summarized and discussed below. These are divided into subsections focused on vehicle hardware selection, wind tunnel testing, and flight testing.

5.1   Hardware Selection

An objective of this work is to not only, as outlined in the described research plan, develop and demonstrate a controller capable of performing the specified task in simulation, but to ultimately additionally demonstrate and assess its performance in flight. Specifically, the intent is to demonstrate this on an RC fixed-wing vehicle in both manual and autonomous flight. In keeping with the "supersonic" context of the work, the RC airframes selected for testing were a scale F-15C and a scale F/A-18E, both produced by MotionRC, a commercial RC vehicle manufacturer. Both airframes have an approximately 38-inch wingspan, a takeoff weight of 6.75 pounds, and are each propelled by a single 90mm ducted fan powered by a single 6S 5000mAh LiPo battery. The F/A-18E, unlike the F-15C, additionally includes 3D twin-engine thrust vectoring. With the selected batteries, each vehicle has a nominal maximum flight time of 3-4 minutes.

The decision to include both airframes in our testing was driven by two primary factors. First, preliminary planning allowed for the possibility of designing and implementing a custom thrust vectoring solution. For this reason, an airframe was required that did not come pre-equipped with thrust vectoring. An additional airframe pre-equipped with thrust-vectoring, however, was desirable in that it could both serve as inspiration in designing and implementing a custom thrust vectoring solution, and serve as a backup demonstrator option if complications arose in modifying the other airframe. The second factor, similarly, was simply overall redundancy. If complications arose with one airframe, work could resume with the remaining airframe type. Potential airframe complications identified in a risk analysis included unfavorable flight characteristics even before removal of the vertical stabilizers, insufficient flight time for performing adequate data collection flights, insufficient payload mass or volume requirements for the added avionics and instruments, etc.

The selected COTS RC airframes do not come pre-equipped with flight computers; as such, additional hardware must be installed and configured to allow for tasks such as data logging, SAS-assisted manual flight, and autonomous waypoint navigation flight. The primary hardware selected for this purpose was the 3DR Pixhawk flight computer. The Pixhawk is a small (2.0" x 3.2" x 0.6", 1.3 oz) hobby-grade flight computer that features a 168 MHz 32-bit STM32F427 Cortex processor, a 32 bit STM32F103 failsafe co-processor, 256 KB of RAM, and 2 MB of flash memory. Avionic instrumentation includes an ST Micro L3GD20H 16 bit gyroscope, an Invensense MPU 6000 3-axis accelerometer / gyroscope, an ST Micro LSM303D 14 bit accelerometer / magnetometer, and a MEAS MS5611 barometer. A variety of RC-centric interfaces are included, as well as I2C and USB interfaces. The flight computer supports the popular and open-source ArduPlane flight software and accompanying Mission Planner ground control station software. This specific flight computer was selected primarily due to prior familiarity with both its hardware and software.

5.2   Wind Tunnel Tests

Two wind tunnel tests were conducted in the Oran W. Nicks Low Speed Wind Tunnel (LSWT) at Texas A&M University in order to obtain stability derivatives for modeling the aircraft dynamics. The LSWT has a 7' x 10' test section that is capable of dynamic pressures up to 100 psf. The first test was conducted on the scale F-15 model in two configurations: with and without vertical tails. Due to recent construction at the LSWT, the test was forced to use the tunnel's external balance and turntable mount, which allowed for only sideslip angle sweeps. Accordingly, the aircraft was positioned at a fixed angle-of-attack and several sideslip angle sweeps were conducted with different control surface deflections. Runs were conducted over several dynamic pressures representative of different flight conditions.

The second test was conducted on the scale F/A-18E model, again in two configurations: with and without vertical tails. For this test, the aircraft was mounted on the High Attitude Robotic Sting (HARS) system. The HARS system allows for both angle-of-attack and sideslip angle sweeps to be conducted. The F/A-18E is shown in the standard configuration on the HARS system below.


The first two test runs for each configuration were sweeps over the angle-of-attack and sideslip angle at 0 psf to obtain static tare data. Additionally, a sweep over dynamic pressure was run to determine if the results were Mach-independent, which was found not to be the case. After these initial runs, angle-of-attack sweeps (-5:1:15 deg) and sideslip angle sweeps (-4:2:20 deg) were run at two dynamic pressures representative of flight conditions (10 psf and 15 psf) with different control surface deflection and vectoring conditions in order to determine control power derivatives. Dynamic derivatives (e.g. C_{Lq}, etc.) were not obtained.

Prior to conducting tests of the thrust vectoring effectiveness of the aircraft, a brief lull in the test activities occurred in order to inspect the model. It was found that the front fuselage of the model had plastically deformed during the testing; this was largely due to reduced structural stiffness due to changes in the structure made to accommodate the HARS balance mount. Aluminum tape was used to reinforce the structure, as seen in the photo of the F/A-18E in the tailless configuration below. Since the forward fuselage structural integrity was degraded, the alpha sweep was changed to remove the negative AOA values so that structural loads would be in compression and not tension to reduce the chance of structural failure.

After the standard configuration runs were completed, the vertical tails were removed from the aircraft. Unlike the F-15C scale model, whose vertical tails are removable, the F/A-18E scale model has permanently attached verticals. These were cut off with a knife and the result covered with aluminum tape. Due to the structural issues described in the above section, the modified alpha sweep was used for all future runs. Otherwise, the same runs were completed for the tailless configuration as for the standard configuration.

Example coefficient data from the F-15 test is shown below, which plots the yawing moment coefficient versus the sideslip angle. The data show a linear trend within approximately 15 degrees of positive/negative sideslip, with a positive trend, indicating that the static directional stability derivative C_{n_β} is positive, which indicates stability.
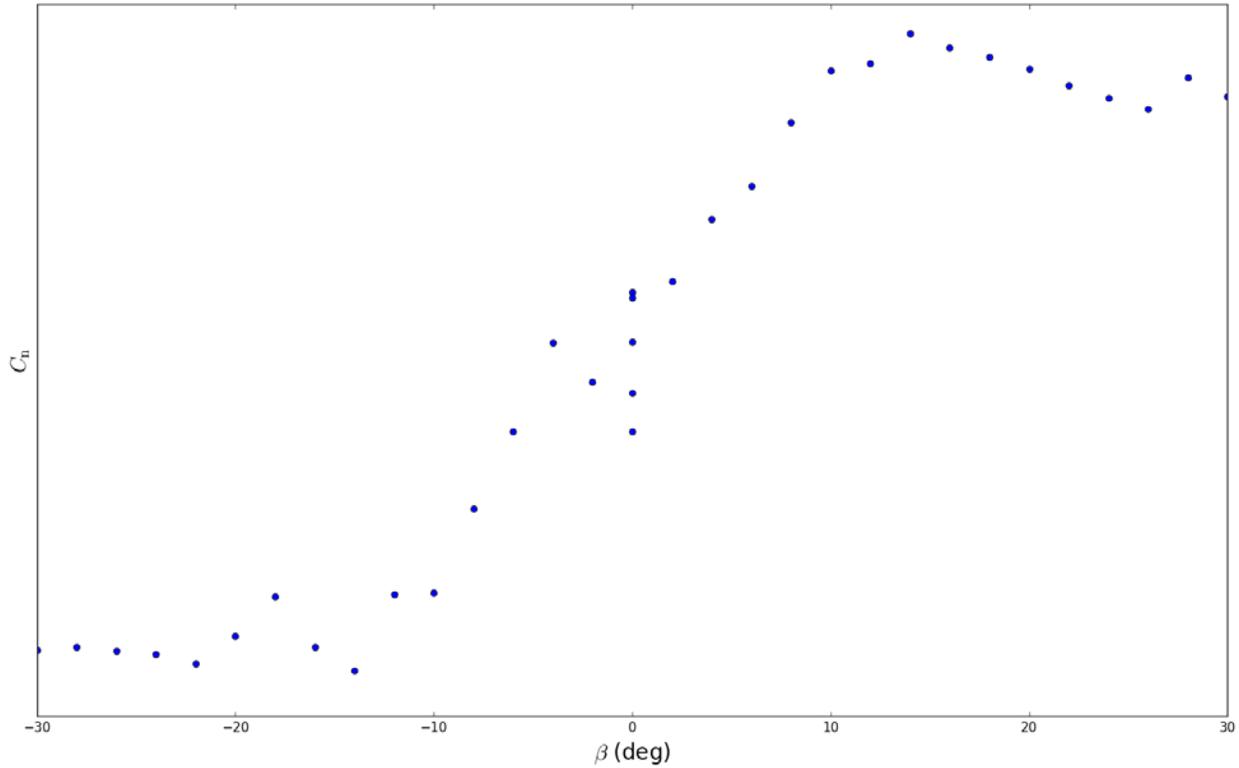
The stabilizing effect of $C_{n_\beta} > 0$ is shown in the figure below.
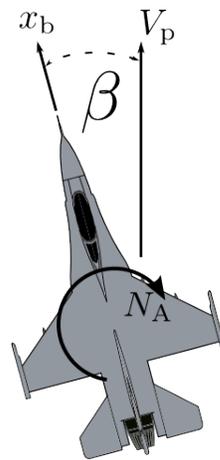
Positive yawing moment N_A tends to reduce sideslip angle β.
Consequently, the **static directional stability derivative**, C_{n_β}, is positive for static stability.

Data for a tailless configuration of the F-15 is shown below. Note that for the F-15, later runs were made assuming symmetric aerodynamics, so only -30:2:4 values of sideslip are shown. Observe the linear trend and the negative slope, indicating that without the tails $C_{n_\beta} < 0$. This is an expected result, as the vertical tails are required for directional stability.
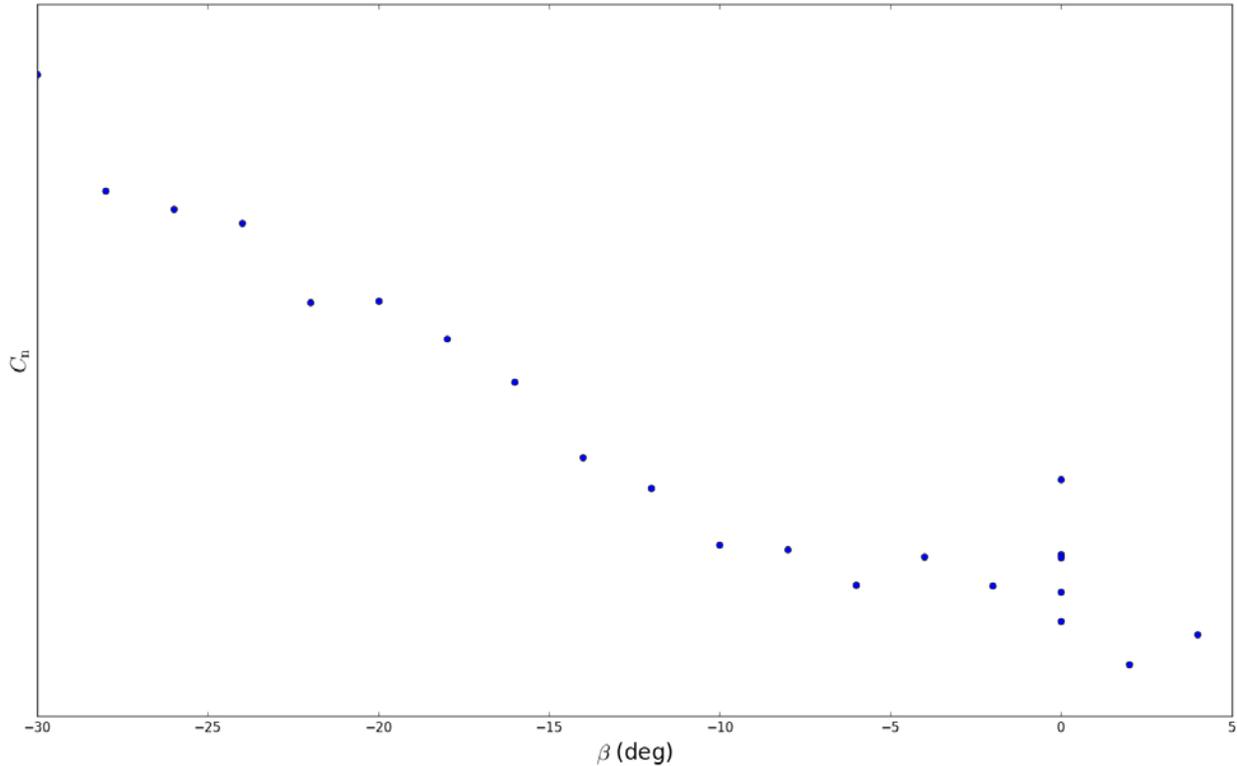
6.   FLIGHT TESTING

A series of flight tests were conducted at the Texas A&M University RELLIS Campus with both the F-15C and F/A-18E vehicles. All testing to-date has been performed as manually piloted flights with inclusion of the vertical stabilizers and control surfaces. The primary purpose of these flights has been to qualify and build operational familiarity with the respective airframes. A secondary purpose has been to qualitatively assess and compare the handling characteristics of each vehicle. Qualitatively speaking, the F/A-18E has been found to be the more stable airframe of the two, although its flight time is slightly less than that of the F-15C. Specifically, the F/A-18E has a flight time of approximately 2-3 minutes, versus 3-4 minutes for the F-15C.

Due to the more benign handling qualities, additional flight testing with a Pixhawk flight computer installed on the F/A-18E has focused on identifying controller gains for the vehicle with its vertical tails. The vehicle, with vertical tails, has been flown in a SAS-assisted manually piloted configuration and is in a state in which it could be flown autonomously if required. These gain-tuning and verification flights have been performed to both qualify the installation and configuration of the flight computer and instrumentation, and to build additional experience in operating the vehicle in a SAS-assisted flight mode. Finally, these flights have tested and verified the Pixhawk flight data collection capabilities, enabling ongoing and future flights in which

vehicle performance can be quantitatively assessed with and without the vertical stabilizer control surfaces and thrust vectoring enabled.

7. SUMMARY

Phase II of this program saw the model of the tailless supersonic vehicle developed, wind tunnel tested, and control laws designed. The full flight testing program was cut short due to the end of the contract, but the initial results were promising and merit further investigation. This will allow the full potential of the methods and analysis used to be evaluated, including the specific shortcomings which were identified to cause problems in the academic setting for aircraft design.

Contact Information

Dr. John Valasek
Director, Vehicle Systems & Control Laboratory
Department of Aerospace Engineering
Texas A&M University
3141 TAMU
College Station, TX 77843-3141

(979) 845-1685
        -6051 (FAX)

valasek@tamu.edu

INTEGRATED RESEARCH/EDUCATION UNIVERSITY AIRCRAFT DESIGN PROGRAM DEVELOPMENT

1 JAN 2015 – 31 MAY 2016

UNIVERSITY OF COLORADO BOULDER FINAL REPORT

PI: RYAN STARKEY
SUBAWARD NO.: 757226
PRIME AWARD NO.: 9550-14-1-0027/AFOSR
SPONSOR: UNIVERSITY OF WASHINGTON

i

Contents

iv

1. Executive Summary

The Integrated Research/Education University Aircraft Design Program Development at the University of Colorado Boulder was successful in integrating meaningful hardware design, manufacturing, and testing into both undergraduate and graduate design courses. Specifically, the project achieved the following:

1. Completed design, manufacturing, software-in-the-loop testing, and hardware-in-the-loop testing of the Engineering Test Unit low-cost, high speed unmanned aircraft with complete traceability to the supersonic variant.

2. Completed planning for a series of high-speed taxi tests (up to 120 knots) for execution at Front Range Airport, Colorado.

3. Captured and documented lessons learned for manufacturing of the final, Mach 1.4 capable UAV.

4. Completed an extensive redesign of our thrust vectoring nozzle facility and implemented a full test program.

5. Integrated a wide spectrum of students; including two senior design teams (9 students each), three graduate project teams (12-14 students each), a MS thesis student, a PhD student, 7 independent study students, and 2 Jr-level students.

This final report documents the work completed under this project primarily under the AY2015-2016 GoJett graduate design project. Other projects, including the REAPER senior project, while not explicitly fully funded by this project, benefited synergistically from the design tools, growing student expertise, and facilities developed under the integrated research and education program.

2. <u>INTRODUCTION</u>

The "Integrated Research/Education University Aircraft Design Program Development" project at the University of Colorado Boulder has three primary tasks:
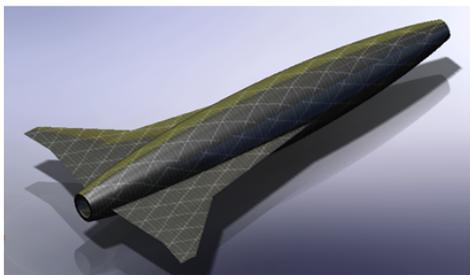
1. Research into low cost, high speed UAV development.
2. Research into tailless supersonic vehicle design and operation.
3. Educate undergraduate and graduate students on the process of aircraft design while performing tasks 1 and 2.

All three tasks started at the University of Colorado around 2010 under the guidance of the PI and were augmented and refocused by the start of the AFOSR effort in 2014. The guiding mission statement and project progress are given in the following images.
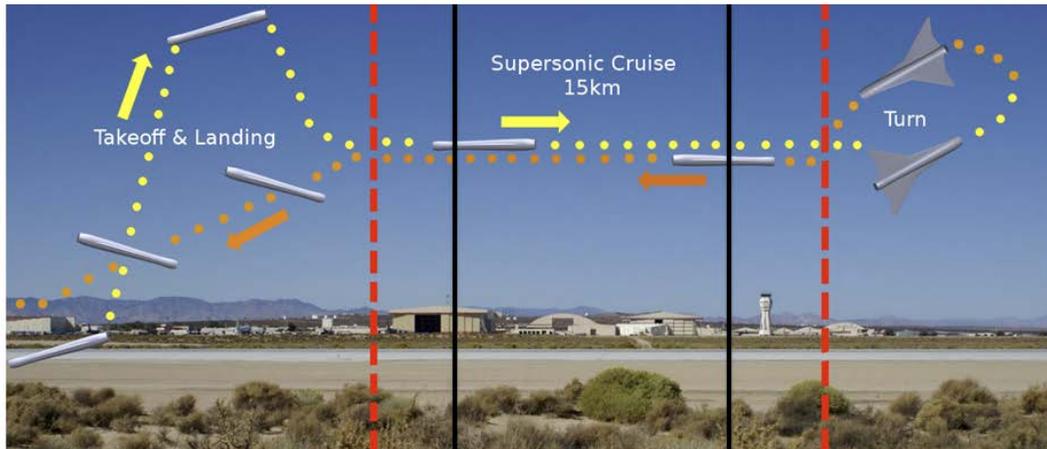

3

FAI Mission Profile


Takeoff & Landing
Supersonic Cruise 15km
Turn

- Two 15 km cruise sections in opposite directions
- 5 km approach sections
- Maintain level flight (± 100 m) through speed run and approaches
- 2000 m ceiling above cruise course at all times

GOJETT – AIAA-2012-5531

8

Design Solutions

- Custom afterburning turbojet engine with 200+ lbf thrust
- Fluidic injection thrust vectoring system for control
- Sears-Haack fuselage design with pitot inlet
- Cranked delta wing with elevons
- Tailless design with modular vertical stabilizer
- Redundant flight computers
- Lift-off at 60 m/s

GOJETT – AIAA-2012-5531

4
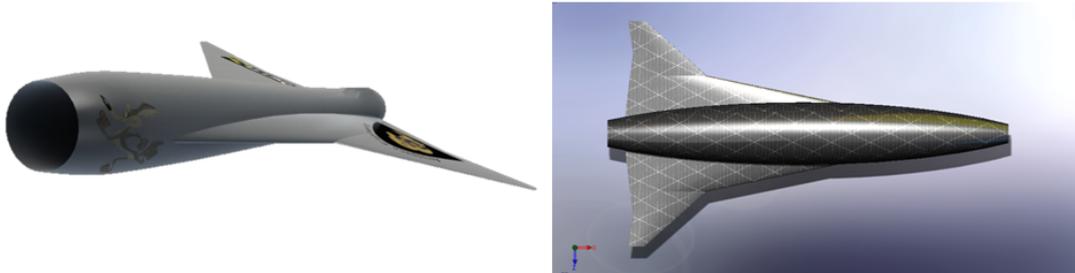
Subsonic Flight

- From Fall 2013 on, focus has been on preparing the ETU for a subsonic flight test
  - Typically 10-12 team members
  - Divided up into 7-10 subsystems
- Emphasis on finalizing subsystem designs, testing and validating, manufacturing and integrating

Engineering Test Unit

- 6' long x 5' wide (50 lb dry weight)
- All ETU components have been designed and manufactured for supersonic flight even though this aircraft will only go to Mach 0.4 (NM UAS FTC limitation for now).
- Future flights will require restricted airspace
- University ITAR concerns

GoJett Graduate Project

11

Proprietary, Ryan P. Starkey, CU/Starkey Aerospace Corporation

ETU System History Spring 2012

Systems:	CAD:	Propulsion:	Landing gear:	Telecom:
Mass budget	Initial design	AMT 450	Oleo shock	Haigh-Farr Antenna
Volume budget	of everything	Afterburner	strut system	RF transceiver
		Variable nozzle		Ground station (BS)
		Inlet diffuser		

Controls:
Elevon + rudder
design

Structures:
Composite skin
+ Aluminum
bulkheads
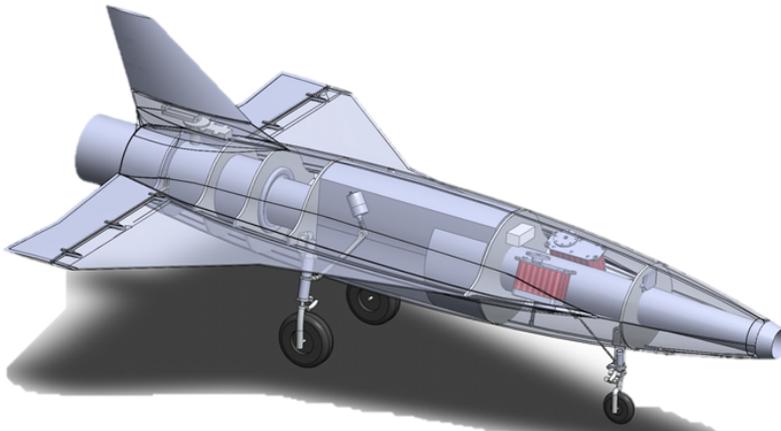
12

ETU System History Fall 2013

Systems:	CAD:	Propulsion: redesign	Landing gear: redesign
Update budgets	New bulkheads, engine	JetCat P200-SX	Century Jet Models Inc.
Analyze fuel	Higher fidelity	Shapiro analysis	pneumatic system
requirements		Remove afterburner	
		Remove variable	
		nozzle	

Telecom:
FCU + MCU chosen
Sensor schematic

Power:
Power budget
Voltage requirements
Current requirements

Controls:
Manufacture
testing

Structures: redesign
Spar location
Bulkheads

13

6

ETU System History Spring 2014

Systems Engineering
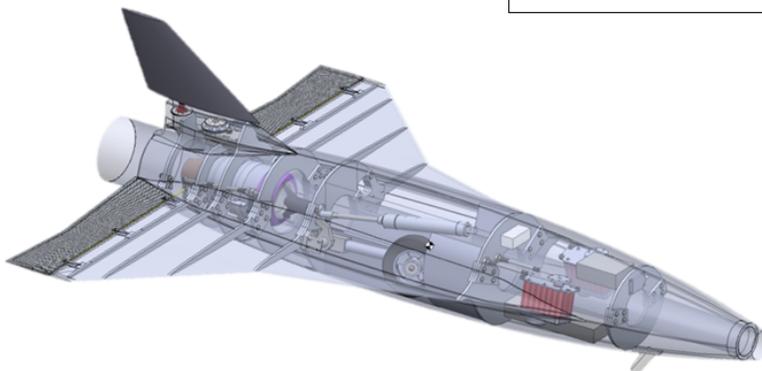
| Systems:
Fuel tank design
Jettechusa | CAD:
New landing gear
Higher fidelity | Propulsion: redesign
Testing
Inlet CFD analysis | Landing gear:
Drop test
Door design | Power:
New PDB
Update
requirements |
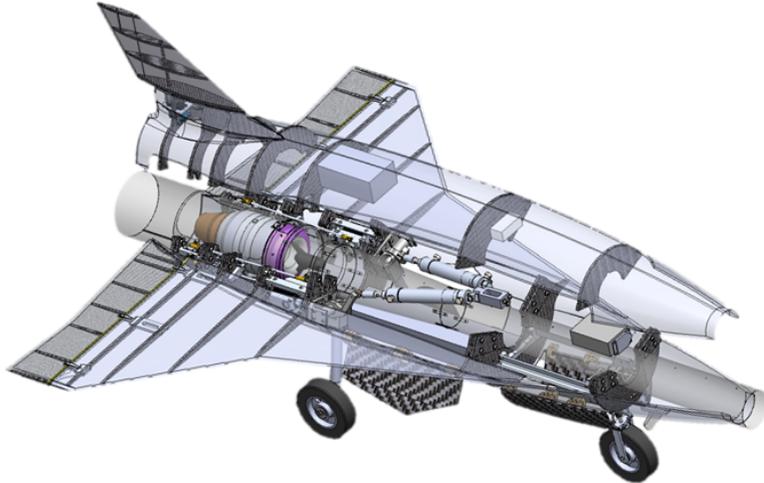
Telecom:
Antenna testing

Controls:
Redesign rudder
manufacture

Structures:
Spar analysis
Tolerance analysis
outsourced

Aerodynamics:
Detailed takeoff analysis

14

Spring 2015

- Reached design freeze on March 23rd
- Pushed into manufacturing and integration
  - GoJett skeleton manufactured and integrated
- Power board redesigned and populated
- Software nearly complete
- Landing gear redesigned (nearly completed...)

- Integration and testing focus
- All remaining parts manufactured
- Power board tested with components
- FPV systems designed, tested, manufactured
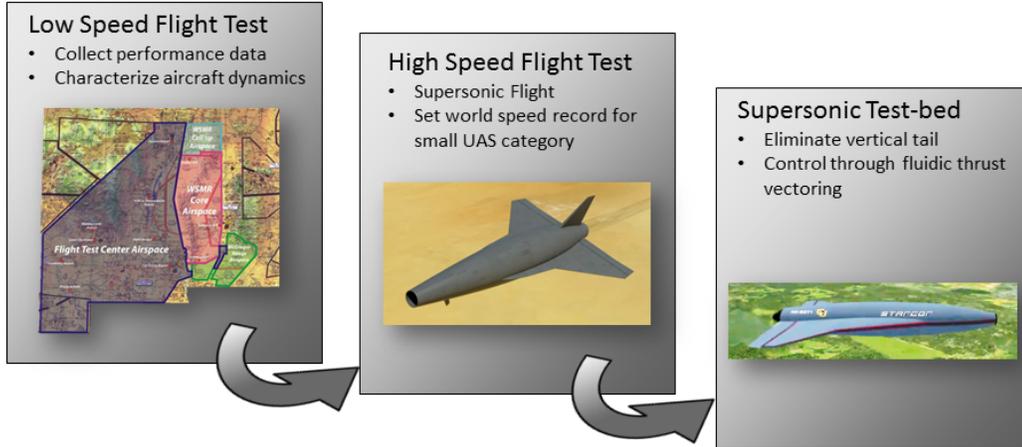- Landing gear redesigned, tested, and integrated
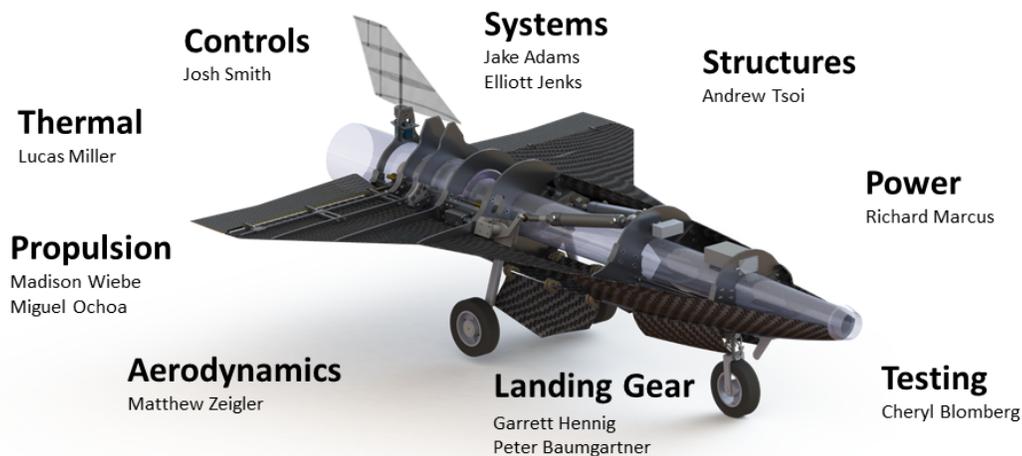

They grow up so fast :')

Systems Engineering

21

8

The Future of GoJett

Low Speed Flight Test
- Collect performance data
- Characterize aircraft dynamics

High Speed Flight Test
- Supersonic Flight
- Set world speed record for small UAS category

Supersonic Test-bed
- Eliminate vertical tail
- Control through fluidic thrust vectoring

System Breakdown

Controls
Josh Smith

Systems
Jake Adams
Elliott Jenks

Structures
Andrew Tsoi

Thermal
Lucas Miller

Power
Richard Marcus

Propulsion
Madison Wiebe
Miguel Ochoa

Aerodynamics
Matthew Zeigler

Landing Gear
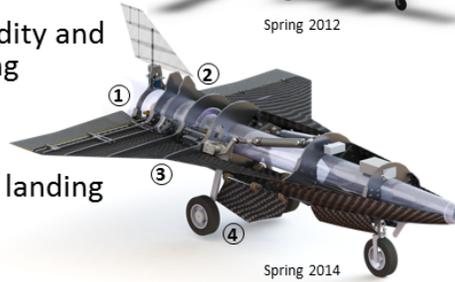Garrett Hennig
Peter Baumgartner
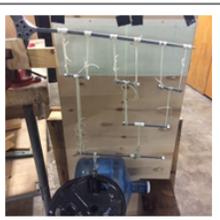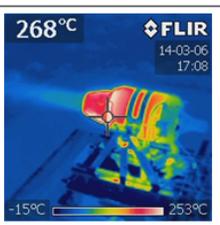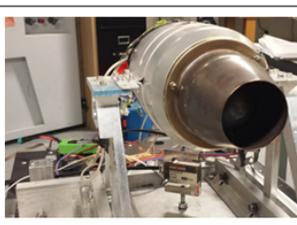
Testing
Cheryl Blomberg

21

9

Finalized Design

1. *JetCat P200-SX* turbojet engine with custom-built inlet provides up to 50 lbs of thrust
2. Aircraft controlled by titanium gear servos for elevons and actuating vertical stabilizer
3. Bulkheads and wing-spars improve rigidity and factory of safety of aerodynamic loading
4. Landing gear design uses pneumatic actuation system to retract and deploy

    LG supports 110 lbs at 128 mph during landing

Spring 2012

① ② ③ ④

Spring 2014

Testing and Validation

Structures Testing
- Wing spar stiffness
- Material comparison
- Failure mode analysis

Landing Gear Testing
- Spin-up drop testing to simulate landing conditions

Thermal Testing

Temperature measurements for
- Engine and exhaust
- Power board
- Battery

268°C ◆FLIR
14-03-06
17:08
-15°C   253°C

Propulsion Testing
- Static engine thrust
- Fuel consumption

Manufacture for Integration

Carbon Fiber Skin

Vertical Tail

Main Gear

Nose Gear

Power Board

Mounting Parts
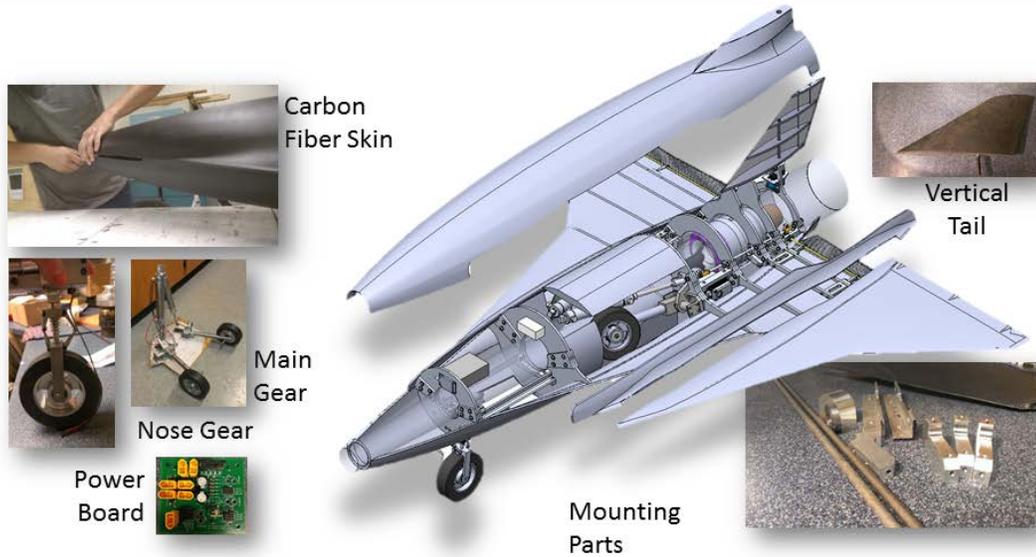
Detailed Design/Validation

268°C FLIR
Propulsion

Aerodynamics

Landing Gear

Control/DAQ

Electronics

Inlet/Ejector

Wind Tunnel Testing at USAFA

Mach 1.32 Testing of Tailless Configuration

Proprietary, Ryan P. Starkey, CU/Starkey Aerospace Corporation
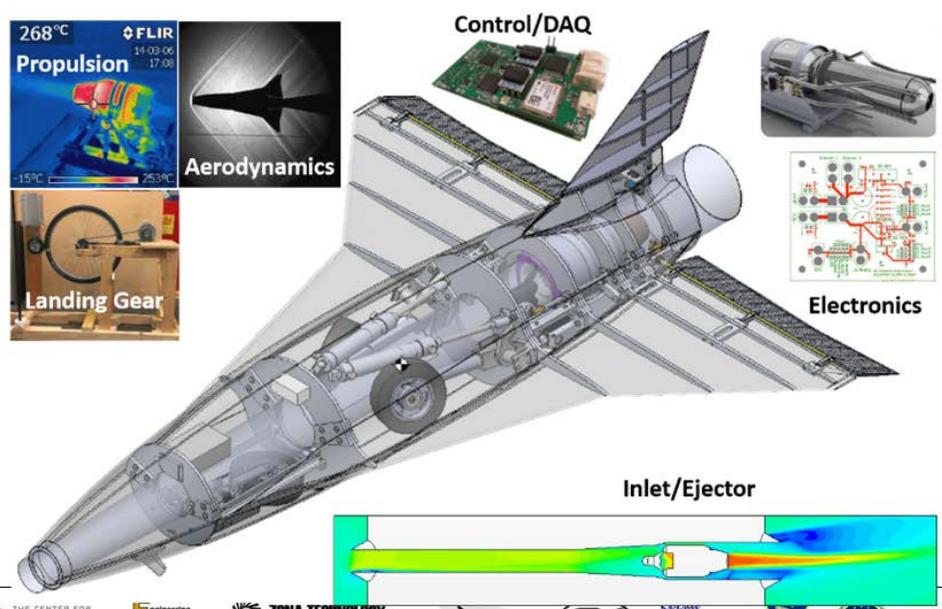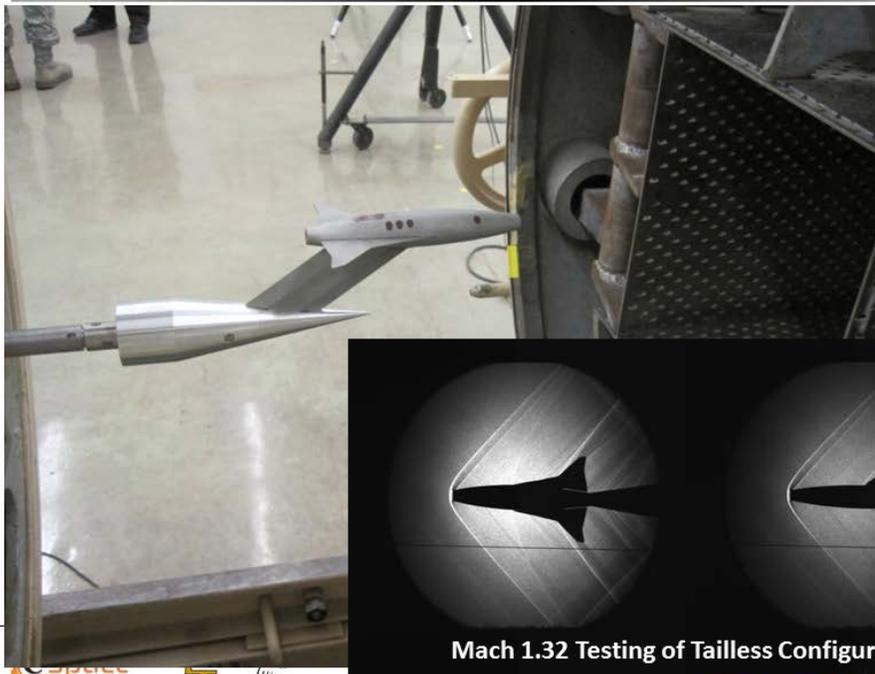
27

USAFA Mach 1.32 Tests
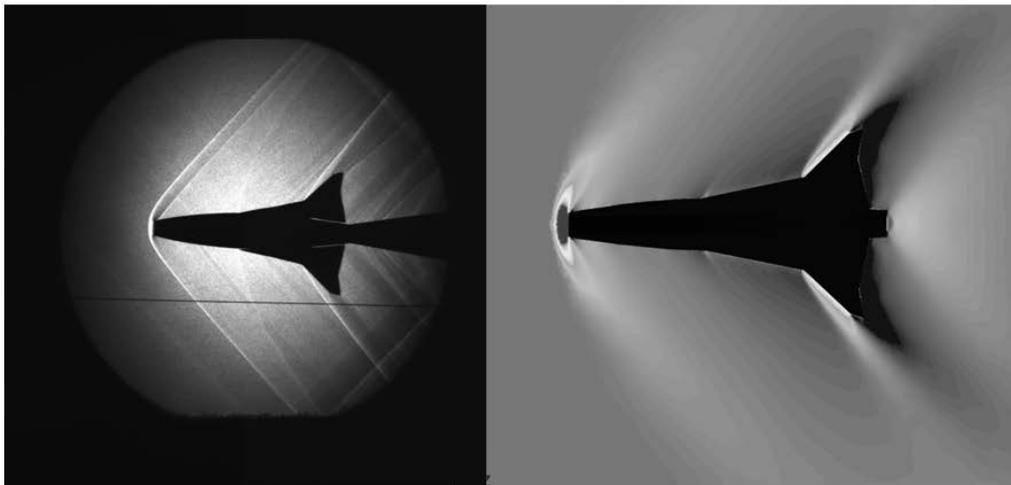
- Double Cranked Arrow wing design
- Sears-Haack analysis used for fuselage design
- Wind tunnel testing at M = 1.32 (USAFA Trisonic Tunnel)
- Extensive computational fluid dynamics (CFD) conducted for validation using ANSYS Fluent and Tecplot

12

Manufacturing Composite Skin

90% of all work went into creating the tool

Special thanks to EBS Carbon for their help and support in building the engineering test unit using their patent pending 3D printed mold technology.

29

Fluidic Thrust Vectoring

NASA Dual Throat Nozzle

- Throat skewing and thrust vectoring
- Similar experiment, but conducted at 20x injection pressures
- Useful validation

CU FTV Nozzle

- Analytical, computational, experimental approach
- On-engine and wind tunnel testing
- Supply and/or engine bleed air
- Adaptable to more test variations
- Wider range of performance criteria to be investigated
- Further design optimization

Image Courtesy of NASA Langley

Main Engine Flow   Injection Site

Thrust Vectoring Nozzle
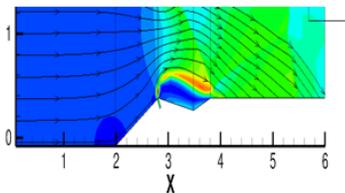
CFD Model for Thrust Vectoring via Fluid Injection

New nozzle configuration under development.

30

13

Concept of Operations

- ETU purpose
- 4 phases
  - Hardware in the loop testing

Phase I. Hardware In The Loop Simulation

Concept of Operations

- ETU purpose
- 4 phases
  - Hardware in the loop testing
  - Taxi operations

Phase II: Taxi Operation – Motion

Concept of Operations

- ETU purpose
- 4 phases
  - Hardware in the loop testing
  - Taxi operations
  - Manually piloted flight

Phase III: Update Autopilot

Concept of Operations

- ETU purpose
- 4 phases
  - Hardware in the loop testing
  - Taxi operations
  - Manually piloted flight
  - Autopilot flight

Phase IV: Autopilot Flight

Fall 2014 Recap
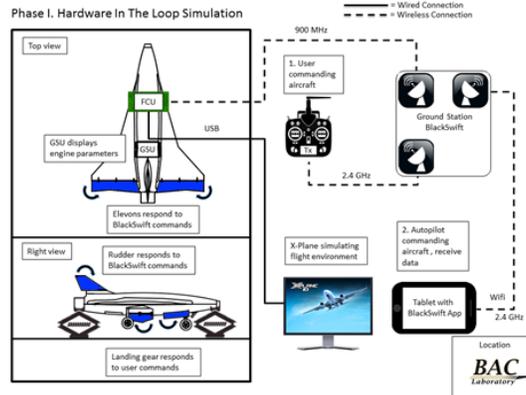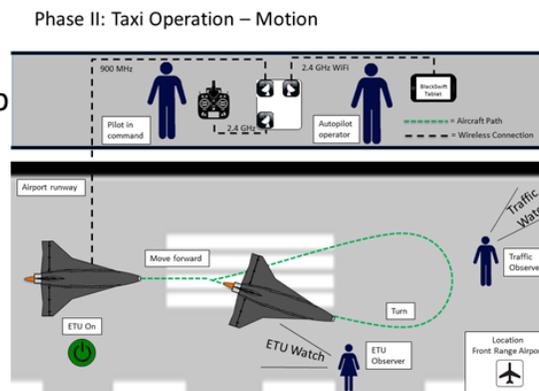
Concept of Operations

- ETU purpose
- 4 phases
- ETU and subsystems requirements flow down

- System: 35
- Propulsion: 12
- Controls: 18
- Landing gear: 14
- Structures: 17
- Thermal: 4
- Electronics: 4
- Software: 20
- Telecom: 17
- **Total: 177**

36

Spring 2015 – Completed CAD

38

16

GoJett Internal CAD
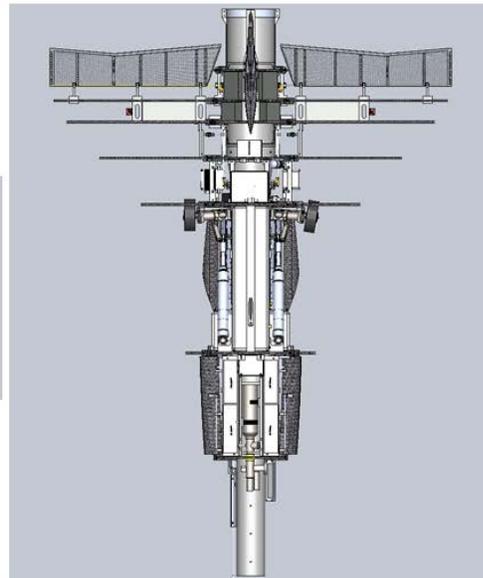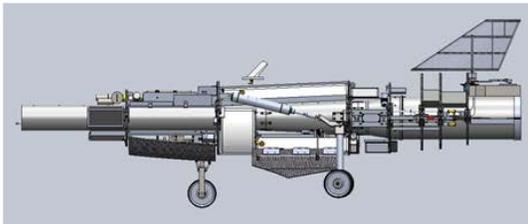
Test Identification

4 ways of verification:
1) Observation
2) Measurement
3) Demonstration
4) Analysis

ETU Examples

Engine/Inlet Thrust Test	-Measures thrust
Nose Gear Drop Test	-Demonstrates 14 CFR part 23 requirements met
Materials Coupon Test	-Finds CF properties to support analysis

17

DISTRIBUTION A: Distribution approved for public release.
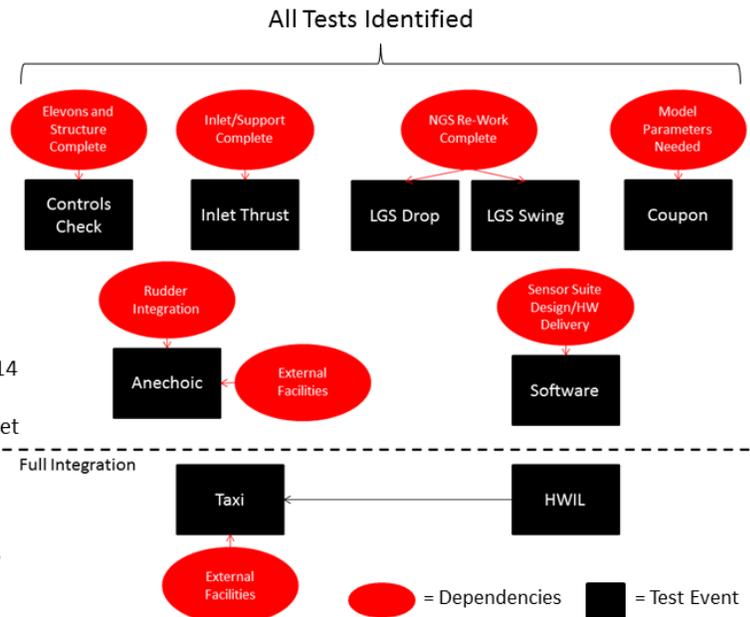
Communication with Front Range Airport

- Email Contact with Bob Lewan, Operations Manager

  BLewan@ftg-airport.com
  303-261-9103

- Has allowed us to come and look at the road
  - Delayed due to weather, time constraints

- Diagrams of Safety and Testing Locations
  - Manila Rd, Watkins, CO

11

12

18
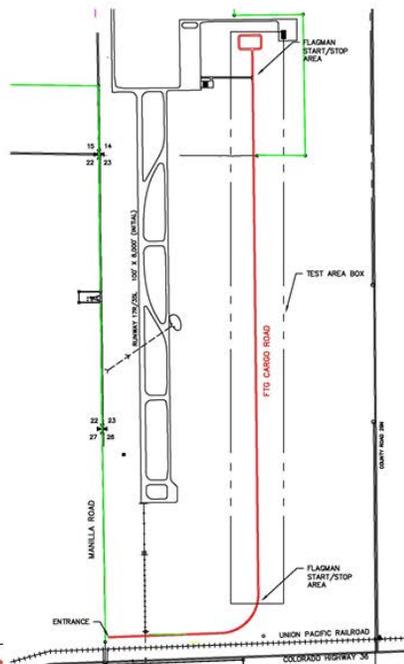
Safety Areas

Primary Safety Area

Secondary Safety Area

13

Testing & Operations

HWIL Test

- Preliminary HWIL Test
- All systems work
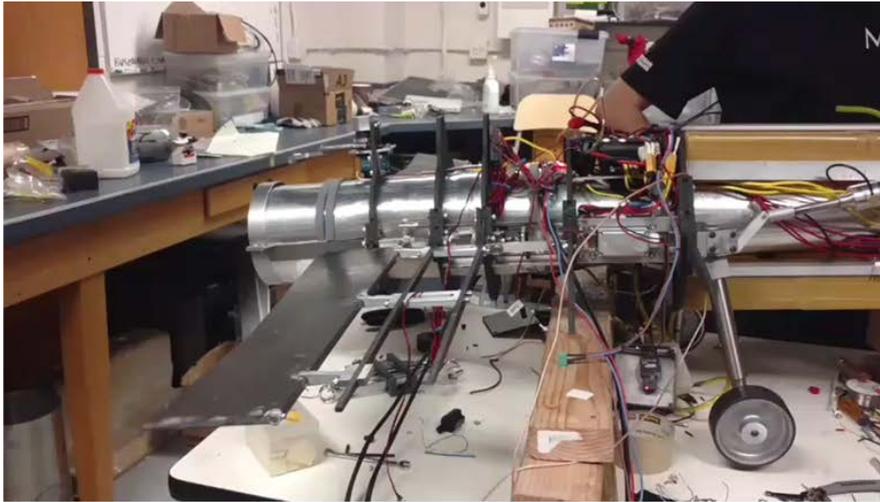
Taxi Testing Plan

- Creation of GoJett ETU Taxi Procedures Document
  - 19 pages of...
    - Test objectives
    - Contact/Emergency Response
    - Set-up diagrams
    - Pre-test, Eve-of, post-test procedures
    - Go/no-go criteria
    - Check-lists
    - Emergency Procedures
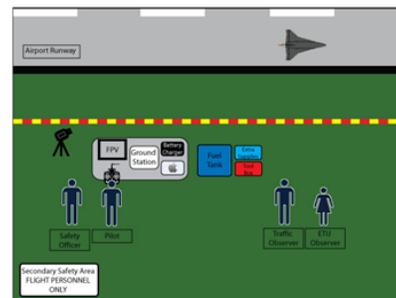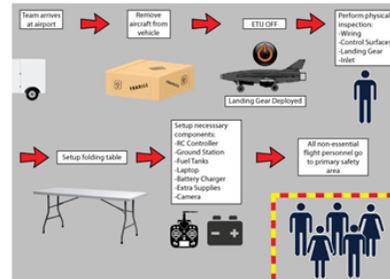
- ETU will only taxi south
- Hill will serve as slowdown section
- Transport vehicle will serve as chase car
- Other personnel will remain north of ETU
- Multiple runs to increase confidence before full speed testing
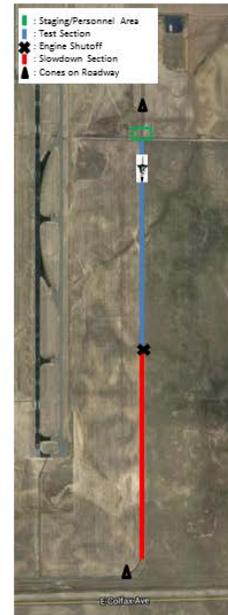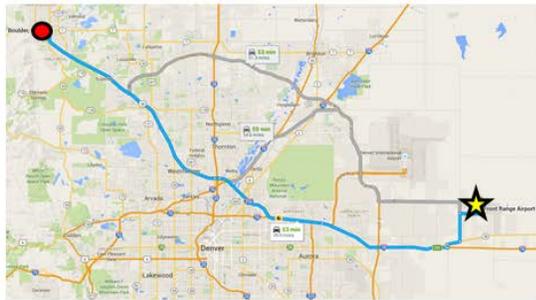
Software

Sensors Suite Definition

Software

Required In-Flight Measurements
- Temperature: Batteries, E-Bays, Engine Burner
- Airspeed, AoA, Side slip angle
- 16x Inlet pressures, 16x Wing pressures
- Wing-tip accelerations
- Elevon/**Rudder** deflection

Added since midterm presentation

Acronyms
ETU = Engineering Test Unit
MCU = Microcontroller Unit
FCU = Flight Computer Unit
ECU = Engine Control Unit
PDB = Power Distribution Board
Ebay = Electronics Bay
DAQ = Data Acquisition
AoA = Angle of Attack

48

CONOPS - Software

Software

Acronyms
AP = Autopilot
SDK = Software Development Kit
SPI = Serial Peripheral Interface
SDIO = Secure Digital Input/Output
EU = Engineering Units

Legend
- GoJett Software
- Provided Software
- Hardware Interface

49

22
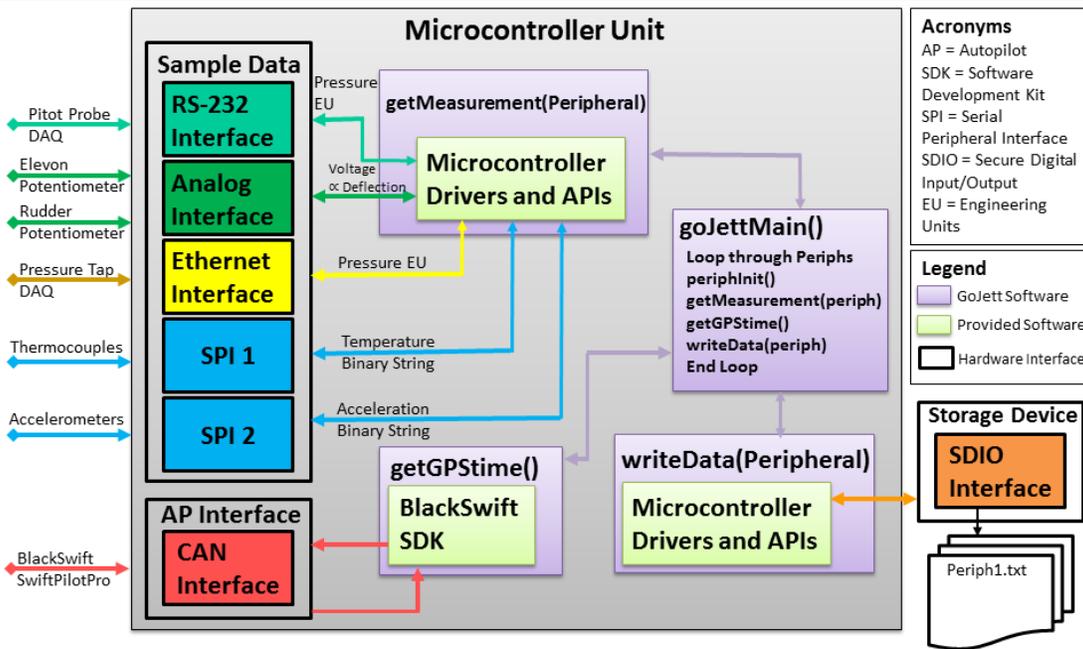
Software

- Accelerometer Calibration
  - Determine link between digital values and acceleration

  Completed: All accelerometers calibrated

- Thermocouple Unit Test
  - Confirm functionality of all thermocouples
  - One thermocouple removed

  Completed: all thermocouples operational

- Potentiometer Test
  - Update code and calibrate

  Completed: All potentiometers calibrated

- Pitot DAQ Test
  - Program pitot DAQ for RS-422
  - Support interface with landing gear controller

  Static Test Completed

62

Communications

23

24
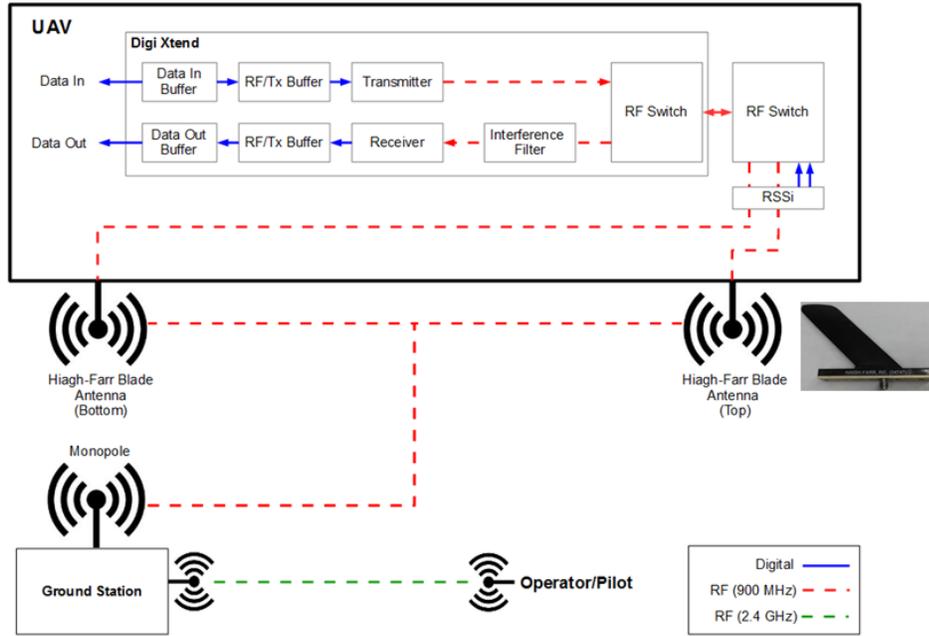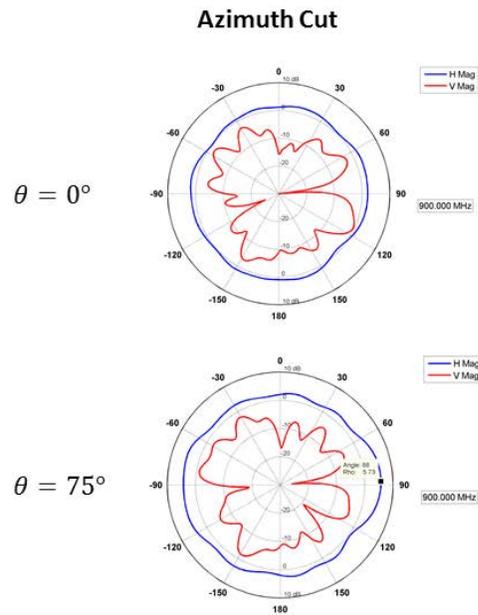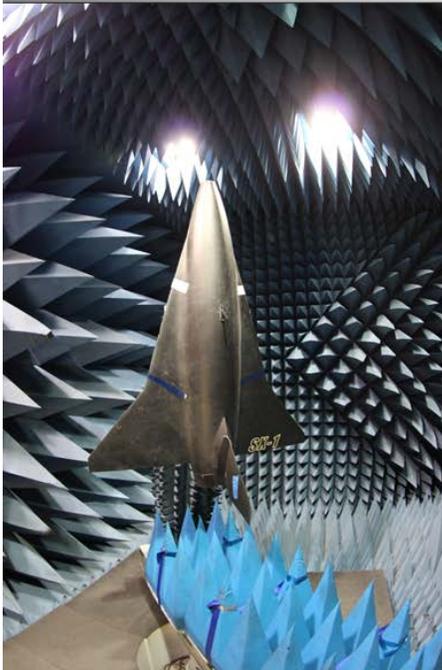
Power

Design Solution

Power

● = ideal diode   ■ = direct battery connection   ■ = fuse

| 20C 4S 5000 mAh | LM2941 LDO 13V 1 A 12-15V 370 mA | KA278R12C LDO 12V 2 A 6-16V 1000 mA | Castle Creations BEC 6V 5 A 4.5-9V 1250 mA |

20C 4S 5000 mAh

2A — LDO — Pitot DAQ

2A — LDO — MCU

DC-DC — A/P

Servo   Servo
HiTec LiPo 4S Servos
6000 mA stall

25C 2S 5000 mAh

KA278R12C LDO
5 V 2 A
3.7-5.5V 100 mA

Servo Servo Servo Servo Servo Servo
6 2S Servos ~6000 mA stall

25C 2S 5000 mAh

2A — LDO — Teensy 3.1

2A — LEDs
6-9V
220 mA

ECU
6.6-9V
4800 mA

Servo
Futaba 4S Servos
6100 mA stall

Board Design

Battery Connections

Ideal Diode Controller

Capacitor (thru hole)

Regulator for Teensy 3.1

Capacitor (thru hole)

Capacitor (surface mount)

MOSFET

Fuse (surface mount)

Fuse (surface mount)

ECU, Teensy 3.1, LED, Rudder Servo, and Auxiliary Servo Connections

Board Design

Heat Sink Outline

Capacitor (thru hole)

Fuse (surface mount)

Regulator for MCU

Regulator for DAQ

Capacitor (surface mount)

Fuse (surface mount)

Capacitor (thru hole)

Capacitor (surface mount)

Capacitor (thru hole)

Elevon Servo Connections

DAQ, MCU, and Autopilot Connections

26

93

Landing Gear

27

Modified System Diagram

LG Door System

Right Door

Left Door

Nose Door

FCU

Sequencer

Retract System

Servo

UP [14]

DN

Compressed Air System

Adjust to 100 psi → [3]

Adjust to 250 psi → [2]

[11]

Servo

DN [12]
UP

800 psi → Bottle Regulator (built in)

3000 psi (max) →

HPA 13ci [1]

Brake System

Brake Valve

Brake Valve

[13]

Left Brake

Right Brake

Legend

—— Pneumatic Line

- - - Electrical Signal

[#] – Bracketed numbers refer to component number as given in the modifications document

101

Propulsion

28

Propulsion

- Custom engine design with afterburner, Variable Area Nozzle / Fluidic Thrust Vectoring
- Expected aircraft thrust to weight ratio > 2 : 1

Compressor Turbine Stator

Inlet

Shaft

Stator Combustor Turbine

Proprietary, Rya

PROJECT FENIX

BIOMITE

DANTE
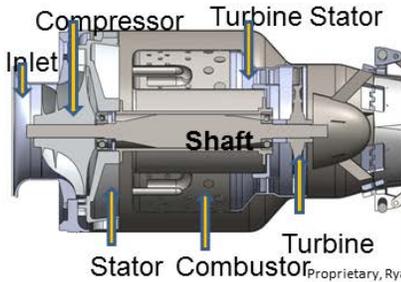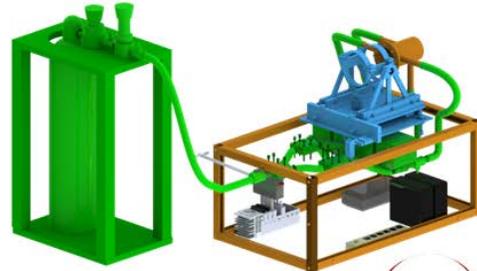
Aerodynamics and Controls

Velocity: Magnitude (m/s)

0.00000   21.231   42.462   63.693   84.923   106.15

140

Velocity: Magnitude (m/s)

0.00000   21.223   42.446   63.670   84.893   106.12
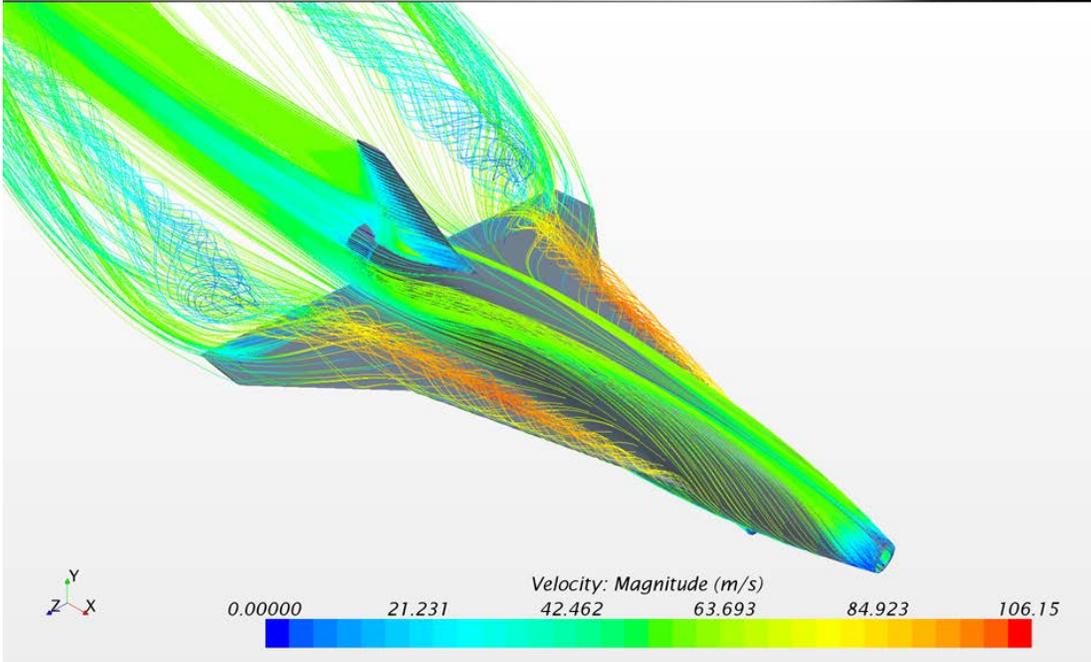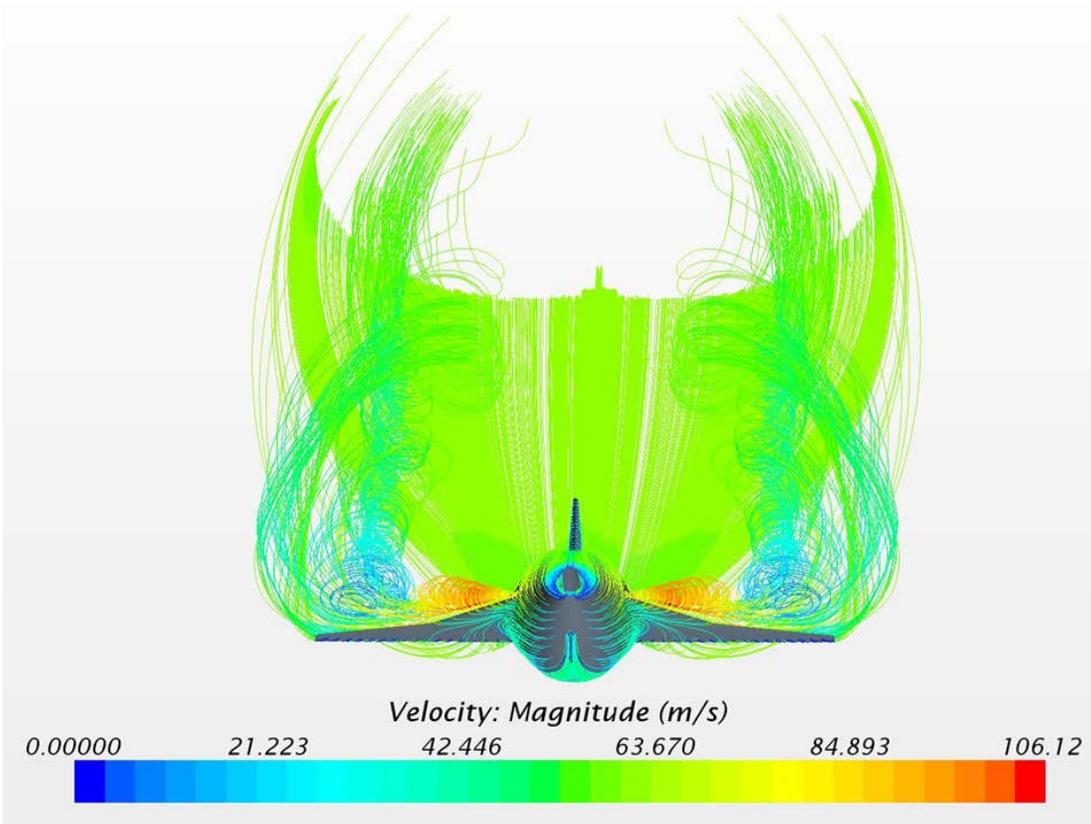
Missile DATCOM results
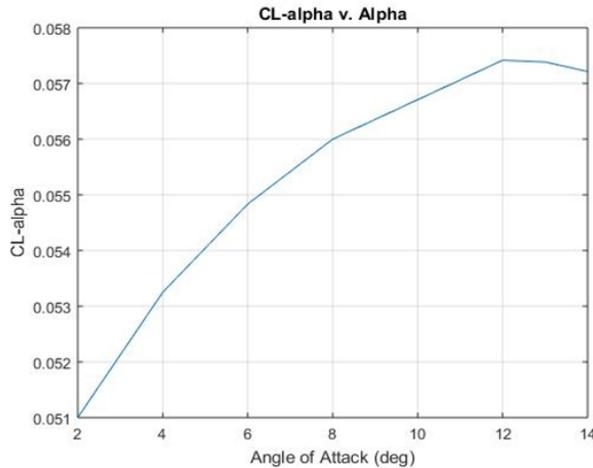
- $C_{L\alpha}$ results

Calculated v. DATCOM results

Method	$CL_\alpha \ (\backslash deg)$
1	0.05
2	0.0637
3	0.0415
4	0.0444
DATCOM	0.0553

72

Combination of Analyses

- Using DATCOM parameters in MATLAB script
- Static Margin calculated using $SM = \bar{x}_{cg} - \bar{x}_{np}$
- Hovers around where we want it
  - 16.38%

76

31

HWIL/Hardware Integration
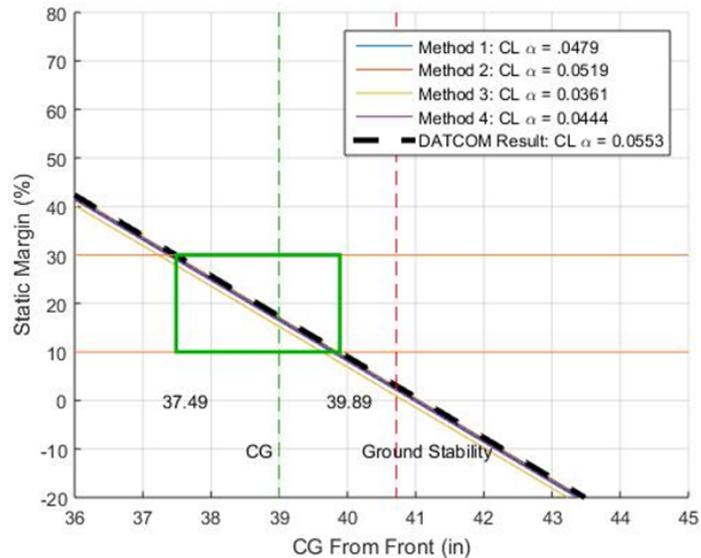
- RC control validated through ground station and autopilot
- Autopilot drives surface, gear and engine controls

FPV
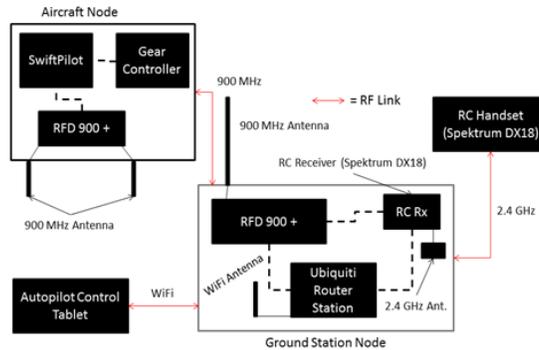
Overview

- Provides live video link over 1280 MHz
- Uses diversity to increase signal reliability
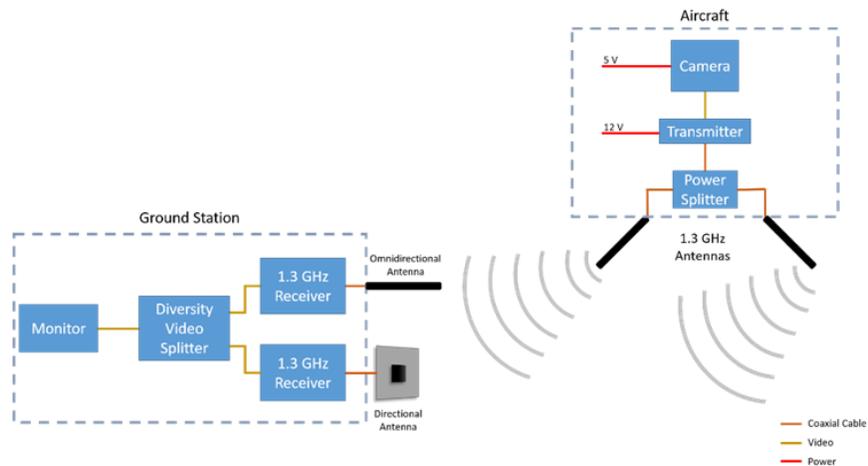
FPV Parts

Ground Equipment   Flight Equipment

33
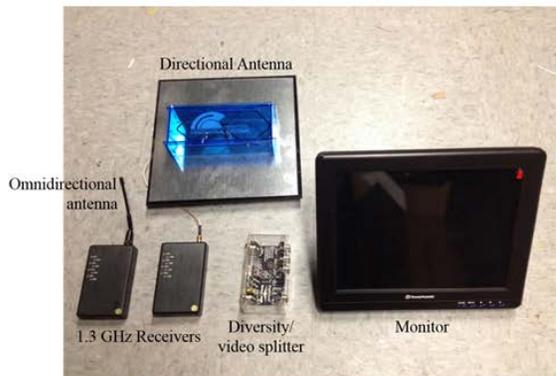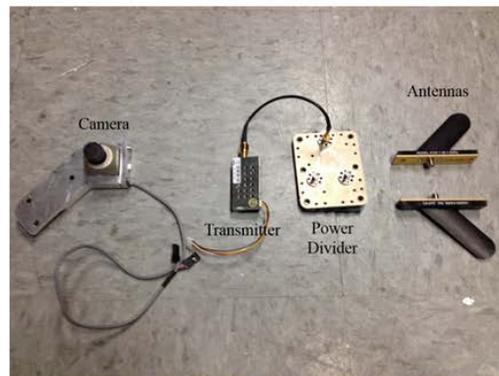
Range Test

- Each antenna was range tested separately
- Aircraft node was driven away from the ground station until signal degraded
- Range meets requirements for taxi and flight testing

Antenna	Observed Range
Dipole	1.2 miles
Biquad	2.5 miles

Completed Ground Station

34

Project Management

Risk Analysis

		Impact				
		Negligible	Minor	Moderate	Significant	Severe
Likelihood	Very Likely	Low Med	Medium	Med Hi	High	High
	Likely	Low	Low Med	Medium	Med Hi	High
	Possible	Low	Low Med	Medium	Med Hi	Med Hi
	Unlikely	Low	Low Med	Low Med	Medium	Med Hi
	Very Unlikely	Low	Low	Low Med	Medium	Medium

Risk Description	Likelihood	Impact	Action	Action Description
Uncertainty in budget (down to roughly $10,000)	Very Unlikely	Severe	Mitigate	• Air Force funding should be understood by the fall semester • Allows time for alternative funding

151

36

3. <u>PROJECT MANAGEMENT</u>

At the end of fall 2015, a schedule was proposed for the spring semester to accomplish taxi testing. A Gantt chart of the proposed schedule is shown below.
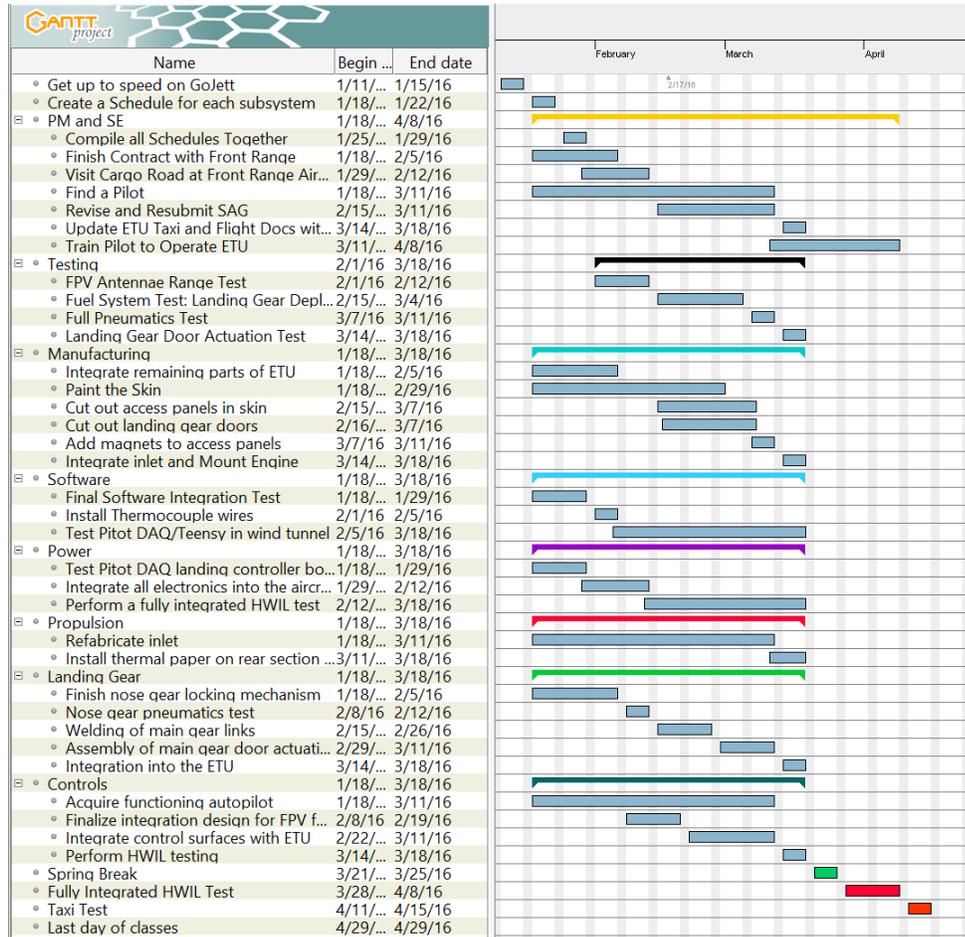
Figure 1: Proposed Spring 2016 Schedule

The proposed schedule was reviewed before creating a new schedule that was used throughout the semester for planning. The updated Gantt chart for the 2016 schedule is shown below.
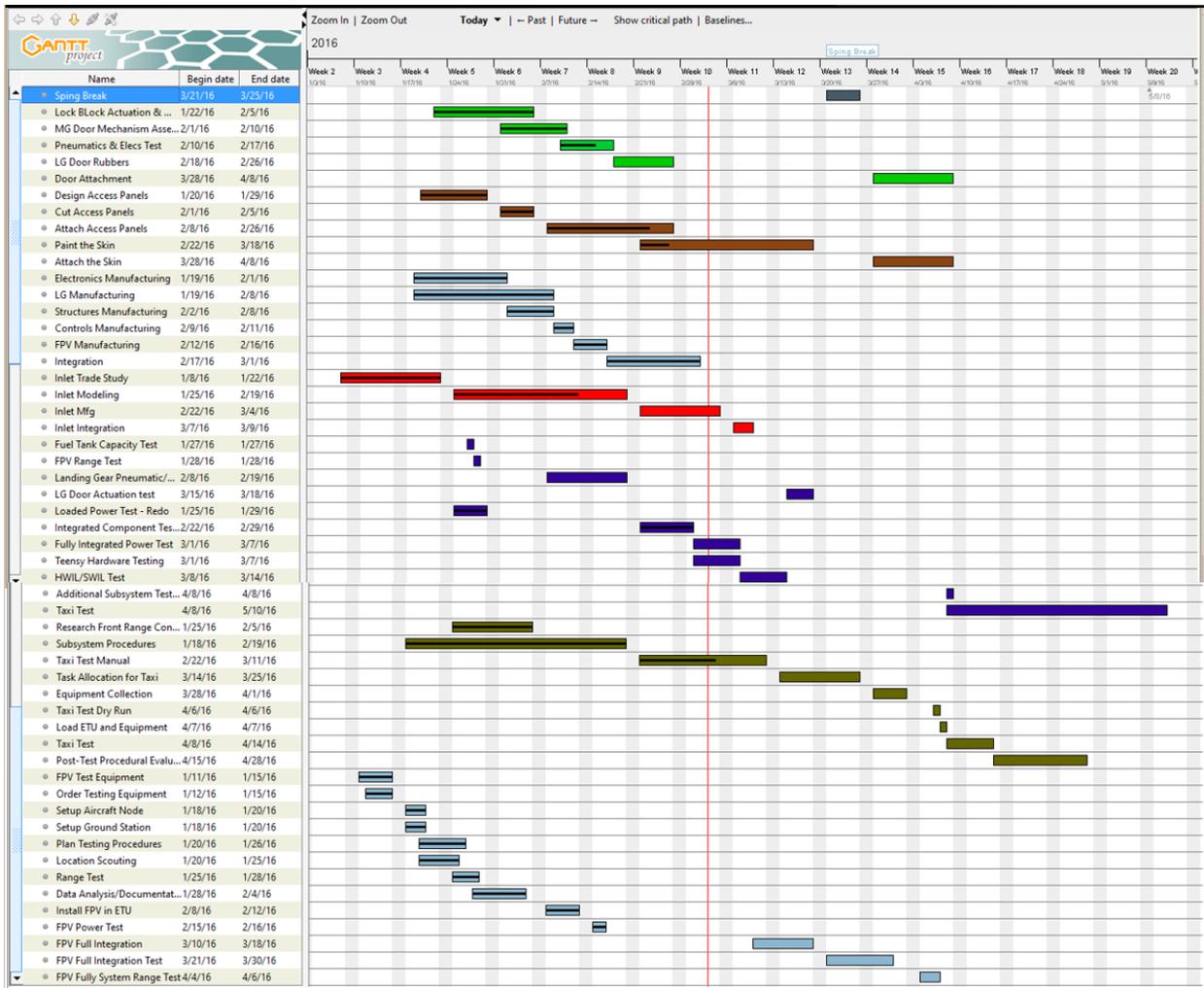
Figure 2: Spring 2016 Schedule

The schedule above is grouped by subsystem with the critical tasks and divisions shown below.
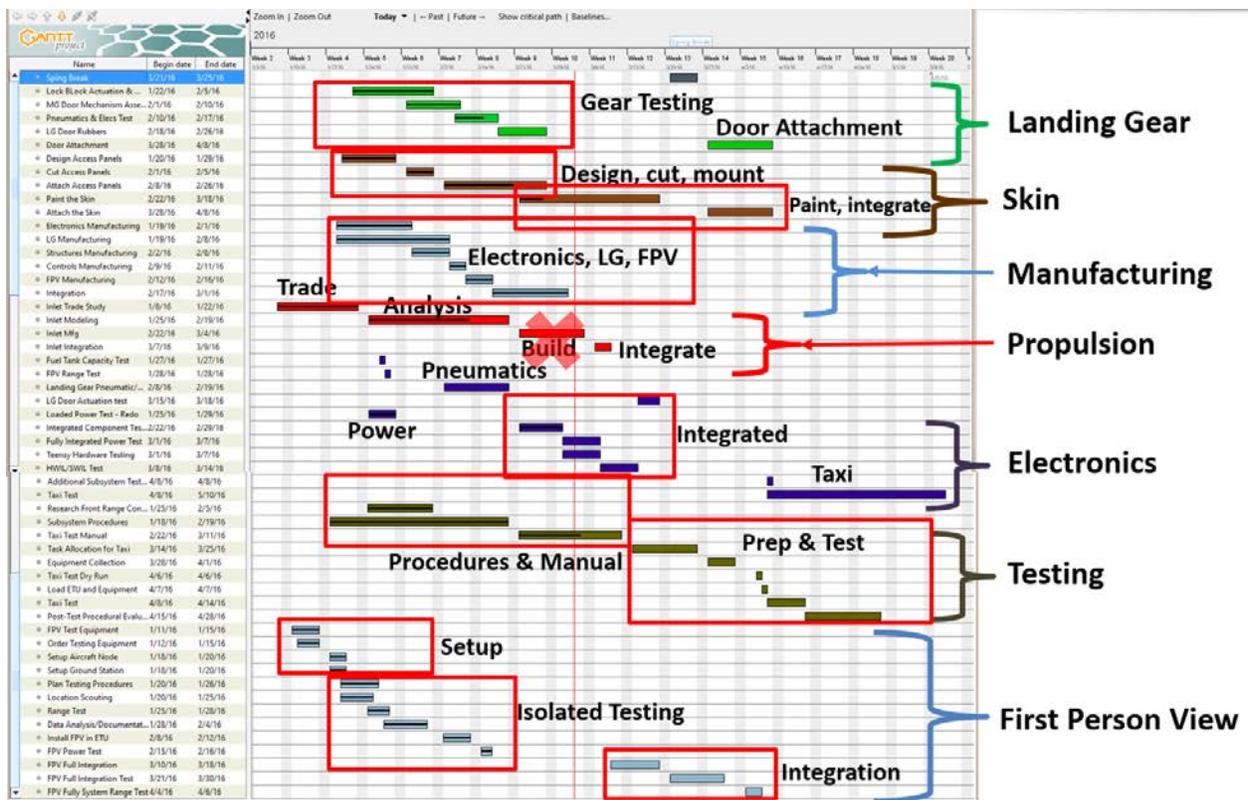
Figure 3: Broken Down Spring 2016 Schedule

The primary changes from the proposed schedule to the final schedule is the removal of the SAG requirements, and including additional time for testing and integration. When determining buffer, the $2, \pi, 5$ rule was used. Using this rule, we applied a buffer equal to 2, π, or 5 times the amount of time the team anticipated each task would take depending on the team's experience. For example, if the team was filled with experts for a task expected to take 1 week, we provided 2 weeks (1 week of buffer) on the Gantt chart. If the team was knowledgeable, but not skilled in the topic, we would provide π weeks for a 1 week task in the Gantt chart. If the team knew nothing at all about a specific topic, we estimated the task would take 5 times as long as our best approximation.

Scheduling was performed using Gantt Project – a free software package used for creating Gantt Charts and organizing project management tasks. Full team meetings were held weekly for approximately 30 minutes each. This weekly meeting was required to regroup the team and keep perspective of the project as a whole. Subsystem meetings also occurred throughout the semester on their own schedule for more detailed discussions.

39

Some of the major milestones and tasks from this past semester are highlighted in the tables below.

In order to prepare for taxi testing, a comprehensive set of test plans were created and executed. Below is a list of some highlights of testing accomplished in various subsystems.

Testing		
FPV Antennae Range Test	2/12/16	2/12/16
Fuel System Test: Landing Gear Deployed	2/15/16	3/4/16
Full Pneumatics Test	3/25/16	3/30/16
Landing Gear Door Actuation Tests	4/14/16	4/18/16

During the first half of the semester, manufacturing was operating using the most human capital of any subsystem. They were working in parallel with subsystem testing for final integration of components into the aircraft. Although integration never ended, machining only occurred in the first half of the semester. After machining was complete, the manufacturing subsystem ceased to exist as a dedicated unit. Rather, those members broke into landing gear, electronics, and integration teams to prepare the aircraft for taxi.

Manufacturing	1/18/16	3/18/16
Integrate remaining parts of the ETU	1/18/16	3/5/16

One of the new subsystems for the spring 2016 semester was the skin. This team worked to properly cut the skin, paint the skin, and mount the skin. The logistics of this turned out to be harder than expected primarily due to outside contract work that caused delays. However, many critical deadlines were hit as outlined below. See section 8 of this report for more information on the introduction of the Skin subsystem.

Skin	1/18/16	3/18/16
Paint the skin	2/28/16	3/15/16
Cut out access panels in skin	2/15/16	3/28/16

40

| Cut out the landing gear doors from the skin | 2/15/16 | 3/28/16 |
| Add magnets to access panels | 3/7/16 | 3/11/16 |

The power system was renamed the electronics subsystem for the spring 2016 semester. Over time, what was the power subsystem started working on more electronics than just the power distribution system, especially including the teensy board and 5 hole probe data acquisition unit. Some critical deadlines for the spring 2016 semester are outlined below.

Power	**1/18/16**	**3/18/16**
Test pitot DAQ landing controller board	1/18/16	1/29/16
Integrate all electronics into the aircraft	1/29/16	2/12/16
Perform a fully integrated HWIL test	2/15/16	3/18/16

The propulsion subsystem was renamed the inlet subsystem. Propulsion analysis and engine testing was complete before Spring 2016, so the work of this subsystem was primarily in the aspect of analyzing the fluid and structural properties of the inlet after damage was found in the fall 2015 semester. The team determined the inlet was safe and did not to be remanufactured. They were able to complete detailed computational fluid dynamics models and finite element structural models as outlined by some of the key milestones below.

Propulsion	**1/18/16**	**3/18/16**
Refabrication decision	1/18/16	2/1/16
CFD Analysis Complete	1/11/16	5/3/16
Structural Model Complete	1/11/16	5/3/16

The landing gear subsystem, like the manufacturing subsystem wrapped up its official recognition during the spring 2016 semester. This subsystem was primarily available for work with the testing subsystem to support the critical landing gear tests before taxi. Very early in the semester there was some final assembly, but most of the work was in integration and test support.

Landing Gear	**1/18/16**	**3/18/16**

Finish nose gear locking mechanism	1/18/16	2/5/16
Full gear pneumatics tests	4/15/16	4/20/16
Assembly of main gear door actuation mechanism	2/29/16	3/11/16

3.1 ETU Operations Manuals

During the spring 2016 semester, the testing subsystem was expanded to including testing and operations. The operations aspect of this subsystem was to provide dedicated personnel to the operations and logistics of taxi and flight. This included development on the taxi and flight operations manual. See section 4 for more information on the status of the operations manual after the spring 2016 semester.

3.1.1 Systems Analysis Guide (SAG)

A diagram of the UAS Flight Test Center Process is shown below detailing the steps that must be arranged before flight testing. This document can also be found in the project management archive from fall 2015.
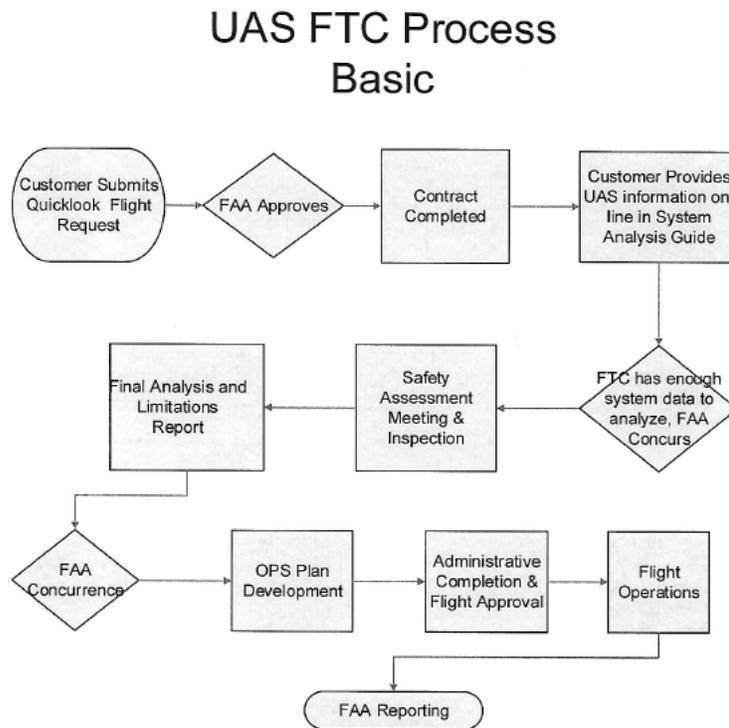
Figure 2: UAS Flight Test Center Process

4. <u>SYSTEMS ENGINEERING</u>

4.1. Systems Engineer Purpose

The systems engineer is responsible for coordinating the tasks for each subsystem including design, integration, and testing. In addition, the systems engineer is responsible for developing and maintaining system specifications, requirements, and a Bill of Materials. There were two systems engineers this semester and the duties were split between them. The SE controlled the master CAD model, to incorporate late changes and assist in integration. Lastly, the systems engineering role includes documenting system configuration changes and ensuring the efficient planning and execution of tasks via proper documentation in order to reach the stated semester goals. The systems engineers will work to complete required pre-flight documentation including the SAG and operations manuals as well. As a reminder, a concept of operations was established for GoJett which can be found in …\Systems\CONOPS as well as revised requirements (…\Systems\REQUIREMENTS). Specific to this semester, the Systems Engineers spent the vast majority of the time working with the skin subsystem to ensure that it was ready for integration, and also with other subsystems to help with their respective integration to the aircraft. The SE also worked with manufacturing to help make additional parts that subsystems needed.

5. <u>**TESTING & OPERATIONS**</u>

By the end of Fall 2015 the GoJett team had completed the actual building of GoJet and the ETU was half way through the testing phase and was ready to go into the final testing phase. For this purpose the goal of the Spring 2016 semester was getting the ETU ready for Taxi test and Flight test. The testing subsystem panned to analyze and test each of the other subsystems and get them ready for flight.

If the team identified that any of the other subsystems or components on the ETU required additional attention or work the testing team would have to help in completing the task directly or reallocate it to some other subsystems to be completed on team. Finally once all the subsystems are individually tested, the testing team will perform integrated tests on the entire GoJett ETU. The project team estimated that with a more aggressive schedule the team would be able to perform the Taxi test by the end of the semester and if all went well even Taxi. So this was set as the end of the semester goal.

5.1. Summary of Subsystem Tests

As stated before the primary goal for the semester was to do the Taxi test. All the work done in Spring 2016 was with the objective of meeting this goal before the end of the semester. Unfortunately we could not meet this goal and had to shift the flight test to a future date due to various reasons. Two of the main reasons for this were the unexpected delay we faced in component failures and Front Range Airport double booking us on the scheduled day of Taxi. The final tests were not performed due to the dismantling of most of the aircraft electronics.

5.1.1 FPV Range Test

The testing in the Spring Semester started off with the FPV Range Testing. For this test we drove out to Cherryvale Lane to get a good 4 mile straight road to test our receivers and antenna. The setup of the ground station is show in the figure below. A mock up of the ETU was made with a cardboard box housing the antenna and each one was tested separately and then together. The cardboard box was placed in a car

which was driven down Cherryvale Lane until the video got hazy and then finally stopped transmitting. As it was placed inside the car it simulated the worst case scenario as the car material is thick. Also the roads were lined with trees posing as obstructions along the way. The outcome of this test gave us a range of approximately 2.5 miles range with both the omnidirectional and the directional antenna on. During actual test these results will be better as the obstructions will not be present.

Figure 4: Ground Station Setup for FPV Range Test Down Cherryvale Lane

5.1.2 Fuel Tank Refilling Test

The Fuel Tank Test was completed in the Fall 2015 semester but without the landing gear deployed. The ETU with the landing gear deployed stands at an angle with its nose pointing slightly upwards which reduces the full capacity of the fuel tanks to curb leaking of fuel. Thus it was decided that the test needed to be completed again to determine the amount of fuel the ETU could carry without leaking having the gears deployed. On successfully completing this test, the results obtained were that the capacity of the ETU fuel tanks is approximately 1.45 gallons of a 5% Oil mixture with Kerosene. This is the maximum fuel that it can hold without

45

leaking. More videos and documents are available on this matter. The fuel needed for Taxi/Flight was estimated to be of the same value, which works out well.

5.1.3 Landing Gear Testing

Having completed the structural testing of the landing gear and successfully conducting drop tests on the gear the only testing remaining were the full landing gear pneumatics testing and the landing gear controller testing.

5.1.4 Pneumatics Testing

The Landing Gear is actuated by a pneumatics system which can be refilled using a paintball tank. This paintball tank needs to be filled up to 4500 psi and the pneumatics tank on the ETU will then fill up to 3000 psi when connected to the paintball tank. The pressure required for deployment and retraction of the gear is 125 psi. The main gear had some issues with friction and pressure build up but those have since been attended to by solving some greasing and friction issues. The nose gear had never been deployed up until this semester and through this test was successfully actuated. The ETU can stand with good stability on its three landing gear once actuated. The nose gear has a delayed reaction to the pneumatic actuation, but it does get actuated efficiently. The pressure can be modified for higher air resistance or friction. Videos for the actuation procedures and the testing itself are available.

5.1.5 Controller Testing

Meanwhile
The landing gear controller has been coded to switch the steering control from the nose gear to the rudder when the ETU hits a high enough speed. It also controls the turning of the nose gear and the landing gear doors. It is time coded as well so as to ensure all these above mentioned events happen in a continuous flow without them simultaneously happening. This test was conducted to test this information and code on the controller to dictate the movement in the landing gear, the steering controls and the landing gear doors actuation.

46
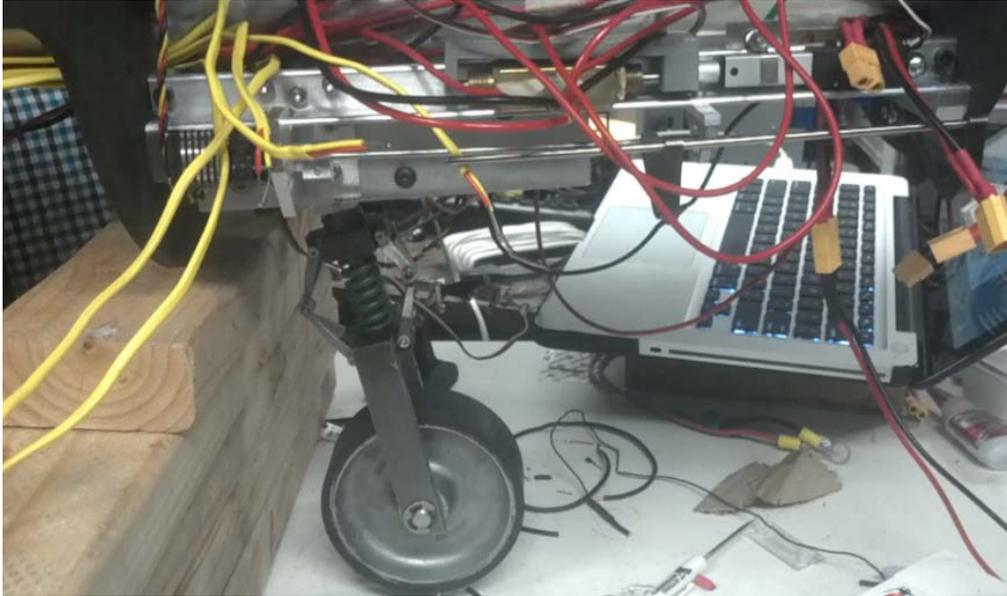
Figure 5: Nose Gear Steering Column

5.1.6 Teensy Test – Pitot DAQ Dynamic Test

This test was conducted in the Wind Tunnel to test if the air probe was correctly reading air-speed data. It was also conducted to check the relay of information and interface between the PitotDAQ and Teensy Board. The results of this test gave us that the wind speed measured by probe is approximately 1.7 m/s more than wind tunnel measurement and on further analysis we were able to determine that there was a discrepancy with the angle of attack 'α' data recorded and repeated tests were carried out for data on various angles of attack. The figure below shows the setup pf the air probe in the wind tunnel with the tubes attached to the PitotDAQ which is in turn connected to the Teensy.

47

Figure 6: Teensy Test and PitotDAQ Dynamic Test Setup

5.1.7 Hardware in the Loop (HWIL) Test

Once all subsystem tests were completed the final step was the SWIL and the HWIL testing. The first preliminary HWIL test was a success with all systems including the elevons, the rudder steering, the flight lights, the pneumatic actuation of the landing gear and the door opening and closing. This test was a success, but it will need to be conducted again in the future.
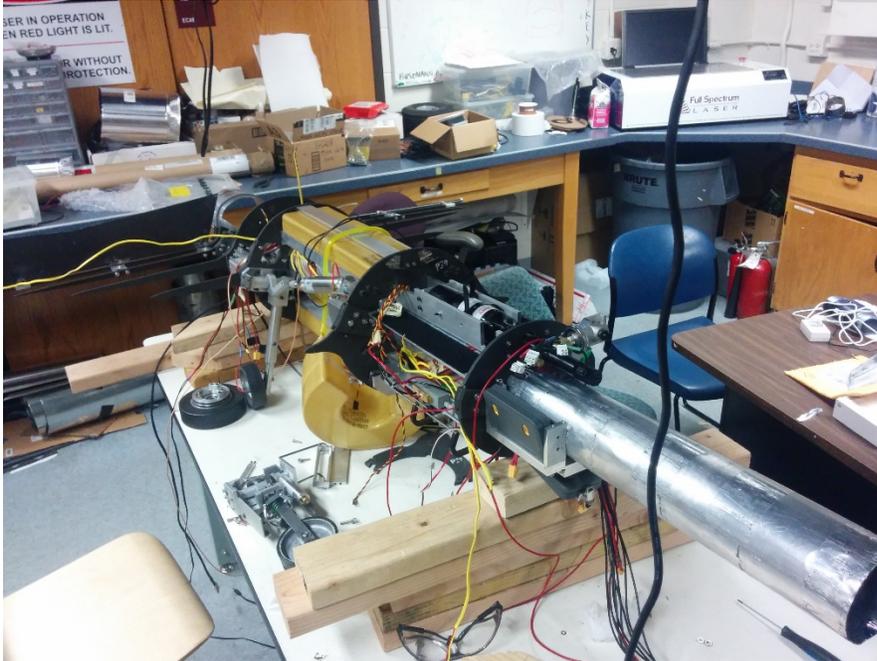
Figure 7: GoJett during the HWIL Testing

5.2. Operations Overview

With any testing program, proper planning and organization can be the difference between test success and failure, despite the actual performance of the system. If setup and operational procedures are not prepared and understood, it is likely that testing will be delayed due to unforeseen complications. If these complications can be planned for ahead of time, it will be possible to either mitigate or troubleshoot them quickly and effectively. As full-system testing is often the most expensive time of an airplane program, it is important to ensure that no testing time is wasted. The Operations Lead for GoJett was responsible for preparing the team for an efficient and successful taxi test. This included reviewing and updating subsystem and overall procedural documents. Also, transportation needs and necessary permissions had to be attained prior to testing.

5.3. Taxi Testing

The main goal for the GoJett team during the Spring 2016 semester was to reach taxi testing. This testing involves all systems functioning and driving the ETU down the runway. Basically, this test serves to demonstrate everything up to the actual airworthiness of the GoJett ETU. In

49

particular, the propulsions system, the landing gear, the controls, the sensor suite, and the structure itself will be evaluated for effectiveness and robustness during taxi. Without these systems functioning properly, the aircraft has no chance of successful flight.

If the propulsion system is not able to effectively propel the ETU down the runway, then there is no chance of successful flight. With the long air-inlet, it is not clear whether proper airflow will be available to the engine. The only way to properly test the propulsion system is to put the aircraft on the tarmac and attempt to drive it down the runway.

For the landing gear, much attention and work has gone into ensuring that the gear will support the ETU during all stages of flight. First, it is necessary to ensure that the gear can be properly extended and retracted. Without gear extension and pressurization, the ETU will not be able to sit idle on the runway, let alone survive a landing. Without gear retraction, the ETU would not be able to reach proper flight speeds due to the increased drag from the extended gear. Also, transportation gets more complicated with the gear extended. Therefore it is necessary to ensure that the landing gear system can be easily extended and retracted. Information gained from taxi testing will assist in increasing the confidence of the system.

The control system is closely tied with the propulsion and landing gear systems as it is used to send engine and gear commands to the respective actuators. Also, the controls are necessary to ensure proper handling of the ETU both on the runway and in the air. For taxi testing, the control to the engine, the gear, and all of the control surfaces will be tested. Also, the nose-gear steering will need to be tested to ensure proper handling of the ETU at low speeds on the runway.

Without data analysis, taxi testing will not be as effective as it could be. Instead, it is necessary to ensure that the surface deflections, airspeed, and internal temperatures can be recorded and used for later analysis prior to flight testing.

50

6.9.1 Taxi Plan

The GoJett taxi plan has been compiled into one document, GoJett ETU Taxi Procedures.doc, which is located in the Operations section of the Drive. This manual, which was compiled over the Fall 2015 and Spring 2016 semesters includes all information on the steps leading up to taxi and the schedule of the actual taxi testing day.

Leading up to taxi, all integration and system testing must be completed. As time will likely be limited during the actual testing day, it is necessary that all systems that can be testing beforehand have been tested successfully. Otherwise the test day may be wasted due to complications that should have been discovered beforehand.

As for the actual operations of the testing day, a taxiway and transportation must be confirmed. The taxiway chosen for GoJett is the cargo road at Front Range Airport, as seen in Figures X and Y. This roadway is approximately two miles longs, which provides plenty of space for the ETU to build up speed and then slow down without brakes. The aircraft will taxi only south, and all personnel will remain north of the testing section for safety as seen in Figure Y. After each taxi attempt, the transportation vehicle, which is following the ETU for safety, will be reloaded with the ETU in the taxi cart. The transportation vehicle will be a nine foot cargo van rented from UHaul. Multiple taxi attempts will be performed with increasing speed as the confidence in the ETU increases.

51

Further taxi details can be found in the GoJett ETU Taxi Procedures, including safety checklists, specific testing sequences, equipment lists, and personnel roles.
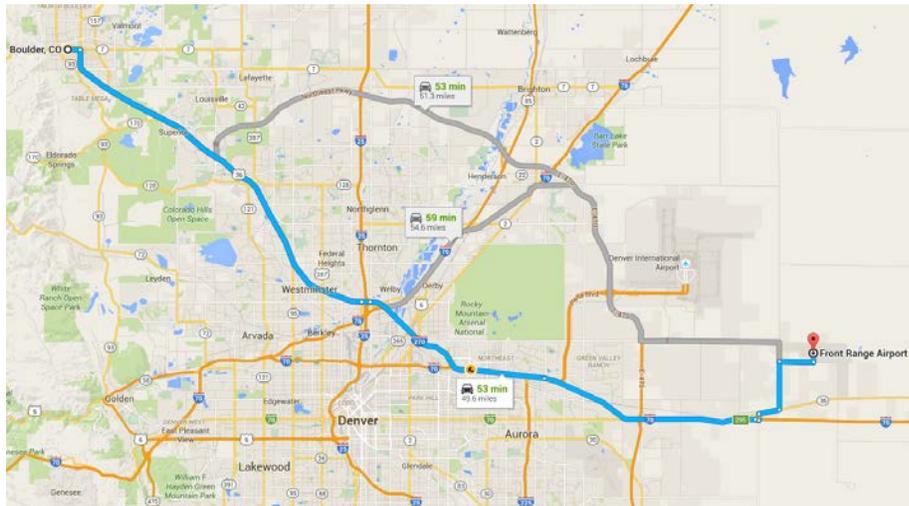
Figure 8: Scheduled Taxi Location

5.4.   Flight Testing

The subsonic flight testing for the GoJett ETU will be the culmination of the work on the current model. This testing will serve to validate the use of a jet engine for the flight of a sub-50kg UAS. Also, the data and best practices from the subsonic ETU can be utilized to assist in the design, manufacturing, and testing for the final supersonic model in the future. The general plan for flight testing is simply to takeoff and then reach a low cruise altitude before returning and landing. The landing gear retraction and extension will also be tested in actual operating conditions along with a proper landing to demonstrate system effectiveness.

52
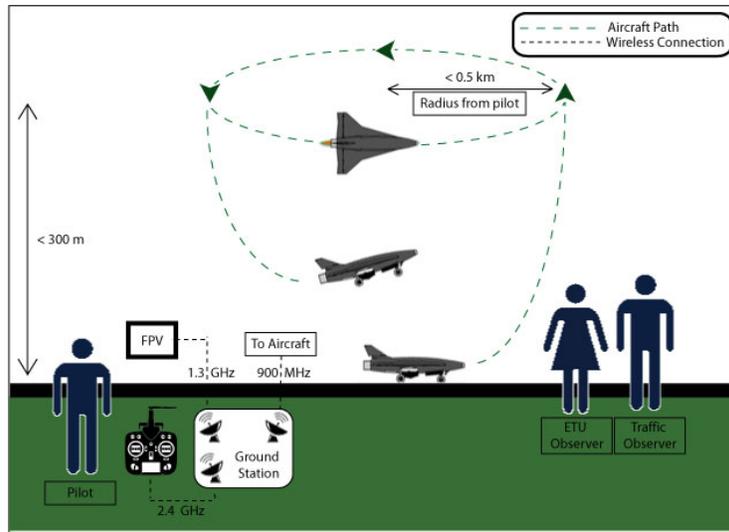
Figure 9: Subsonic Flight Testing CONOPS

6.9.2 To Do Before Flight

Before the GoJett ETU can be flown, many tasks must be completed. First, flight testing is dependent on successful taxi testing. If any systems fail during taxi, flight testing cannot be performed. Assuming successful taxi testing, the data and experience from this testing can be used to improve the chances of a successful flight test.

The location for the final flight testing has been a topic of discussion for some time now. Alocation in Las Cruces, New Mexico was chosen,. An alternative location is White Sands Missile Range (WSMR) due to its remote nature. Confirmation, scheduling, and contracting would need to be performed in order to allow for an eventual flight test at either of these locations.

Much coordination with the FAA will also be needed prior to flight testing. As the ETU will be travelling up to Mach 0.4, there could be dangerous consequences if any of the systems fail. Therefore, it is important that the FAA is heavily involved in ensuring that the ETU is flight ready and that the proper precautions have been taken prior to flight testing. The Systems Analysis Guide has been submitted to the FAA, but this document would need to be completed in more detail if flight testing is ever to be performed.

Prior to Spring 2016, another round of funding was expected from the Air Force, but this money was never received.

53

5.5. Lessons Learned

This semester, the GoJett team had some issues in terms of operational planning, and it is therefore useful to discuss these issues and what lessons can be learned from them.

6.9.3 Scheduling

For most of the Spring semester, the ETU taxi testing was scheduled for early April. As the team got closer to being ready for taxi, the final date was determined and coordinated with Front Range Airport. Unfortunately, the communication between the team and the airport staff was lacking, which led to the roadway being double-booked on the expected taxi date. As this date had been placed late in the semester, there was little time to schedule another test date before the team dispersed for the summer. This, along with a few other setbacks in integration, prevented the team from performing taxi testing as intended. This incident demonstrated the importance of communication with suppliers and resources, especially when those resources must be scheduled well-ahead of time. Otherwise you may fall off of their radar and find yourself without the necessary facilities.

6.9.4 Knowledge Transfer

The key component of the GoJett ETU is the jet engine, which is a highly-complicated system. In previous semesters, the team had completed testing on the engine simply to familiarize the team with its operation. This was not done this semester, which led to a gap in knowledge in regards to the operations of the engine itself. As this system is critical and potentially dangerous, it is vital that the team understands its function and can properly troubleshoot when necessary. Without adequate knowledge of the propulsion system, it is likely that the taxi testing would have been inefficient and potentially dangerous. This demonstrates the importance of knowledge transfer between successive teams, especially in regards to critical systems.

6.9.5 Importance of Planning and Operations

54

The main goal of the Operations Lead this semester was to prepare the GoJett team for taxi testing, but since this testing was not completed much of the work went unseen. This demonstrated that leading up to planned activities, it is not always easy to see the benefit of operational and procedural planning. It is not until things start going wrong that the Operations Lead comes into the forefront and the importance of their work is seen. For example, the loss of the taxiway due to a lack of communication showed how important operational planning can be. All the technical work means nothing if the team does not have the means to actually test its system.

6. <u>**MANUFACTURING**</u>

Manufacturing was one of the top priorities of the GoJett team this semester. There were two major goals for the manufacturing team: machining/fabricating all of the necessary parts and integrating each of these parts with the entire system. The previous semester made excellent headway into both of these tasks, but there was still plenty to accomplish. This section will outline what was done and what needs to be done for each other subsystem on the aircraft.

Each manufacturing task is broken down by subsystem. The tasks which were planned, completed, and still need to be completed will be discussed within each subsection. The subsystems are: Structures, controls, landing gear, propulsion, electronics and power, first person video, and system integration.

6.1. Structures

The structural components for the aircraft had already been almost completely manufactured and integrated on the aircraft, so the team did not plan on doing much work on the structure at the beginning of the semester. Every component was already machined and the only work to be done was to attach the top half of bulkheads 5-7 to the rest of the structure. This was necessary solely to keep the engine available for as long as possible throughout the semester. No work in future semesters is anticipated for the structure subsystem barring a change in the overall design of the aircraft.

6.2. Controls

Similar to structures, the controls subsystem was fully completed before the beginning of the semester. No manufacturing was accomplished for this subsystem because nothing needed to be done. However, the rudder assembly was removed near the beginning of the semester to allow for skin attachment. In future work, the only job that needs to be accomplished for the controls subsystem is to reattach the rudder assembly to the rudder servo after the exterior of the aircraft has been fixed. With this one task, the controls subsystem is complete.

56

6.3. Landing Gear

Landing gear can be split into two groups: the main gear and the nose gear. The main gear was more or less complete by the beginning of the semester. All of the assembly from the pneumatics lines to the gear itself was complete. The only task to accomplish for the main gear was to machine and integrate the main gear door servo mounts and assembly. This assembly is shown in the most recent version of the CAD between bulkheads 2 and 3 (I'm not sure exactly what the part numbers are because the server is currently inaccessible). These parts have since been machined and integrated and therefore no work is anticipated on the main gear.

The nose gear required a significant amount more work due to a redesign that happened at the beginning of the semester. Again, the part numbers for these are unknown because of lack of access to the server, but the entire assembly can be found in the most recent version of the CAD. The beginning of the semester was weighed heavily on machining these parts for the nose gear assembly, finishing with integrating the new parts onto the nose gear assembly. The main addition to the nose gear was a servo to control the lock block rather than using the system that was in place last semester.

Once the nose gear assembly was updated, it was mounted between bulkheads 1 and 2 of the aircraft. The result of this is that both the nose gear and main gear assemblies are completed and fully integrated on the aircraft, indicating that no further work is necessary for the landing gear subsystem.

6.4. Propulsion

For the propulsion system, there were several major tasks to accomplish this semester. The first task was to mount the engine housing and the engine itself to the aircraft. This was largely accomplished last semester, but the final integration of the engine was held to the end of the semester due to requirements of other subsystems. However, this task was fully completed.

The next task was to integrate the fuel tanks with the engine and the engine electronics. This was accomplished by mounting the fuel tanks themselves, then routing fuel lines in the following order: fuel tank, hopper tank, fuel pump, then propane and fuel lines directly to the engine. The

57

fuel tanks sit between bulkheads 2 and 3, while the other components sit between bulkheads 3 and 4. See the propulsion section for more details about this setup.

The final task was to integrate the engine electronics, which consisted solely of the ECU and the electronics onboard the engine itself. The ECU sits on the front of the top of bulkhead 4 and has wires connecting it to the engine and to all three of the fuel pumps. This task was completed.

A separate but related task was manufacturing of the inlet. At the beginning of the semester, the inlet team determined that it was not necessary to build an entirely new inlet. However, a couple of tasks still needed to be accomplished. The first task, which has been completed, was to shorten the inlet to be the length that was specified in the CAD model. This was done simply by using a dremel.

6.5.   Electronics and Power

Electronics was one of the major manufacturing tasks of the semester, taking over a month to accomplish. Machining of all of the electronics mounts was accomplished last semester, so this semester focused on a series of tasks:

The first step was to mount all of the electronics into their respective places on the aircraft. A detailed layout of this can be found by looking at the CAD model. All of the electronics components which did not have mounting platforms were mounted simply by using Velcro and attaching them directly to the bulkheads. When this was finished, all of the power, signal, and ground lines were connected from the power boxes to each component and between components. Upon completing this task, all of the non-engine electronics were mounted to the aircraft and ready for testing.

6.6.   First Person Video

The only manufacturing task for the FPV subsystem was to integrate it with the aircraft. This was accomplished by mounting the camera to the camera mount, which then attached to the left side of the first bulkhead. This connected to the FPV receiver, which then connected to the FPV antennas. The antennas sit between bulkheads 3 and 4 on the skin of the aircraft, while the receiver

sits on the underside of the left battery mount between bulkheads 1 and 2. With this task being completed, nothing else is required for integration of the FPV subsystem.

7. **LANDING GEAR**

7.1. Background and Overview

The purpose of the landing gear subsystem on project GoJett is to facilitate the aircraft's horizontal takeoff and landing on a static, flat surface. The landing gear for the engineering test unit (ETU) currently in development is required to be fully extendable and retractable, and it must be able to withstand all the expected take-off and landing loads, as well as any aerodynamic loads occurring right before or after take-off or landing. Because of the relatively small size of the ETU and the landing gear's requirement to be fully retractable, the landing gear has to be small and compact, while still providing the strength and durability to facilitate a safe take-off and landing.

The landing gear has largely been designed and manufactured in previous semesters. The nose gear was redesigned and manufactured in the Fall 2015 semester. This semester focused on completing the lock block mechanism which prevents the nose wheel from collapsing under landing loads, finishing the main gear door actuation mechanism, and integrating the entire landing gear subsystem into the ETU.

7.2. Nose Gear

7.2.1 Summary

The nose gear was redesigned and manufactured in the Fall 2015 semester. Several drop tests were performed during that semester to verify the design is capable of handling the loads expected during landing. The one aspect of the nose gear that remained to be completed for the Spring 2016 semester was the lock block mechanism. The landing gear is retracted and deployed using pneumatic actuators. Due to space limitations, the pneumatic actuator for the nose gear is not strong enough to securely hold the nose wheel down under landing loads. For this reason, a lock

block mechanism was designed that physically prevents the pneumatic actuator from retracting by blocking the actuator arm using a metal block.

7.2.2 Lock-Block Mechanism

A picture of the completed lock block mechanism is included in *Figure 10*. The lock block is a steel block that fits around the shaft of the pneumatic actuator. When the block is placed over the shaft, the actuator is unable to retract and the nose gear is held in the down position. The lock block is moved into and out of place using a servo connected through an aluminum arm. The lock block slides up and down in two channels, assuring that it moves into and out of place freely. The servo used is a Spektrum S6100 high torque servo. The high torque servo ensures that the block will be able to be retracted even if there is pressure on it from the actuator. Also, this is the same servo used for the main gear doors which makes replacing components easy in the event of a failure.
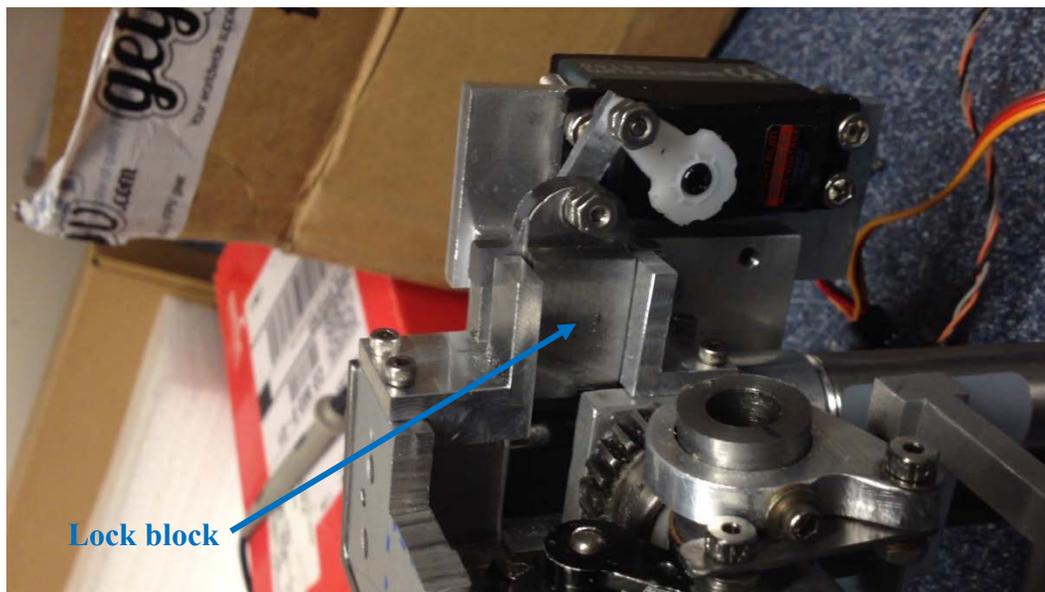

Figure 10: Lock block mechanism in the unlocked position

The lock block mechanism was tested outside of the aircraft, as well as after being integrated. The design has performed reliably during all tests. The nose gear has been completed and fully integrated into the ETU.

60

7.3.   Main Landing Gear

The main landing gear was mostly completed at the beginning of the Fall 2016 semester. The main gear was integrated into the ETU, excluding the door actuation mechanism. The focus of this semester was to complete the door actuation mechanism and fully complete the landing gear.

7.3.1 Main Gear Door Actuation System

The main gear doors needed powerful servos for their actuation. Last semester, Spektrum S6100 High Voltage High Torque Surface Servo were chosen for the doors. The servos have been mounted in the ETU using the mounts in Figure 12. To complete the main gear, the linkage between the servo and doors needs to be attached. The servo mounts though initially were designed as in Figure 3, once they were manufactured and placed in position, it revealed that the inner side of the mount came in contact with the inlet. Thus we had to modify the mount by cutting the vertical section of the inner side down to a height which accommodated only one hole for mounting the servo. The other problem with the mount design was that the main gear scraped the mount during motion. For this we chamfered the outer side of the mount and solved the problem. The modified mount and welded linkage is seen in Figure 4.

61
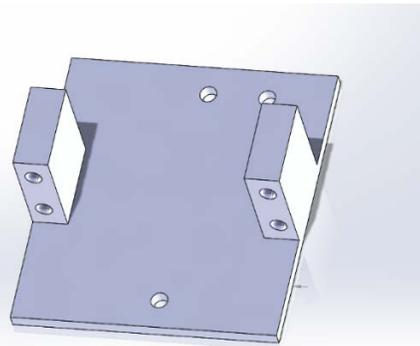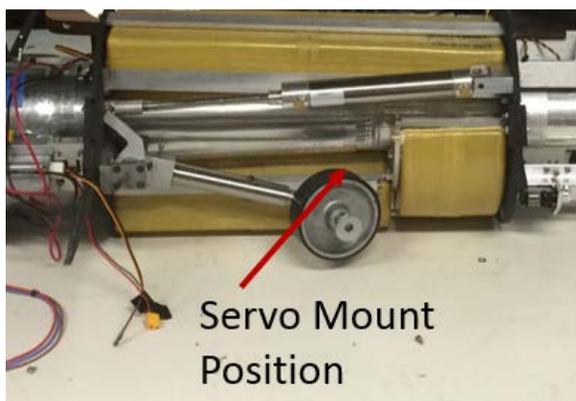
Figure 11: Main gear servo mount position and CAD model
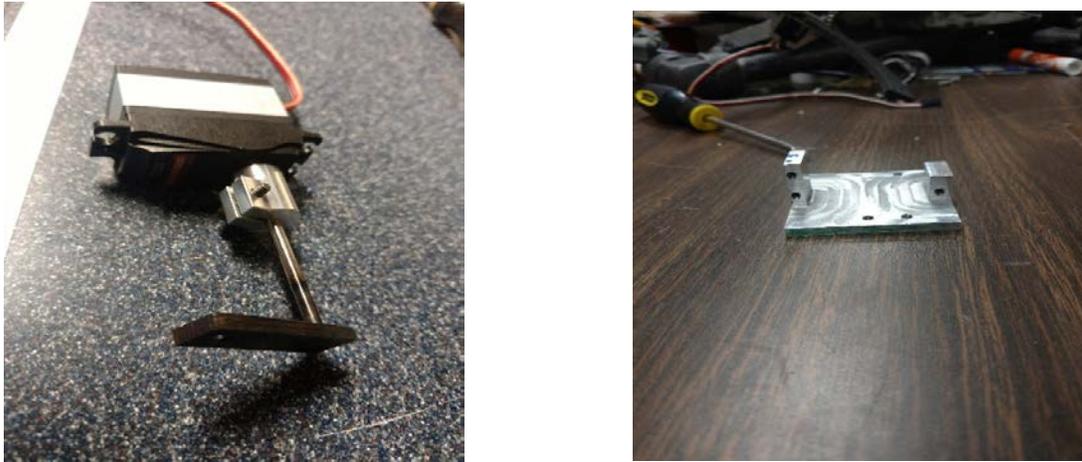
Figure 4: Welded linkages and modifies servo mount

A 4-bar linkage mechanism is discussed in the Spring 2014 Final document. This design was modified to remove the gears by lining up the servo coupler and the mechanism. The smaller link of the 4-bar linkages was remade out of steel to facilitate the welding of the steel shaft from the coupler to the smaller link. The smaller link along with the larger link will then be connected to the door cut from the ETU skin through hinges and thus the main gear door will be actuated.
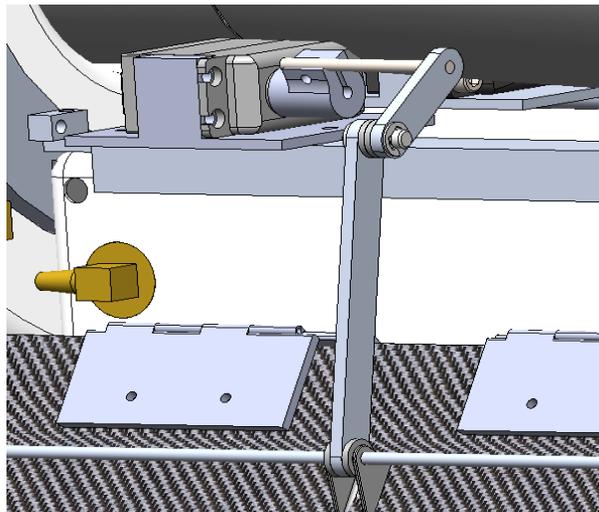
Figure 12: Main Gear Actuation System

For the main gear actuation mechanism, all manufacturing has been completed and the entire system is assembled together.

62

7.4. Landing Gear Controller

The landing gear controller is the electronic circuit board responsible for correctly deploying and retracting the landing gear, as well as steering the nose gear. The LG controller acts as the interface between the autopilot and the landing gear subsystem. The LG controller receives an input from the gear and rudder channels on the autopilot. When the gear channel changes from up to down, the landing gear controller sequences the correct deployment of the doors, landing gear, lock block, and steering. When the gear is in the down position, the LG controller uses rudder inputs from the autopilot to steer the nose gear.
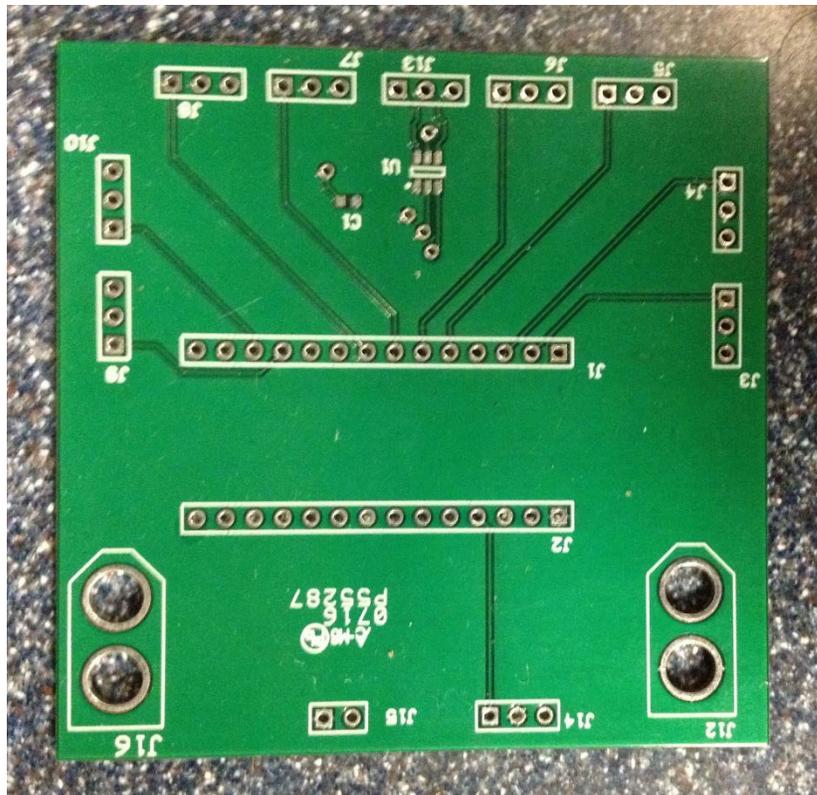
Figure 13: Landing gear controller PCB

Most of the code for the landing gear controller was completed last semester, but had to be rewritten this semester due to the server failure. The PCB for the controller was designed, ordered, and tested. The LG controller PCB is shown in Figure 14. The Teensy 3.1 mounts in the center of the board, and connections for all of the servos are around the edges. The board was populated and the Teensy mounted. A full system test confirmed the operation of the

63

landing gear controller by successfully deploying and retracting the landing gear while GoJett was suspended off of the ground in the lab.
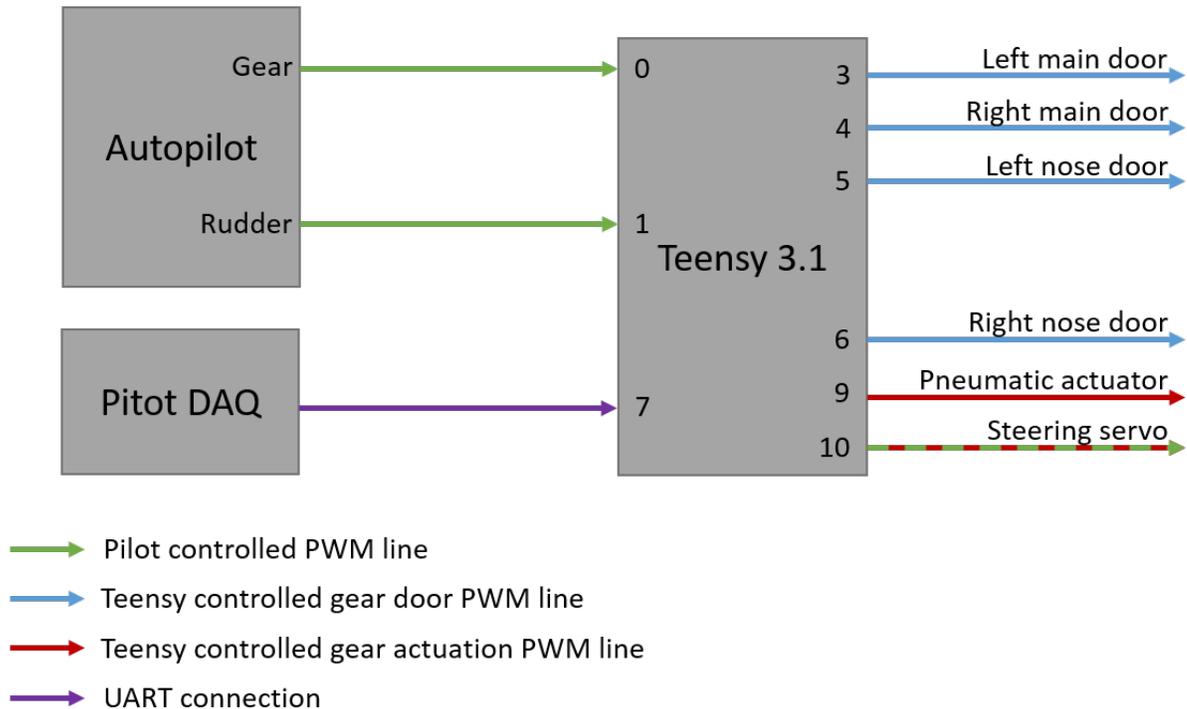
Figure 14: Landing gear controller connections

The landing gear controller is a Teensy 3.1 programmed using the Arduino IDE and mounted on a custom PCB. The inputs and outputs from the landing gear controller are listed in Table 2.1. All outputs are PWM signals to various servos. The LG controller also distributes power to all of the landing gear servos. When the controller detects that the gear channel of the autopilot is cycled from down to up, the controller will first turn the nose gear to 90°, unlock the lock block, then trigger the pneumatics to retract, and then finally close the main gear and nose gear doors. When the gear is signaled down, the controller first opens the doors, triggers the pneumatics to lower the gear, locks the lock block, and then rotates the nose gear back to center.

64

Inputs	Outputs
1. Gear PWM Channel 2. Rudder PWM Channel 3. Pitot DAQ RS-422	1. Main door left servo (PWM) 2. Main door right servo (PWM) 3. Nose door left servo (PWM) 4. Nose door right servo (PWM) 5. Steering servo (PWM) 6. Pneumatic actuation servo (PWM) 7. Lock block servo (PWM)

The rudder PWM channel is used to steer the nose gear when the gear is down and the aircraft is travelling less than 30 m/s. The airspeed is monitored from the Pitot DAQ RS-422. To use the LG controller, power simply needs to be applied by flipping the main power switches on the ETU. The aircraft should always be initially powered up with the landing gear down. This is because the landing gear does not have any sensors to detect position, so it needs to start in a known position.

The code for the LG controller is located on the server. A basic outline of the landing gear controller code is as follows. All of the pin numbers, servos, servo positions, delays, and other variables are defined at the top. The Setup() function starts the serial connection to the Pitot DAQ, sets up the interrupts for reading the PWM signal from the autopilot, and then commands to gear to the down position. The gear and rudder signal are read from the autopilot using external interrupts so that the gear_pwm_value and rudder_pwm_value are automatically updated. The main loop first checks the value of gear_pwm_value sees if the position of the gear needs to change. If a change has been commanded, then the loop calls the function to either raise or lower the gear. Next, the controller reads the current velocity from the Pitot DAQ UART connection. If the aircraft is travelling less than the critical speed then the rudder commands are translated to the nose gear steering servo, if the aircraft is travelling faster than the critical speed then the steering servo is held straight.

65

8. __ELECTRONICS__

8.1. Introduction

The electronics subsystem consists of the power distribution system in addition to all of the electrical flight components. During the Spring 2016 semester, the electronics subsystem was responsible for integrating all of the wiring and the electronics into the engineering test unit, performing isolated testing on critical flight components, and performing a fully integrated test in preparation for a high speed taxi test. The electronics subsystem was also responsible for assembling and testing the landing gear controller board, which supports power to the landing gear servos and allows communication between the landing gear controller and the pitot DAQ in order to provide the capability of locking the wheels once a certain speed is reached.

8.2. Power Distribution System Description

The power distribution system is a two bus system that is designed to supply the required power to all of the flight components. The system contains a 2S bus and a 4S bus, each containing two batteries. The power distribution system was designed such that each bus draws power from the battery with more charge. The power distribution system was designed to be failure tolerant to one battery. Thus, one battery on each bus could fail without causing immediate loss of power to the critical flight components. The components that were deemed critical were the rudder servo, the elevon servos, the engine control unit (ECU) and the autopilot. If a battery fails, there is a minimum endurance of 5 minutes under the remaining battery. A diagram outlining the power distribution system is shown below

66
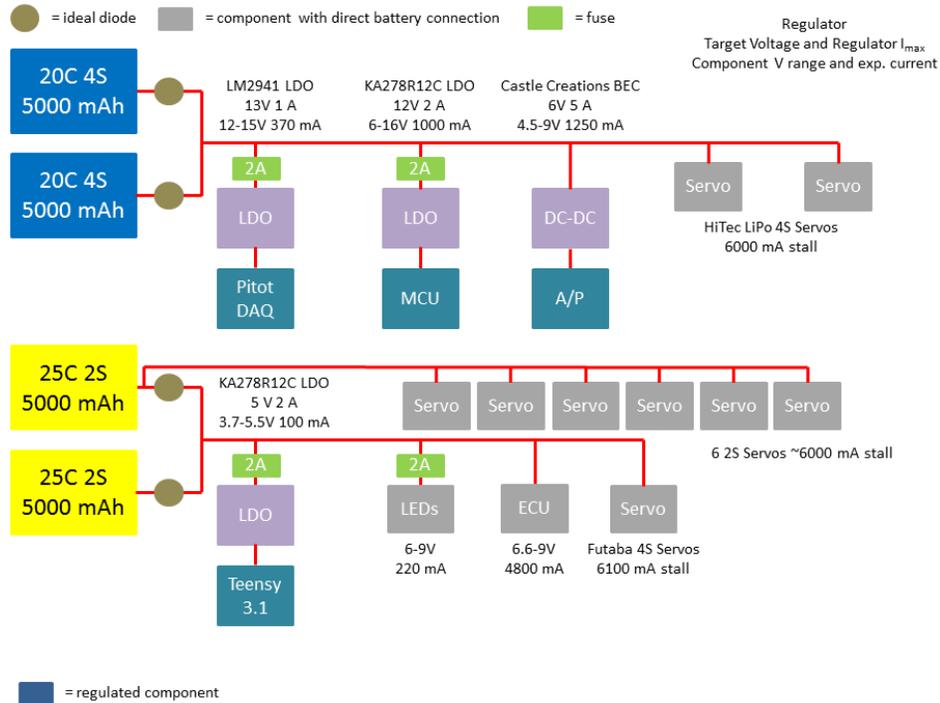
Figure 15: Power Distribution System

As the diagram shows, some of the components require regulation, but others draw current directly from the batteries. It is also important to note that the landing gear servos draw power directly from a single battery on the two bus system. Therefore if that battery were to fail the landing gear servos would no longer be function. The power distribution was tested under load in the previous semester and was integrated into the aircraft.

8.3. Assembly and Integration

8.3.1 Assembly

In terms of the assembly, the electronics subsystem was responsible for assembling the landing gear controller PCB that was designed in the previous semester. The landing gear controller board contained many through-hole parts and only two surface mount parts; therefore, the board was assembled by the electronics subsystem. A diagram of the board is shown below

67
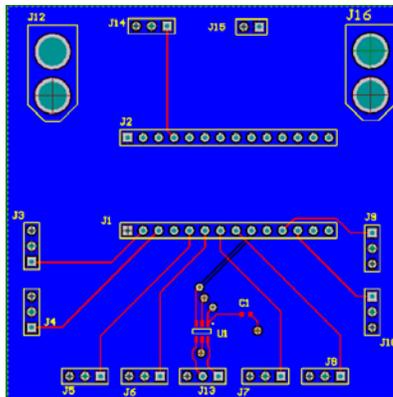
Figure 16: Landing Gear Controller Board

The landing gear controller board was successfully assembled by the electronics team and was then subject to electrical testing.

The only other assembly that the electronics team was required to do was to assemble some of the connectors to various flight components. The majority of the flight components were powered either through XT-60 connectors or through JR type connectors, which are most commonly used for servos. These connectors were assembled in order to establish a power connection between the power distribution system and the various components.

8.3.2 Integration

The state electronics integration at the beginning of the semester was minimal. The power boxes had been mounted and the wiring on the power box end was connected but none of the flight components had been mounted. An image of the power distribution system mounted on the aircraft is shown below.

68

Figure 17: Power System Mounting

As the image above demonstrates, the power box is mounted and the connectors are attached; however, the wiring is still incomplete. The wiring was placed through the corresponding connectors in each of the bulkheads in the previous semester, but wire management and harnessing had yet to take place.

Before the wiring could be completed, the electronics had to be mounted to the aircraft. This included the pitot DAQ, the ECU, the MCU, the autopilot, the landing gear controller, and the aircraft lights. The elevon servo and the rudder servos had been mounted in the previous semester. During the course of the spring 2016 semester, each of the components mentioned above were mounted into the aircraft successfully. The next step was then connecting all of the power wires to each of the components and managing the cables. This was a complicated and time consuming task given the number of wires that needed to be connected and the fact that all of the slack on the wires needed to be removed which required shorting and lengthening the wires as needed. The electronics subsystem connected the wires to the corresponding components one bay at a time. Once this process was completed, the electronics subsystem bundled and harnessed the wires appropriately.

It was important that the wiring was secured in the aircraft in order to prevent loss of signal during taxi or flight. The vibrations from taxi or flight could potentially cause the wiring to

69

separate and even short, which is extremely dangerous. Therefore, the wires in each bay were bundled carefully using cable ties and were mounted to different parts of the aircraft.

There were many issues encountered during the integration of the electronics. The first main issue was a miscommunication in the location of the power buses. The wiring for the 4S bus was placed on the side of the aircraft and the wiring for the 2S bus was placed on the bottom of the aircraft. As it turned out, the 2S bus was on the side of the aircraft and the 4S bus was underneath, forcing the electrical system to redo all of the wiring installed in the previous semester. The second main issues had to deal with grounding. Due to space constraints, only one power wire could be sent from each box through the first bulkhead. Thus, the ground lines had to be split in order to connect to all of the components. To accomplish this task, a ground bus was placed in each of the bays in order to support ground connections to all of the components in that bay. After performing testing with the electrical system, it was observed that some of the ground connections were loose and even disconnected. This promoted the change of the grounding method. A stronger type of ground connector was obtained that provided both a stronger connection and better strain relief. Each of the original ground bars were then disassembled and replaced with the new connector.

8.4. Testing

The tests that were performed on the electrical system are outlined in this section

8.4.1 Landing Gear Controller Testing

There were many tests involving the landing gear controller board. The first test performed was a continuity and power test on the landing gear controller board. The continuity test was to ensure that the board did not have a power to ground short and the power test was to ensure that power was being distributed correctly. If these tests were not conducted, the board could short or perform incorrectly while being directly interfaced with other electronics. This could prove dangerous and could potentially result in serious damage to the critical flight components. Once these tests were complete, the next test was a functional test. During this test, the teensy was connected to the board and a single servo was attached to one of the outputs. The teensy was to control the servo being tested.

70

During the test, the teensy was successfully able to control the one servo that was attached. Therefore, the next step was to mount the landing gear controller board to the aircraft in order to perform a fully functional test with all of the servos. During this test, the landing gear controller board was hooked up to the landing gear, pneumatics, and steering servos to determine if they could be properly controlled. The result of the test was a success, with all of the servos responding in the expected manner.

The other test conducted with the landing gear controller board was a dynamic test with the pitot DAQ. The landing gear controller board receives velocity data from the pitot DAQ so it was important to verify that the data from the pitot DAQ could be received by the landing gear controller board. In order to do this test, the pitot DAQ had to be moving to simulate the data collection that would take place during taxi. To simulate this condition, a wind tunnel was used. The pitot probe was mounted in the wind tunnel and it was connected to the pitot DAQ. The pitot DAQ was then connected to the landing gear controller for data collection. The wind tunnel was run at various air speeds in order to test the capability of the system. The results of the test showed that the airspeed data was being correctly sent from the pitot DAQ to the landing gear controller. The landing gear and testing and operations section can be referenced for more detailed information on the nature of this test.

8.4.2 Isolated Component Testing

Before the fully integrated HWIL test, the electronics subsystem conducted isolated testing on select flight components. This was done in order to evaluate the performance of each component without being interfaced with the rest of the system. This can help to identify issues with the integrated system if the performance of the particular component doesn't match when being tested with the whole system as opposed to being tested stand alone.

The first component tested was the autopilot. The autopilot was to be used to control the elevon and rudder servos. The autopilot test in a previous semester was a simple power

71

test to test the distribution system under load. This test, on the other hand, was designed to test the autopilot's ability to control the rudder and elevens. During the test, the autopilot was powered by the power distribution system with feedback from the indicator lights onboard the autopilot. The RC controller was then used to control the rudder servo through the autopilot. During the test, it was apparent that no signal was being sent to the rudder servo. In order to check if the rudder servo was bad, it was tested stand alone with a power supply. The rudder servo responded to the power input, eliminating that as the source of the issue. The manufacturer of the autopilot was then contacted to obtain information regarding the lack of a signal. The manufacturer claimed that the autopilot needed a regulated 5V supply in order to properly function. The team used a multimeter to check the power to the autopilot and it was found to be 6V. The manufacturer said that anything around that voltage would prevent the autopilot from functioning. The autopilot was then attached to a 5V regulated supply that was used to power the landing gear controller. The test was repeated and the autopilot was able to run the servo. The performance, however, was not anywhere near the level required for a control surface. The lag time between moving the stick on the RC controller and seeing a deflection of the surface was very long, on the order of a few seconds. In addition, there was a lot of noise to the point where the rudder would move sporadically without moving the stick on the RC receiver. This type of performance is unacceptable for an aircraft control surface. The team decided that until the autopilot could be fixed, the RC receiver would be used instead. This was mounted on the aircraft and then tested in the same way as the autopilot. It was seen that the RC receiver outperformed the autopilot as there was little noise and a really fast response time.

Other than the landing gear controller testing, which was outlined above, the only other component that still required functional testing was the light controller. For this test, the light controller was powered from the power distribution system and was tested to ensure that the aircraft lights and beacons all performed as expected. This test was successful and all of the lights and beacons functioned as expected.

72

8.4.3 Fully Integrated HWIL Test

The last major test conducted by the electronics subsystem was the fully integrated HWIL test. In this test, all of the electronics were mounted and they were all to be powered and used simultaneously in order to simulate their function on the aircraft during taxi.   This was done in a series of stages with each power bus being turned on separately to test the components on each box. Then, both boxes were powered to see how all of the flight components would operate together. The results of the test indicated that all components were working correctly except for the engine control unit. When the engine control unit was powered on, the solenoids were constantly running and one of the beacons began flickering at a much higher frequency. This performance did not match what was specified in the manual so the electrical subsystem did a series of tests to determine the underlying issue. The first test was designed to indicate whether cross talk was an issue. If there was any coupling between the throttle input and the beacon, the signal might inject onto the beacon line and cause the beacon to flicker at a higher frequency. To determine if this was the case, the two signal lines in question were separated and shielded. After applying this new configuration, power was again turned on but the problem persisted. The next test involved removing different connections to the ECU to determine if a certain connection point was causing the issue. It was found that when the connection to the engine was removed and put back in place, the problem stopped. However, after the connection was restored, a spool up of the engine was attempted. The engine was unable to spool up so the next step was to check the connection to the engine. In order to do this, the bulkheads and the engine had to be removed, which set the project back due to the time required. After inspection of the engine connections, it was determined that both the cable assembly and the connectors were not the root cause of the issue. After more rigorous testing, it was concluded that there was a problem with the ECU that was internal. It was believed that there was an intermittent short that was causing all of the issues. Since there were no schematics provided by the manufacturer on the ECU, it could not be determined what connections inside the ECU might be problematic. Thus, the ECU needed to be replaced.

8.5. Conclusions

The electronics subsystem made considerable progress during the spring 2016 semester, taking the ETU from not having any electronics integrated to having all electronics and wiring

73

installed and having all components individually tested along with an integrated HWIL test. The aircraft would have been ready for a taxi test.

9. CARBON FIBER SKIN

The Carbon fiber skin was created in 2012 by the structures subsystem using 3K grade carbon fiber for the skin and a coarser 1K grade bi-weave for the control surfaces. It was handed over in two sections, the top and the bottom half, presumably to be bonded post the internal system integration. Following 2012 little to no changes were made to the skin. The focus for Spring 2016 semester was to get the skin ready to taxi and learn about carbon fiber in the process.

Figure 18: Shows the skin with doors and panels cut out

9.1. Goals

As mentioned earlier, little to no work was done on the skin post 2012, hence the main goal for this semester was to get the skin ready to taxi and seal the system post integration. To achieve the goal, various tasks had to be completed which are enumerated as follows:

- Design access panels: These panels grant access to vital onboard electronics, pneumatic and fuel systems. However, it was identified that the skin lacked in stiffness, hence it was essential that the surface area cut out be minimum.

- Cut access panels: Cutting the access panels is a challenge by itself, ideally to maintain stiffness and still have access, the previous team should have cut out panels while laying up the carbon-fiber sheet. The benefits for this process are twofold, firstly, the skin would have a cutout, without the residual opposite flex resulting from cutting post-cure. Secondly, carbon-fiber dust is highly poisonous and known to cause cancer when inhaled.

- Making skirts to support the panels: This process could have been completely avoided had the structural engineers designed panels before curing with a technique called gradient recess layup which involves increasing the size of a recess gradually and have a complementary fitting part.

- Painting the skin: The skin had to be painted with an aerospace grade epoxy-paint following the color scheme set by the FAA

- Trimming Operations: As the skin was not entirely symmetrical and fell in the way of the control surfaces, it had to be trimmed. Additionally, a slot had to be cut to accommodate the FPV. If the engineers had a little foresight, the FPV could have been positioned more suitably. The current configuration demands both halves of the to be trimmed, which can be an arduous task

- Bonding both halves of the skin: the skin had to be integrated into the frame of the aircraft.

- Mounting the doors

- Sealing the aircraft: The aircraft has to be sealed for aerodynamics reasons.

The tasks were identified to achieve the goal, although some of the tasks could have been completely avoided had the previous engineers shown some foresight. However, this is a learning experience and a lot more can be taken from mistakes than successes.

9.2. Scheduling

A Gantt chart was made after identifying the tasks and a schedule was made as follows, prior to painting, every process was on schedule, but there was a derailment during the painting process, the details of which are discussed in a later section.
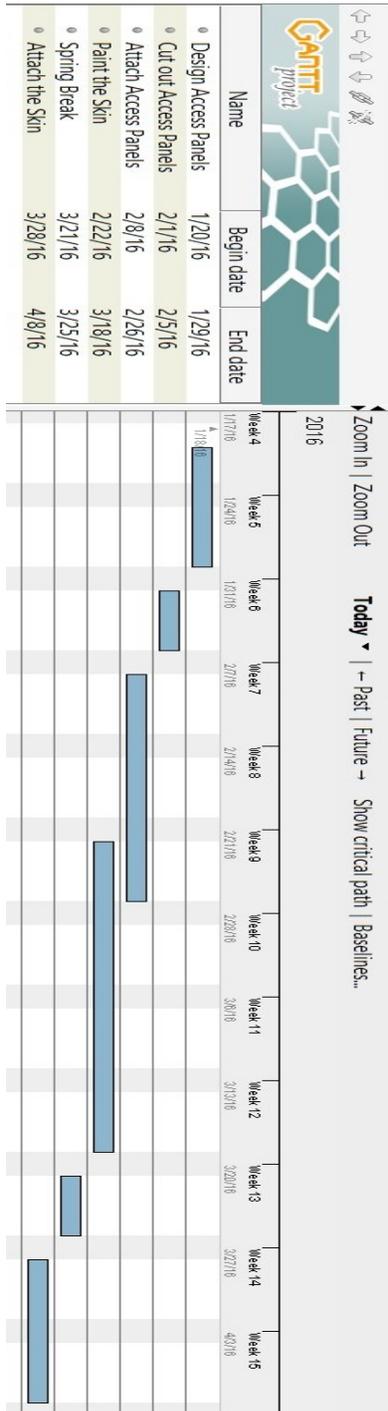

Figure 19 Gantt Chart

77

9.3. Tasks Completed

Design of access panels: Access panels were designed by meeting with the entire team and coming to a decision collectively on the location and size. A Paper Mache template of the top half of the skin was made to get visual estimate of the location and size The front right access panel is over the power board. The two symmetric access panels give access to the battery and the pneumatics reservoir. The rear access panel on the top makes the ECU accessible. The bottom panels are the doors for the landing gear and the bottom rear panel covers the LED board. Access panels were cut on the model to validate the size and positioning of the panels.
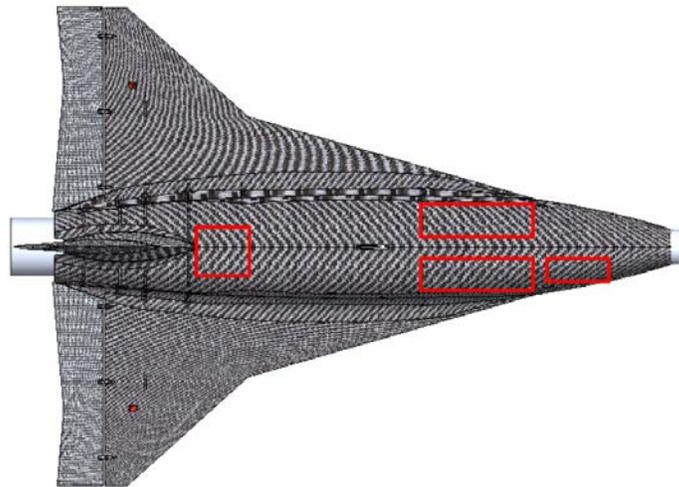

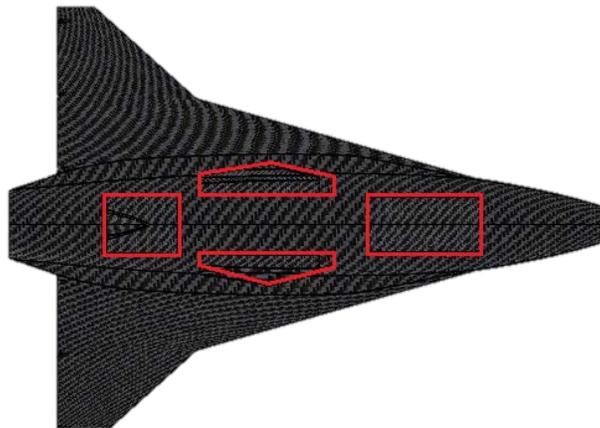*Figure 20 shows the access panels in the top half*

Figure 21 Shows the doors and panels in the bottom half

78

Figure 22 Shows the paper Mache mold.

Cutting the Access Panels: Cutting the access panels is not a complicated procedure. However, it demands skill in the usage of a Dremel. The panels were marked with thread and taped to the surface. A Dremel was used to cut the panels. A metal cutting head with the speed of 25,000 rpm was used in the cutting procedure. It is vital that the panels are not sanded in the edges as this will affect the fit of the panel. **It is very important to take precaution while cutting the panels as inhaling carbon fiber dust can cause cancer. It is advised to use masks for breathing and a vacuum to suck the dust as the cutting takes place. It is also recommended to thoroughly wash hands to eliminate accidental ingestion.**

Figure 23 Cutting the access panels

79

Painting the skin: The paint used on the skin was purchased from The paint was purchased from a 'Aircraft Paint Supply' in Ohio. The supplier Mr. Dave Seymour (*dave.seymour@aircraftpaintsupply.com*) sent the following quote for Imron Paint:

PRIMER		
Components Parts by Volume		
Corlar 13550S Epoxy Primer 3 Part	1 / quart – Imron Epoxy Primer 13550S	-$90.61
Corlar 13150S Epoxy Activator 1 Part	1 / pint – Imron Activator 13150S	-$49.72
13756S VOC-Exempt Reducer 2	1 / quart – Imron Reducer 13756S	-$46.46
PAINT		
Components Parts by Volume		
Imron AF3500 Color 2 Parts	1 / quart P2333EJ Gloss Black	-$101.80
13100S Activator 1 Part	1 / quart 13100S	-$90.60
13765S Reducer 0.25	1 / pint 13765S	-$24.65
Imron AF3500 Color 2 Parts	1 / quart P7016EJ – Zepher Orange	-$232.90
13100S Activator 1 Part	(Included Above)	
13765S Reducer 0.25	(Included Above)	
	Subtotal:	$636.74

The skin was handed over to Motor Sports Concepts (Mr. Jarod Swantkoski, 303 286-9498) an auto body shop in Denver for painting. Originally, we had asked the paint shop at CU Boulder, but they were not equipped to handle the 3-part epoxy paint. Due to a misunderstanding between the paint supplier and the painting shop, it took 3 weeks for the paint to dry, when it should have taken approximately one week.

The following images show the finished paint job:

Figure 24 Painted skin

80

10. <u>FIRST PERSON VIEW (FPV)</u>

10.1. FPV Summary

The FPV subsystem is responsible for transmitting a live video feed from the aircraft to the ground station. This live view from the aircraft is used by the pilot to control and navigate the aircraft.

All components for the FPV system were selected and purchased in the Fall of 2015. This semester, the FPV system was fully assembled and tested, both at the component and system levels. This included a range test to verify the operational range met the system requirements, as well as a full integration test to verify full system operation of the aircraft following integration.

10.2. FPV System Description

The first person video (FPV) system is responsible for transmitting live video data from the aircraft to the ground station for the pilot to use while flying. The system mostly consists of off the shelf FPV components for RC aircraft as well as aerospace grade antennas. The system operates at 1.3 GHz (specifically 1280 MHz) which was chosen to not interfere with the 900 Mhz control signal, and 2.4 GHz RC handset link to the ground station. This frequency falls within the 23 cm band which requires a minimum of a Technician Class HAM radio license to operate legally in the United States. A Technician Class License is easy to obtain and grants privileges to operate all VHF/UHF Amateur bands. The specific components of the FPV system are described below. Figure 37 shows a high level diagram of all major components in both the aircraft and ground station FPV nodes. Each item is described in detail in the following sections.
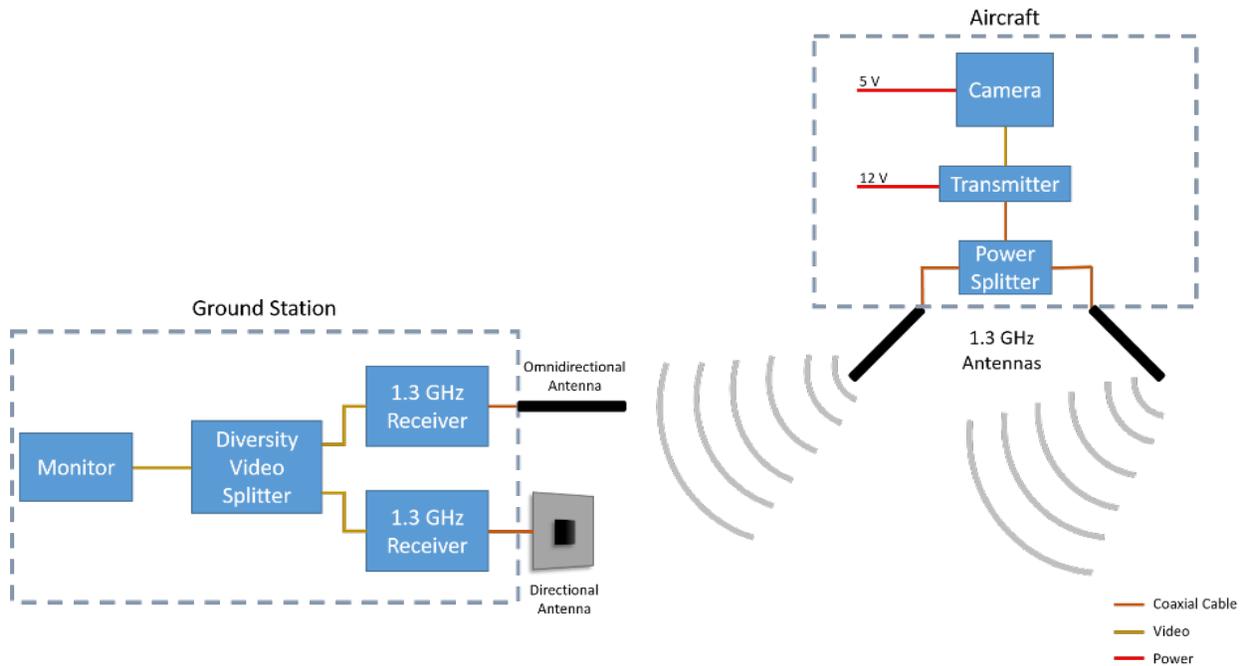
81

Figure 25: FPV system diagram

The FPV system operates at 1280 MHz and uses two transmit antennas and two receive antennas. Two transmit antennas were required on the aircraft to achieve full coverage around the aircraft and to eliminate shielding from the carbon fiber skin. One antenna is placed on top of the aircraft, and one on the bottom so that one will always be visible for any orientation of the aircraft. Both antennas are linearly polarized and are aligned 90˚ rotated from each other which eliminates interference between the two. The power from the video transmitter is equally split between the two antennas.

The ground station uses two antennas in order to receive the best quality signal. One antenna is a directional antenna and the other is omnidirectional. The directional antenna should receive a much stronger signal most of the time, but in the case that the aircraft goes out of view of the directional antenna, the omnidirectional is included as a backup. A diversity splitter is used to select the video feed from which ever antenna has the strongest received signal strength. This diversity setup should give a reliable video signal at all times during the flight test. All of the FPV components are listed in Table 4.

Table 2: FPV system components

Aircraft Node	
Component	**Part Number**
Camera	FatShark PilotHD V2
1.3 GHz Transmitter	1.2-1.3 GHz LawMate 1000 mW Transmitter
Power Divider	Haigh-Farr 2 Way Power Divider
Transmit Antennas	Haigh-Farr 1.3 GHz Blade Antennas
Ground Station	
Component	**Part Number**
Monitor	Lumenier LCD 12.1" FPV Monitor
Diversity Video Splitter	EagleEyes FPV Station
2 Receivers	1.3 GHz LawMate Deluxe Portable High Sensitivity Receiver
Omnidirectional Antenna	Dipole Antenna included with receiver
Directional Antenna	IBCrazy 1.3 GHz BiQuad Antenna

10.3. Ground Station Node

The pilot interfaces with the FPV ground station through the monitor for viewing a live video feed from the aircraft. The ground station uses two antennas each connected to a separate receiver to receive video from the aircraft. The antennas are connected through a diversity controller so that the video from the antenna with the stronger signal is displayed on the monitor.
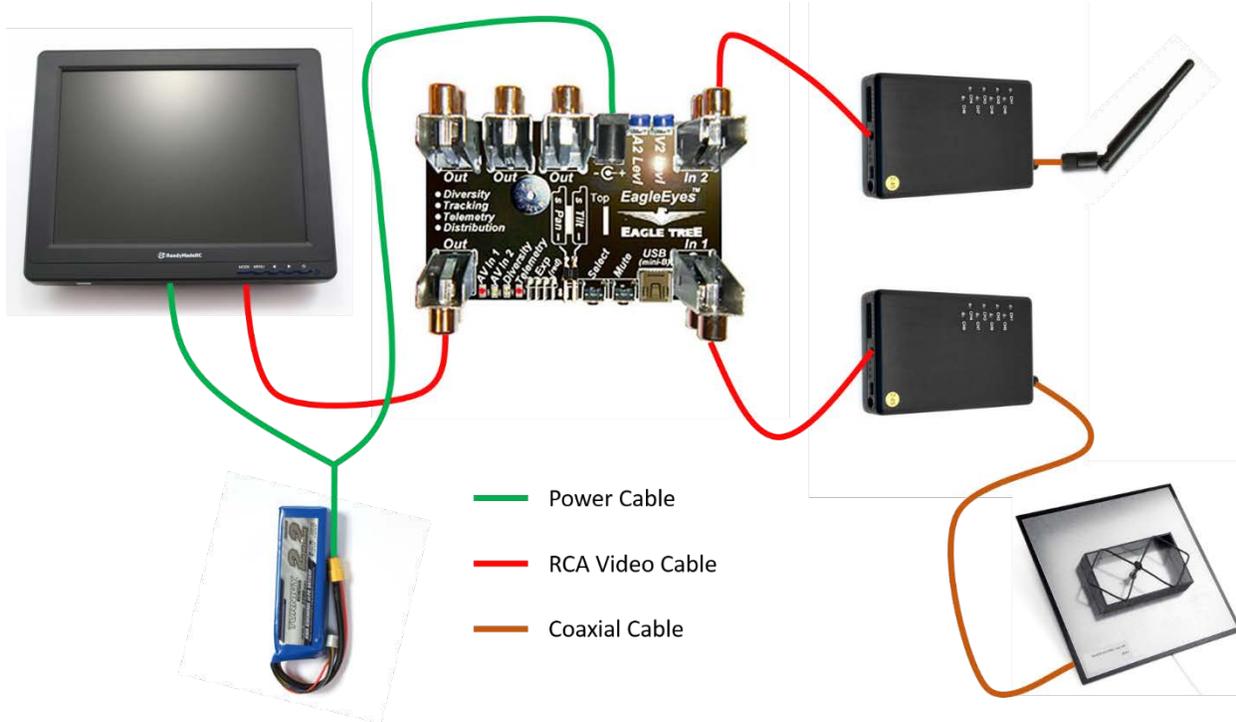
83

Figure 26: FPV ground station detailed connection diagram

10.4.1 Monitor

The monitor is a 12 inch monitor from ReadyMadeRC. It is a display specifically designed for flying RC aircraft with FPV. This is important as it does not go to a blue or black screen when the signal fades. While flying FPV it is common for the strength of the received video signal to fluctuate, and this monitor is designed to still show the video signal even if it is weak. This is contrary to most TV and computer monitors which will just display a blue screen if the signal is not strong enough.

The monitor can be powered by 6-24 V. This is commonly done using the included 12 V wall adapter, or a 3S Lipo battery while in the field. The monitor has inputs for video from the splitter, and power. In order for the monitor to correctly display the signal from the camera, the monitor needs to be set to PALi. This has already been done and should not need to be changed again.

10.4.2 Video Diversity Splitter

The video splitter is an EagleEyes FPV Station from GetFPV. This splitter can be used for displaying the aircraft video on multiple displays, or attaching a recording device to save the video. The splitter also includes a receiver diversity function which is used to choose the stronger signal of each of the two antennas. Each receiver is connected to the splitter, and the one with the best video signal will be output to the monitor. Antenna diversity was deemed necessary to ensure that the video signal will always be strong as this is the main interface that the pilot has for flying the aircraft. A loss of video signal would be a very high risk scenario that would most likely result in loss of the aircraft.

10.4.3 Receivers

The receivers are 1.3 GHz Deluxe Portable High Sensitivity Receivers from GetFPV. These receivers were chosen as they operate at the correct frequency and include a standalone battery for power. The receivers can be switched between different channels within the 1.3 GHz band and should be set to match the channel of the video transmitter which is 1280 MHz. Each receiver connects to an antenna and provides video out to the video splitter. **THE RECEIVER SHOULD NEVER BE POWERED ON WITHOUT AN ANTENNA ATTACHED.**

10.4.4 Omnidirectional Antenna

The omnidirectional antenna is a standard 3 dB dipole antenna that came with the receiver. This antenna achieves nearly isotropic coverage, with nulls above and below the antenna. This antenna is mostly provided as a backup to the directional antenna which should be receiving a stronger signal most of the time.

10.4.5 Directional Antenna

The directional antenna is a BiQuad linearly polarized antenna from ReadyMadeRC. This antenna has 11 dBi of gain with a 50° beam width. The radiation pattern of this antenna is shown in Figure 39. This antenna will work at much greater distances than the omnidirectional dipole antenna.
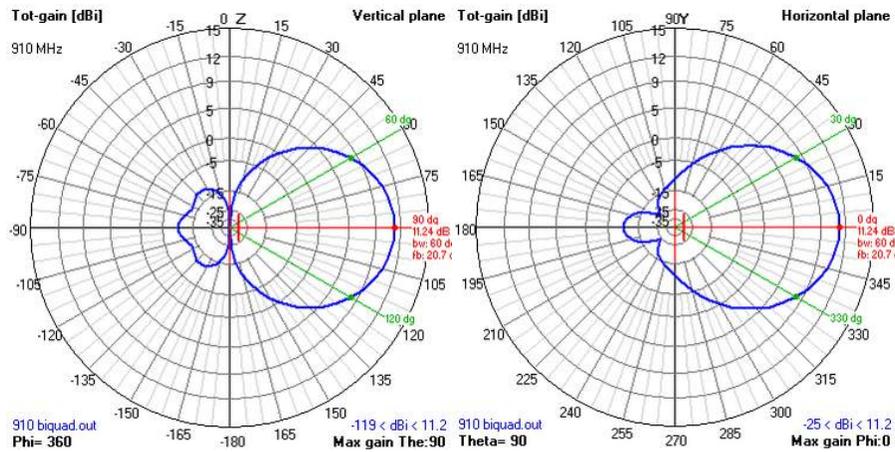
85

Figure 27: Directional antenna radiation pattern

This antenna will need to be actively pointed at the aircraft during flight to ensure that the aircraft always remains within the beam. This will be done by a member of the team during flight test.

10.4. Aircraft Node

The aircraft includes a camera from which the video will be transmitted to the ground station. This is accomplished through a transmitter, power splitter, and two antennas which are described below.

10.5.1 Camera

The camera is a FatShark PilotHD V2 camera from GetFPV. This camera was chosen because it has the ability to record onboard video which will be useful to review after the flight test. The camera is mounted on the front of the aircraft pointing forward. It is powered by 5 V and has a video output which is connected to the transmitter.

10.5.2 Transmitter

The video transmitter is a 1.3 GHz LawMate 1000 mW transmitter from GetPFV. The transmitter was chosen because it has high power which is important for good range, and since the power is being split between two antennas. Video from the camera is connected to the transmitter, and the antenna output is connected to the power divider. The transmitter is powered by 12 V. Since the transmitter is such high power, it becomes very hot after a few minutes of operation. It needs constant airflow over the casing in order to cool properly. **THE TRANSMITTER**

86

SHOULD NEVER BE POWERED ON WITHOUT AN ANTENNA ATTACHED. THIS COULD DESTROY THE TRANSMITTER.

10.5.3 Power Divider

The power divider comes from Haigh-Farr and has the part number 2169F-FB. This power divider splits the power from a transmitter of 1.0 - 1.8 GHz equally between the two outputs. This power divider was chosen since it is the same manufacturer that designed the antennas.

10.5.4 Transmit Antennas

There are two FPV transmit antennas on the aircraft. These antennas are from Haigh-Farr and have the part number 6103. These antennas are designed to work for 1.25 – 1.4 GHz which includes the frequency of transmitter being used. These antennas were chosen because of their aerodynamic design, and because these type of antennas have already been tested with aircraft skin for the control system. Since these antennas are basically the same as those used for the control system, it is possible to conclude that they will also work well with the aircraft skin. Both antennas are linearly polarized and are mounted at 90˚ angles to each other to ensure that they will not interfere.

10.5.5 Mounting

A mount was designed to hold the camera at the front of the aircraft while trying to minimize air resistance. The design attaches to the first bulkhead and comes out of the skin at 45˚. The design can be seen in Figure 40. The mount has been installed in the aircraft.

Figure 28: FPV mount CAD design.

10.5. Range Test

One of the major goals of the Spring 2016 semester was to perform a range test of the FPV subsystem to characterize its reliable operating range. This was accomplished by installing the aircraft node of the FPV subsystem in an aircraft mockup with the antennas in a similar orientation to the actual aircraft. The ground station was set up at the top of a hill, and the aircraft node was driven away from the ground station. One person monitored the live video feed on the ground station and recorded the distance at which the video degraded to a point no longer usable for flight. By testing the range on the ground with the aircraft node inside of a car, this gives the maximum operating distance under worst case conditions. Trees and hills along the road block the line-of-sight degrading the video signal. During taxi and flight, there will be a clear line-of-sight to the aircraft and the range will be much better than during this test. Each antenna was tested individually and together as full system. A range of 1.2 miles was observed for the dipole antenna, and 2.5 miles for the biquad antenna. During the full system test, the ground station was observed to correctly select the stronger video signal.

The distances observed during the range test verify that the FPV subsystem will be sufficient for taxi and flight testing. Following this test the aircraft node was installed inside of the aircraft and wired to the power system.

10.6. Conclusions

The FPV system was fully completed, integrated, and tested during the Spring 2016 semester. The system is installed in the aircraft and is ready for taxi test.